DECLARATION

I hereby declare that all the work presented in this thesis is my own, unless otherwise stated within the text, and that the thesis has been composed by myself.

Iain J. McGee

AN IMPLANTABLE MULTICHANNEL BIOTELEMETRY SYSTEM

by

Iain J McGee

Thesis presented for the degree of
Master of Philosophy
at the
University of Edinburgh

December 1974

To my wife and children in lieu of
time I should have spent with them

A C K N O W L E D G E M E N T S

The help and guidance of J. Jordan and M.A. Reid, under whose supervision this work was carried out, is gratefully acknowledged. My thanks are also due to J.H. Filshie, of the Poultry Research Centre (ARC) in Edinburgh, for his invaluable advice and encouragement, and to many other colleagues who have contributed in different ways. In particular, I should like to thank W. Templeman for his mask-making and photoreduction work, B. Wilkie who performed the metal depositions, J. Moir who etched and bonded the transmitters, and J. Clarke who typed the thesis.

Finally, I should like to thank Professor W.E.J. Farvis of the Department of Electrical Engineering, for the use of the facilities of his department, and together with J. Murray and A.D. Milne, past and present directors of the Wolfson Microelectronics Liaison Unit, for the help and support they have given to the PRC Telemetry Group, throughout their development program.

C O N T E N T S

LIST OF SYMBOLS USED IN THE TEXT

A	Area	m^2
$\overset{o}{A}$	Angstrom Unit	m^{-10}
A_r	Effective Aperture	m^2
a	A constant	-
B	½ IF Bandwidth	Hz
b	b-value of a thermistor	^oK
C	Channel Capacity	bits/sec
D	Modulation Index	-
d	Penetration Depth	m
dB	Decibel	-
dl	Incremental Length	m
E	Electric Field Strength	v/m
E_v	Bridge Supply Voltage	v
e	2.71828	-
e_o	Output Voltage	v
e_{max}	Maximum Temperature Error	^oK
f_c	Carrier Frequency	Hz
f_{IF}	Intermediate Frequency	Hz
f_m	Message Bandwidth	Hz
G_r	Antenna Gain	dB
H	Magnetic Field Strength	amp/m
Hz	Hertz	sec^{-1}
h	Signal-to-Noise Voltage Ratio	-
h_o	A temperature increment	^oK
I	Current	amps
i	Current	amps
J	Bessel Function of the first kind	-

l	Length	m
N_v	Noise Voltage	v
n	A variable	-
P_d	Power Flux Density	w/m^2
P_r	Received Power	w
p	Order of Bessel Function	-
Q	Q-factor	-
R	Resistance	Ω
R_r	Radiation Resistance	Ω
R_s	Sheet Resistance	Ω/square
S_v	Signal Voltage	v
T	Temperature	^oK
t	Temperature	^oK
V	Voltage	v
V_r	Received Voltage	v
v	Voltage	v
w	Width	m
x	Distance	m
Z_o	Intrinsic Impedance of Free Space	Ω
β	Relative Bandwidth	-
γ	Criterion of Significance	-
Δf	Frequency Deviation	Hz
ε	Permittivity	Farads/m
λ	Wavelength	m
μ	Permeability	Henries/m
π	3.14159	-
ρ	Bulk Resistivity	Ωm
σ	Conductivity	i/v

τ	Response Time	sec
Ω	Ohm	v/i
ω	Angular Frequency	rad/sec

LIST OF ABBREVIATIONS USED IN THE TEXT

AC	Alternating Current
AGC	Automatic Gain Control
AM	Amplitude Modulation
ARC	Agricultural Research Council
DC	Direct Current
ECG	Electrocardiogram
EEG	Electroencephalogram
EMG	Electromyogram
FDM	Frequency Division Multiplexing
FET	Field Effect Transistor
FM	Frequency Modulation
FSD	Full Scale Deflection
GPO	General Post Office
HMSO	Her Majesty's Stationery Office
HO	Home Office.
IF	Intermediate Frequency
IRIG	Inter Range Instrumentation Group
MRC	Materials Research Corporation
NPO	Capacitor Dielectric Material (Negative/Positive/Zero)
PAM	Pulse Amplitude Modulation
PCM	Pulse Code Modulation
PDM	Pulse Duration Modulation
PM	Phase Modulation
PPM	Pulse Position Modulation
RCA	Radio Corporation of America
PRC	Poultry Research Centre
RF	Radio Frequency

SAW	Surface Acoustic Wave
TCR	Temperature Coefficient of Resistance
TDM	Time Division Multiplexing
VCO	Voltage Controlled Oscillator
VHF	Very High Frequency

LIST OF ILLUSTRATIONS

LIST OF ILLUSTRATIONS (contd)

APPENDIX

SUMMARY

The results of investigations carried out by the author, into the feasibility of producing a multichannel radio-telemetry system compatible with chronic implantation in small animals, and the relevant GPO telemetry regulations, are reported.

Some aspects of RF propagation from small implanted antennae are considered in Chapter I, and the design of a practical RF transmitter is presented. The results of investigations into biological signal and telemetry channel bandwidths are reported in Chapter II and reasons are given for the choice of an FM/FM multiplex system. Various miniaturisation techniques are assessed in Chapter III and the arguments in favour of the use of a thin film hybrid technology are presented. Aspects of the technology which lead to constraints in circuit design are also considered.

The design of a number of component modules of a potential multichannel system is described in Chapter IV, and thin film layouts for some of these are presented, together with some performance data.

INTRODUCTION

The application of radio-telemetry to the field of physiological parameter measurement is rapidly becoming more widespread. (Kimmich and Vos, 1972). The availability of semiconductor active devices and micro-miniature discrete components has enabled the construction of high-performance telemetry transmitters, within limits of size and weight, acceptable for use with the larger animals.

Radio-telemetry can permit biological variables, such as temperatures, pressures and bio-potentials, to be measured under realistic experimental conditions, with a minimum of interference to normal behaviour patterns. The elimination of trailing wires from transducers to monitoring equipment reduces stress to the subject, and can permit complete freedom of movement during exercise. Problems due to lead induced transients and mains-hum pick up are reduced, and potential danger to the subject from failure of mains-powered monitoring equipment is eliminated. In many cases, particularly in the study of animals in their natural habitat, radio-telemetry may prove to be the only satisfactory method of measurement.

If the entire telemetry transmitter and power supply can be implanted within the body of the subject, the level of stress to the subject may be reduced still further. Long-term bio-potential data retrieval is made possible without the need for maintenance of the skin/electrode interface, and the possibility of infection is eliminated, where leads from internal electrodes would otherwise have

to pass through the skin.

Many implantable radio-telemetry devices have been described since the earliest 'Endoradiosondes'. (Mackay, 1957)*. The majority of such implantable devices have been based on either a 'squegging' oscillator, whose performance has been analysed by Lin and Ko (1968), or on a single transistor Colpitts or Hartley oscillator, with provision for frequency modulation, as described by Green and Shore (1969), Marshal and Celebi (1970) and Brown (1971). Such devices have only very few components to keep them small and light, nevertheless reliability can be a problem. (Barr, 1972).

More complex circuits, of improved performance, using sub-carrier oscillators, have been described by Michael and Weller (1968) for use with Rhesus Monkeys, and by Riley (1970) in sheep and cows. These circuits also use a single transistor RF oscillator, where a single tuned circuit is used for both carrier generation and radiation. These two functions, however, are mutually antagonistic, since for efficient radiation the antenna must match well into the surrounding medium, and for good carrier frequency stability, the frequency determining elements must be insensitive to changes in that medium. Recent developments in microelectronics have made possible the construction of more complex and reliable circuitry, within dimensions which have previously been considered acceptable for implantation in small animals.

Such devices were required by scientists of the

* p.12.

Agricultural Research Council's Poultry Research Centre[1] (PRC) in Edinburgh to facilitate work on avian physiology, and a liaison between the PRC and the University of Edinburgh, Department of Electrical Engineering[2], evolved. Since 1967, the author has been employed by the PRC and has been working in the Department of Electrical Engineering on the development of implantable telemetry transmitters. It was considered that a Thin Film Hybrid Technology would best satisfy the requirements of this project. Initial work on the electron-beam evaporation of metals and the influence of deposition parameters on film properties was therefore carried out concurrently with work on subtractive photo-lithography and component attachment. This led, in 1970, to the establishment of a standard process based on a Ni-Cr/Au/Si-O film system. (Filshie and McGee, May 1974). This process has been used for the fabrication of two single channel telemetry transmitters to handle the avian ECG/EEG signals, and deep-body temperature. (Filshie and McGee, June 1974).

Considerable experience has now been gained in the use of these devices 'in vivo', for the continuous monitoring of single biological variables. It is now apparent that simultaneous monitoring of more than one such parameter will greatly facilitate the physiological work by eliminating the need for multiple experiments. The succeeding chapters present the results of investigations carried out by the author, into the feasibility of producing a micro-miniature multi-channel telemetry transmitter, compatible with chronic implantation in 'Gallus Domesticus' and existing GPO telemetry standards.

CHAPTER 1

RADIO TELEMETRY

1.1 GPO Telemetry Regulations

The use of radio-telemetry devices for medical and biological applications in the UK is restricted by the HO* to licenced users. Mandatory minimum standards of performance have been specified for three permitted classes of devices and are published by HMSO (1968) in Performance Specifications Numbers:-

W6802 for Class I devices

W6803 for Class II devices

W6804 for Class III devices

A brief summary of the most important requirements for telemetry transmitters follows.

Class I devices must normally be wholly contained within the body of an animal or man, and must have useful range, when used in conjunction with appropriate receiving equipment, not appreciably in excess of 1.5m. Operation is permitted on any frequency within the band 300kHz to 30MHz, provided that the mean DC power input to the transmitter does not exceed 5mW if operating continuously, or 1mW if pulsed. The RF bandwidth is undefined, but emissions at any frequency other than that of the carrier and sidebands comprising the modulation envelope are considered spurious, and their field strength, when measured at 10m distance from the transmitter in any plane, must not exceed 50μV/m.

* Home Office.[34]

Class II devices must operate in the frequency band 102.2 to 102.4 MHz. Specification no. W6803 states that 'Amplitude or angle modulation up to a maximum of $\pm$50kHz is permitted'. The maximum un-modulated carrier power must not produce a field strength greater than 10μV/m at a distance of 15m in the same horizontal plane as the transmitter. Spurious signal power, ie lying outwith the band 102.2 to 102.4 MHz, is measured in the absence of modulation and no individual spurious component may exceed a field strength of 10μV/m at a distance of 3m in the same horizontal plane as the transmitter. The carrier frequency must be such that 'significant emissions' shall be contained within the band 102.2 to 102.35 MHz. This condition must be satisfied over a temperature range of 0^{o}C to 40^{o}C, and throughout the full range of battery voltage.

The maximum range of operation of Class II devices is not explicitly stated in the GPO specifications. The maximum permitted field strength of 10μV/m at 15m distance allows the range to be calculated if the gain of the receiving antenna and the receiver sensitivity is known. The free-space wavelength (λ) at 100MHz is $\approx$ 3m. Consequently, at a distance of 15m the induction field is insignificant and the radiation field strength falls off linearly with distance. An example of this range calculation for a Class II device is shown below. The standard expressions used in the evaluation are taken from Connor (1972).

A field strength of 10μV/m is equivalent to a Power Flux Density (P_d) of

$$P_d = E.H = \frac{E^2}{120\pi} = 2.65 \times 10^{-13} \text{ w/m}^2 \qquad (1.1.1)$$

where E = 10μV/m

and $H = \frac{E}{120\pi}$

The effective aperture (A_r) of a half-wave dipole (whose gain (G_r) is x 1.62 or 2.17 dB) operating at λ = 3m is given by

$$A_r = G_r \frac{\lambda^2}{4\pi} = 1.16\text{m}^2 \qquad (1.1.2)$$

The power received (P_r) by the half-wave dipole at 15m distance is therefore

$$P_r = P_d.A_r = 3.05 \times 10^{-13} \text{ watts} \qquad (1.1.3)$$

But $P_r = \frac{V_r^2}{4R_r}$ where V_r is the voltage developed across the receiver aerial terminals and R_r is the antenna radiation resistance = 73Ω.

$$\therefore V_r = (4P_rR_r)^{1/2} = 9.4\mu V \qquad (1.1.4)$$

The sensitivity of the Leak[3] Delta FM Receiver, whose performance is investigated further in Chapter II, is quoted by the manufacturers to be 2.5μV aerial input for a 30dB output s/n ratio. The effective maximum range for a 30dB s/n ratio is therefore

$$15 \times \frac{9.4}{2.5} = 56 \text{ metres}$$

Class III devices also operate within the band 102.2 to 102.4 MHz, and are permitted a maximum unmodulated carrier power output such that the field strength shall

not exceed 10μV/m when measured at a distance of 200m in the same horizontal plane as the transmitter. Specification no. W6804 states that 'Amplitude or angle modulation up to ±5kHz is permitted', but operation is restricted to two spot frequencies within the band, viz CHANNEL A - 102.36 MHz and CHANNEL B - 102.39MHz. Carrier frequency drift must not exceed ±3kHz over a 0°C to 40°C temperature range, and over the full working life of the battery. Spurious signal power is again measured in the absence of modulation. The power of any individual spurious signal, at a frequency removed from the carrier by more than 20kHz, shall not cause a field strength of greater than 10μV/m at a distance of 3m in the same horizontal plane as the transmitter, under all conditions of use. An additional point in the Class III specifications is that the spot frequency of 102.375MHz may be used for control of transmitters working on either CHANNEL A or CHANNEL B.

The GPO specifications also cover associated receiving equipment and lay down performance requirements which are much tighter for 100MHz equipment than for the band below 30MHz. Class I device users are merely required to optimise receiver performance, and to limit spurious radiations from the receiving aerial to a field strength of 50μV/m at 10m distance. The specifications relating to receivers for use with Class II and III devices, include quite stringent requirements relating to rejection of unwanted signals, spurious responses and spurious emissions from the receiving aerial. One consequence of these requirements for Class II and III device users is that

most commercial FM broadcast receivers covering the band 88 to 108 MHz, would not comply with the requirements without modification. (Weller and Manson, 1972). Commercial broadcast receivers covering the Class I frequency range are usually designed for A.M. reception. Unfortunately, there are considerable advantages in the use of FM for implantable Class I devices.

The legal user is thus constrained either to purchase a relatively expensive receiver designed specifically for telemetry applications, or to involve himself in considerable modification of relatively cheap receivers. This applies to all three classes of operation.

1.2 RF Propagation

The equations which describe the alternating electric and magnetic fields produced by a small electric or magnetic dipole source, consist of two terms which are added. (Kraus, 1950)*. These can be considered to represent two superimposed, but not independant, electromagnetic fields. The first term represents the near or induction field which consists of electric and magnetic field components which are 90^{o} out of phase. In free space, this field returns its energy to the dipole source. Its field strength varies as the inverse square of the distance from the source has a maximum value along the dipole axis and a minimum, of half that value, in the perpendicular plane. The second term represents the far or radiation field which consists of electric and magnetic field components which are in phase. The energy of this

* p8

field is effectively detached from the source, and propagates through space. Its field strength varies inversely as the distance from the source has a maximum value in the perpendicular plane and is equal to zero along the dipole axis. At distances from the source, in the perpendicular plane, of less than $\lambda/2\pi$ (where λ = the wavelength in the medium concerned), the near field predominates, and at distances greater than this the far field becomes increasingly dominant.

The radiation resistance (R_r) of an elementary electric dipole, of length dl, operating in free space, can be derived from Maxwell's field equations as:-

$$R_r = 80\pi^2 \left(\frac{dl}{\lambda}\right)^2 \text{ ohms} \quad : \text{Kraus (1950)}^* \qquad (1.2.1)$$

where λ is the operating wavelength in free space.

This expression is derived on the assumption of a uniform current distribution along the length dl, and can be justified for $dl < \lambda/10$. For dipole lengths of $\lambda/10$ to $\lambda/4$ a linear current distribution may be assumed, if one end is grounded. For $dl > \lambda/4$ a sinusoidal current distribution may be assumed.

If the above expression for R_r is evaluated for $dl = \lambda/3$, the error involved in the use of the uniform current approximation is in the region of 5%. The radiation resistance of a $\lambda/2$ folded dipole, similarly evaluated, appears as 197Ω, as against 173Ω if a sinusoidal current distribution is used, giving an error of about 8%. The great majority of practical antennae for use with small animals will be much smaller than $\lambda/2$, even at 102MHz (where $\lambda/2 \approx 1.5$m). The above expression for R_r may therefore be used as a good approximation.

* p 137

The radiation resistance (R_r) of a small magnetic loop antenna of area (A)m^2 operating in free space may be similarly derived as:-

$$R_r = 320\pi^4 \left(\frac{A}{\lambda^2}\right)^2 \text{ ohms} \qquad (1.2.2)$$

on the assumption that the loop dimensions are such that negligible phase change occurs around the loop circumference. This is generally true for loops whose radii are $< \lambda/10$. (Kraus, 1950).*

If these expressions are evaluated for antennae whose dimensions are compatible with implantation in small animals, values of R_r are obtained which are very much smaller than the intrinsic impedance of free space (Z_o) of 377Ω. Such small antennae are therefore inefficient radiators, and in general steps must be taken to improve their radiating performance.

The effective length, and hence the radiation resistance of a small electric dipole, operating below its self resonant frequency, may be increased by 'base-loading' the dipole elements with a lumped impedance at the driving points. (Mackay, 1970)†. This technique may be used to bring a small dipole into resonance at the transmitter frequency, and can result in a high-Q system. The structure is, however, vulnerable to changes in antenna geometry, and to the presence of nearby dielectric materials. Both of these factors can cause de-tuning, resulting in a reduction in transmitted power if the antenna is driven at a constant frequency.

The effective current and radiation efficiency of a small loop antenna may be readily increased by incorporat-

* p167

† p.247.

ing more than one turn, thus increasing the effective current. This structure can be tuned to resonance with a capacitor, to produce a high Q resonant antenna. The structure may be de-tuned by the proximity of ferromagnetic materials, and to a lesser extent by the effects of dielectric materials contributing to the self-capacitance of the coil. In work with small animals, this is less of a practical problem than that of maintaining a base-loaded electric dipole, in resonance. Increased magnetic flux densities may be readily obtained from a small loop antenna by inserting small pieces of high permeability, eg ferrite, material into the loop. Such materials can have extremely small losses, even in the region of 100MHz. Materials capable of concentrating electric flux to any appreciable extent are invariably lossy at these frequencies. One further practical point regarding tuned magnetic loop antennae is that their impedance may be readily made significant compared with typical circuit impedance levels. This allows more convenient matching of the antenna to the transmitter than is possible with short dipole antennae.

1.3 Implantation of Antennae

The majority of standard texts on antennae theory are concerned mainly with the far field radiation of relatively efficient antennae systems operating in free space. (Kraus, 1950), (King, 1956). In most biological radio-telemetry work, the transmitting antenna is either implanted within, or operates in close proximity to,

living tissues. The mathematics involved in the description of the near and transition fields of small inefficient radiating elements is complex, especially if their interaction with a finite volume of body tissue is taken into account. Living tissue has a high water and ionic content and, consequently, both its permittivity ($\mathcal{E}$) and conductivity (σ) are quite high. Its magnetic permeability (μ) is, however, close to that of free space. ($\mathcal{E} = 80, \sigma = 0.4$ mho/m, $\mu = 1$). (Schwan, 1960). The field strength of a transverse electromagnetic wave passing through an isotropic medium is attenuated exponentially with distance (x) by an attenuation factor (α) which increases as the square roots of both the conductivity (σ) and the permeability (μ) of the medium, and as the square root of the frequency (ω) of the wave. The penetration depth (d) in this situation is defined as the propagation distance at which the E-vector has fallen to $1/e$ (=0.37) of its original value (E_o), ie

$$E(x) = E_{(o)}\, e^{-\alpha x} \quad \text{where } \alpha = \left(\frac{\omega\mu\sigma}{2}\right)^{1/2} \text{ nepers/m} \qquad (1.3.1)$$

α is therefore equal to $1/d$, and can also be shown to be equal to $2\pi/\lambda$ where λ is the wavelength in the medium: Mackay (1970).*

Most experimental work on penetration depths in biological tissue has been carried out in the frequency range used for microwave dia-thermy (2450MHz), with particular attention being paid to the heating effects of the absorption process. Such work is well reviewed by Schwan and Piersol (1955). Typical values of penetration depths

* p.436

at 100MHz, however, are quoted by Schwan (1960) as 2.5cm for muscle, 4.0cm for skin, 12cm for fat and 30cm for bone and yellow marrow.

Radiation equations describing the fields produced by small loop antennae immersed in a medium of defined permitivity and conductivity have been developed by Bolie (1962)* to aid the choice of optimum carrier frequencies for implanted devices. He has predicted, by a numerical evaluation based on his analysis, that no serious loss due to tissue absorption should occur to the field at 10cm from a 0.5cm radius loop, excited at 100MHz, and immersed in body tissue. This analysis is, however, based on a constant energising current in the loop. If, as is frequently the case, the radiating loop forms part of a series or parallel tuned circuit, the effect of the conductivity of the surrounding medium is to reduce the Q-factor of the resonant circuit, and thus to reduce the circulating current. As pointed out by Bolie, any boundary across which μ, ε or σ suffers a discontinuity, will require an appropriate auxiliary treatment. Since this is the case where the transmitting antenna is implanted and the receiving antenna is not, the problem of estimating the power loss due to reflection at the body surface remains. This is obviously a situation where reliance must be placed on experimental data, where this is available.

Buchanan et al (1968) have investigated the signal strength polar diagrams obtained from small transmitters operating in the 84 to 108 MHz region, before and after

* p 94-105

implantation in Rhesus Monkeys. They have observed 'no change of consequence' in the polarization and directivity of the radiation field patterns so obtained. Their field strength measurements show a considerable variation in attenuation on implantation, from device to device, but a figure of -3dB is typical. They attribute these results to loading of the oscillator's tuned antenna circuit, rather than to signal absorption by body tissues. Four of the sixteen implants studied produced an 'anomalous' increase in signal strength, typically about +3dB, but up to +6dB in one case.

This anomalous increase in signal strength on implantation in a lossy medium has also been reported by Ko and Neuman (1967) and Mackay (1970)*. A theoretical explanation has, however, recently been produced by Ko et al (1972). They have shown that if a radiating loop is implanted within a conductive sphere, 'resonance' effects occur whenever the loss-tangent of the conductive medium is close to one and the diameter of the sphere approaches the effective wavelength in the medium. For loss tangents greater than one, resonance occurs where the sphere diameter is less than the effective wavelength.

In particular, in a muscle-like medium where the loss tangent at 100MHz is 1.975 and the effective wavelength is 0.282m, an increase in the radiation field strength by a factor of up to 1.75 can be obtained. This effect occurs at a sphere diameter of 0.2m where the loop is unencapsulated, and at 0.4m where the loop is encapsulated in a 3cm diameter sphere of $\varepsilon = 3.5, \sigma = 0$ and $\mu = 1$. (Ko et al, 1972).

* p.355

The work of Schwan (1960), Bolie (1962), Buchanan (1968) and Ko et al (1972), thus supports the author's experience that implantation of small transmitters at 30MHz and at 102MHz, in chickens, results in a small change in signal strength, which has not proved troublesome in practical experimental situations.

1.4 Effect of GPO requirements on Antennae Design

The design of antennae systems for use in biomedical radio-telemetry must be based on the considerations discussed in the previous sections, in conjunction with the GPO requirements.

For Class I devices, the highest permitted carrier frequency is 30MHz, corresponding to a free-space wavelength (λ) of 10m. Since the maximum range of operation is 1.5m which is less than $\lambda/2$, the induction field predominates at the receiving antenna, and omnidirectional reception is, in principle, feasible. Optimum antennae designs are achieved by maximising the capacitative or magnetic coupling between the transmitting and receiving antennae. Operation towards the high frequency end of the permitted band is desirable from this point of view. If a small electric dipole antenna is used, its Q-factor is reduced, on implantation, by the conductivity of the body tissue and its effective length is increased because of the reduced wavelength inside the body. The net effect is that charges appear on the surface of the body, causing it to behave as a lossy dipole of variable geometry. The electric induction field so produced will induce charges on any nearby surfaces, and the carrier signal may be

received by appropriately placed electrodes. Such a dipole will be de-tuned by body movements and the proximity of nearby dielectric materials. It must therefore be driven by a relatively stable carrier frequency oscillator of such power that the resulting carrier amplitude fluctuations can be tolerated.

If a magnetic loop antenna is used, smaller dimensions are in general possible if high permeability ferrite cores are used. As mentioned in the previous section, the major effect of implantation is to reduce the Q-factor of the antenna coil, thus reducing the circulating current. This effect can be minimised by encapsulating the coil in a conveniently large volume of low-loss dielectric material. The high permittivity of the biological medium can cause an increase in the inter-turn capacitance of the coil. This effect is also minimised by encapsulation, and may be further reduced by placing a suitable metallic shield external to the encapsulation and so constructed as to avoid producing a 'shorted' turn around the coil. If the coil is driven from a fixed frequency source, the effect of the residual de-tuning on implantation is to reduce the circulating current still further. If, however, the coil is part of the frequency determining element of the oscillator, the effect is to reduce the frequency of operation. For Class I devices, this can usually be tolerated because of the wide range of permitted operating frequencies.

The optimum receiving antenna for such a coil takes the form of a loop of wire in the plane of the transmitting

loop. If this cannot be arranged, the two planes should be parallel. The optimum loop diameter is then equal to the separation beween the planes: Mackay (1970)†. A circular loop of about 1.5m radius (ie circumference $\approx \lambda$) would be self resonant at 30MHz. Loops of smaller diameter than this will appear inductive and may be series resonated with a capacitor to improve their matching to the low-impedance aerial terminals of conventional receivers. Reception close to a long wire, or a matrix of long wires or loops, is also possible.

Class II devices do not have to be implanted but are intended to be used with an integral antenna. This is interpreted by the GPO* Radio Regulatory Division[4] to mean that the antenna must be contained within the body of the transmitter, and the use of a whip antenna is precluded. Considerations of space available within any practical device once again favour the use of a small loop antenna. The toroidal radiation field pattern of a small loop is such that, if the plane of the loop can be maintained approximately horizontal, uniform radiation in a horizontal plane can be achieved. A suitable receiving antenna could then be a horizontal electric dipole, as the radiation field E-vector is horizontal in this situation.

The transmitting antenna considerations for Class III devices are essentially the same as for Class II devices, viz. an integral antenna must be used. The permitted range of operation is, however, about thirteen times greater than that of a Class II device.

* now HO[34].
† p. 231.

On the basis of preceding sections, a small loop antenna, probably incorporating ferrite materials, best fulfils the requirements of Class I, Class II and Class III operation, where work with small animals is involved. Such a loop will operate, for Class I devices, as the primary winding of a loosely coupled transformer, and omnidirectional reception is in principle possible. Omnidirectional reception of a Class II or III device can be achieved if a 'spinning field' can be generated. This can be accomplished if a second resonant loop is mounted perpendicular to the first, and driven 90^{o} out of phase. This can be achieved by 'critical' coupling of the two coils: Mackay (1970).*

1.5 An RF Oscillator

In all physiological and behavioural experiments, it is important that the use of radio-telemetry does not adversely affect the environmental conditions of the subject. For instance, in the study of battery hens, the birds 'natural environment' is a cage of small dimensions (usually less than 0.75m). The limited range of a Class I transmitter is therefore no problem, as the receiving antenna may consist of a loop of wire around the cage. Birds housed in deep-litter or free-range conditions are free to roam over wider areas, and the increased range permitted under Class II or III conditions would be highly advantageous.

As mentioned in the previous section on Implantation of Antennae, a small shift of carrier frequency can usually be tolerated of a Class I device, because of the

* p.237

wide range of permitted operating frequencies. The antenna coil may therefore form part of the frequency determining network of the carrier oscillator. For Class II devices, the relatively narrow bandwidth available (150kHz), means that careful consideration must be given to the frequency deviation (Δf) and message bandwidth (f_m) used, to ensure that any carrier frequency drift will not cause significant emissions outwith the permitted band. It is therefore necessary to minimise or characterise any frequency shift after implantation.

Class III devices are permitted the greatest range, but the required carrier frequency stability is such that crystal control of the RF oscillator is virtually essential. The maximum frequency deviation which can be produced in a crystal controlled oscillator is a function of the mode of oscillation of the crystal. In general, the higher the overtone of oscillation of the crystal the less is the percentage deviation that can be produced. (H.M. Brash, Personal Communication).

100MHz crystals using bulk piezo-electric effects typically operate in the third or fifth overtone mode and insufficient deviation is available for wideband FM. Class III transmitters, therefore, generally use a low-frequency, fundamental-mode crystal oscillator, followed by a number of frequency multiplier stages, to produce the required carrier frequency. Typical examples of this design approach are described by Castelfiori and Dubini (1972) and by Stalberg and Kaiser (1972).

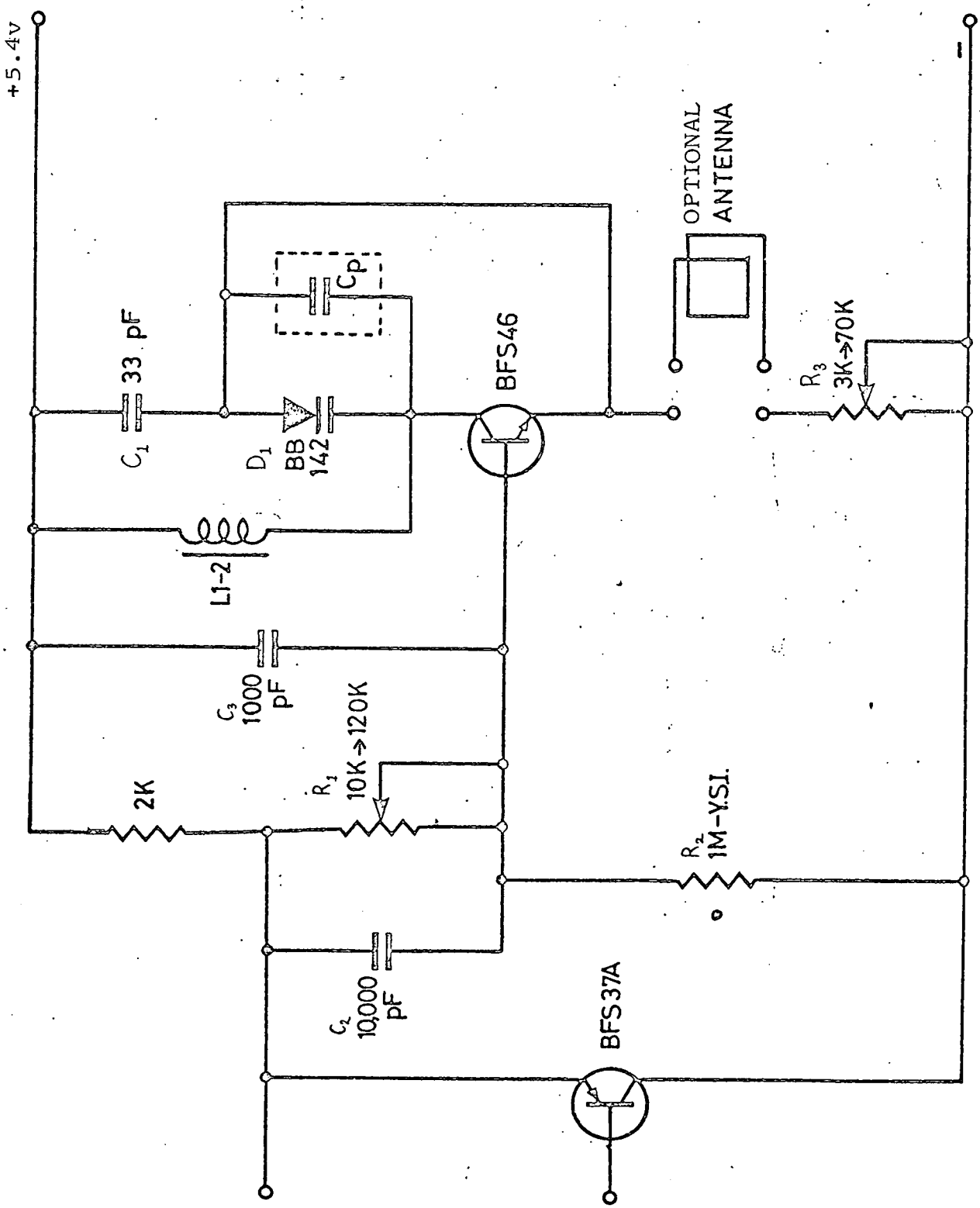

Figure 1.5.1 Colpitt's Oscillator : Schematic Diagram

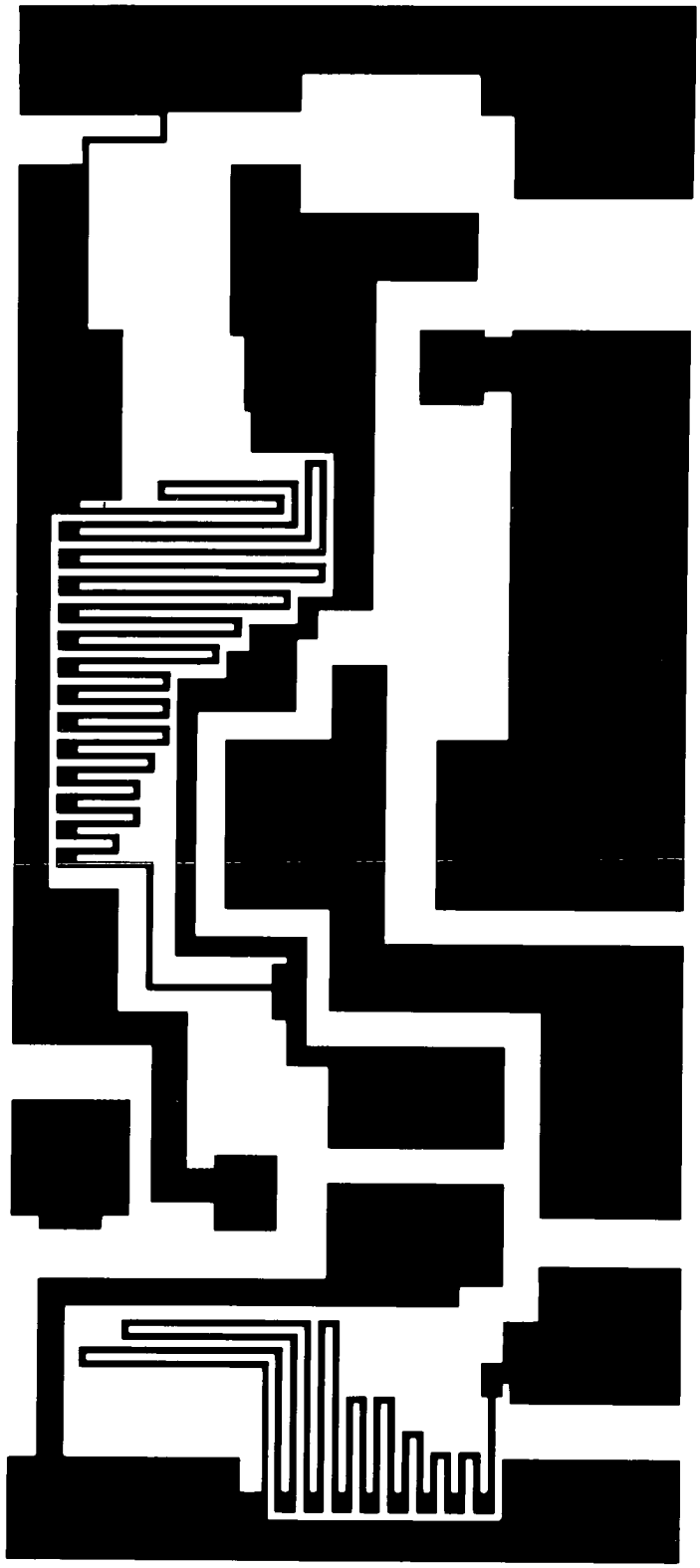

Figure 1.5.2 Colpitt's Oscillator: Thin Film Layout

Such transmitters are invariably too large and consume too much power to be considered for implantation in small animals. This situation may, however, change as oscillators based on Surface Acoustic Wave (SAW) devices become available. Such oscillators can have frequency stabilities approaching that obtainable from conventional bulk crystal oscillators and are capable of direct wideband FM generation (Lewis, 1973). An SAW device suitable for Class II operation is currently under development at the Royal Radar Establishment[5], Malvern, but samples will not be available for evaluation until 1975.

An RF oscillator capable of driving small loop antennae in accordance with Class I and II conditions was therefore developed and laid out in thin-film form by the author, in cooperation with Dr. J.H. Filshie of the Poultry Research Centre. A schematic diagram of the oscillator is shown in Figure 1.5.1. The Thin Film layout, on a substrate size of 0.5 inches x 0.25 inches, is illustrated in Figure 1.5.2. Frequency modulation of this oscillator is achieved by the application of a message waveform to a varicap diode (D1) in the frequency determining network. C_1 serves as a DC blocking capacitor for the varicap bias voltage and, in conjunction with the diode capacitance of around 11pF, provides a feedback factor of about one-third, while reducing the RF voltage swing across D1 by the same factor. This results in a reduction of the carrier distortion that is otherwise introduced where the RF voltage swing across D1 is significant compared with the reverse DC bias voltage. The author has relied heavily on the results of

investigations (presently unpublished) by Dr. Filshie into the linearity of this modulation technique and the carrier distortion introduced. Typically, second and third harmonic levels are measured on an Airmec[6] Wave Analyser Type 853, as more than 25dB down on that of the unmodulated carrier. Typical modulation sensitivity is 13kHz/mV at 102MHz.

The power output of the oscillator can be altered by means of the ultrasonic wire-bonding options provided on R_3.

Practical experience of implanted use of this oscillator has been gained at 27 to 30MHz and at 102.36MHz. In both cases the antennae used consisted of a few turns of 36 SWG copper wire wrapped around a 4mm diameter Aladdin[7] former Type 8A-4387 (fitted with a 6mm Aladdin 'R7' grade ferrite slug). Resonance in the 27 to 30MHz region was obtained with 11.5 turns, and resonance at 102.36MHz was obtained with 3.5 turns. Typical Q-factors obtained were 138 at 30MHz and 25 at 102.36MHz. These values fell to 124 and 20 respectively when the coils were embedded in the paraffin wax mixture described in section 3.8. The R7 grade material is not intended for operation above about 50MHz, and lower high-frequency losses should be possible using R9 grade cores. It has not proved possible to obtain these as yet but data published by Aladdin indicates that Q-factors of 50 to 60 should be possible using R9 cores at 100MHz.

Antennae coils such as these have a positive temperature coefficient of inductance leading to a decrease in

centre-frequency on implantation. This effect is minimised by deriving the varicap bias voltage from a potential divider which includes a thermistor (R_2) with a negative temperature coefficient of resistance. Provision of ultrasonic wire-bonding options on R_1 enables a wide range of positive antennae temperature coefficients to be equalised.

The Class I devices gave satisfactory reception when implanted sub-dermally in chickens and run on a supply voltage of 4.35 volts at currents of about 120μA in the RF transistor. The chickens were kept in experimental cages measuring 40cm x 45cm x 55cm high and the receiving aerial was a loop of wire around the cage, series tuned with a 3-30pF beehive trimmer. A Dynatel[8] DRT3 receiver was used. The required transmitter power for an acceptable signal-to-noise ratio at the receiver output is a function of the level of electrical interference present. In one particularly noisy environment currents of about 400μA were required for satisfactory reception.

The Class II devices operate in a frequency band which is much quieter, and is moreover restricted for use in biomedical telemetry. This, together with the increased efficiency of the small antennae coils at this higher frequency, gives a greatly increased range for a given power consumption. Typical devices operating on a 4.35v supply, and drawing about 820μA, give a range of about 25m when used at 50kHz deviation, in conjunction with a Leak Delta FM receiver fitted with a half-wave dipole antenna. In many applications, the size of the transmitting antenna

may be increased considerably, resulting in much reduced power consumption for a given range. The above figures on power consumption are therefore almost 'worst case' conditions, and a considerable improvement is anticipated when R9 grade ferrite cores become available.

When implanted, these devices have been powered by battery packs consisting of three mercury cells (Mallory[9] type RM 675H). The cells are each 11.56mm diameter by 5.4mm high and have a capacity of 170mAh. These particular cells were chosen as they have the highest capacity per unit volume of the manufactured range. The battery packs weigh about 10gm when fully encapsulated for implantation. The actual life of a 200μA transmitter powered by such a battery pack is usually observed to be about 75 to 80% of that calculated from the published capacities of the batteries. This reduction is associated with the unknown and variable time elapsing between the manufacture and use of the cells, rather than with leakage effects on implantation.

The encapsulation appears quite satisfactory in use, and will be described in section 3.8.

CHAPTER 2

MULTICHANNEL TELEMETRY

2.1 Biological Variables

Considerable insight into animal physiology can be gained from the continuous monitoring of a single physiological parameter. This can allow normal levels to be established, together with typical deviations from these levels. Considerably more information can be gained if these variations can be correlated with observed behaviour patterns, or changes in the environment of the subject. Typical experiments therefore involve establishing the 'transfer function' of the subject by changing the system inputs, eg environmental conditions and diet, while observing the resulting system outputs, eg body and skin temperature, respiration and heart rate. The complexity of the biological system is such that a change in a single input parameter will typically cause changes in a number of physiological parameters. The requirement for a multi-channel telemetry link arises whenever two or more parameters of interest cannot be readily assessed by the observer without disturbing the experimental conditions. In this case, a multi-channel telemetry system can enable correlations between the physiological parameters to be confidently assessed without the need for complex and repetitive experimental procedures, which themselves may invalidate the results obtained.

For example, studies of the 'fight/flight' syndrome in Gallus Domesticus as described by Duncan et al (1974) would be facilitated if skin temperature and heart rate variations were simultaneously available from unrestrained birds. Another subject currently of interest to poultry researchers is the level of stress experienced by birds housed in battery cages, compared with that experienced by free range birds and those housed in deep litter pens. One approach here is to monitor parameters known to be correlated with stress in other less inscrutable animals. No single parameter, however, provides a reliable index and again an implantable multi-channel system would be helpful.

Consideration will now be given to the frequency and amplitude range of some typical biological parameters, with a view to establishing the feasibility of multi-channel telemetry, within Class II constraints.

The great majority of biological events occur fairly slowly. The lowest frequency events are associated with deep-body temperature variations, the action of the respiratory system, chemical activity and internal pressure variations. For these, a frequency response extending to DC is required of the data link. Low frequency events are also encountered in electrical bio-potential measurements associated with the action of the heart, brain and smooth muscle. These bio-potential measurements, however, are complicated by the low amplitudes of the signals observed, where remote electrodes are used, and by the

relatively high and variable bias potentials associated with the tissue/electrode interface. These factors generally place impractically high requirements on the dynamic range of the measuring equipment. Bio-potential preamps are therefore generally AC coupled, with input time constants of from 1 to 5 seconds.

The highest frequency events are encountered in myo-electric activity, particularly if sub-cutaneous electrodes are used. For this application responses extending to 500Hz or very occasionally 2kHz may be required. Transient components as high as 200Hz are observed in the EEG signal recorded from scalp electrodes, although the bandwidth of clinical significance extends at present from about 1Hz to about 30Hz. Fourier analysis of the fairly rapid avian ECG (typically about 330 beats/minute) has recently revealed 85% of the signal power to lie below 100Hz. (J.H. Filshie: Personal Communication). Data bandwidths of less than a few hundred Hertz are therefore required for the great majority of biological parameters presently of interest.

The lowest values of clinically significant bio-potentials are generally agreed to be present in the EEG waveforms recorded from scalp electrodes. (Dummermuth, 1970). Components of about 10μV amplitude may be of interest, although the signal is typically of around 50μV peak to peak. Larger signal amplitudes up to about 200μV may be obtained from cortical electrodes.

The peak to peak amplitude of the QRS complex of the avian ECG signal is typically in the region of 180μV, as

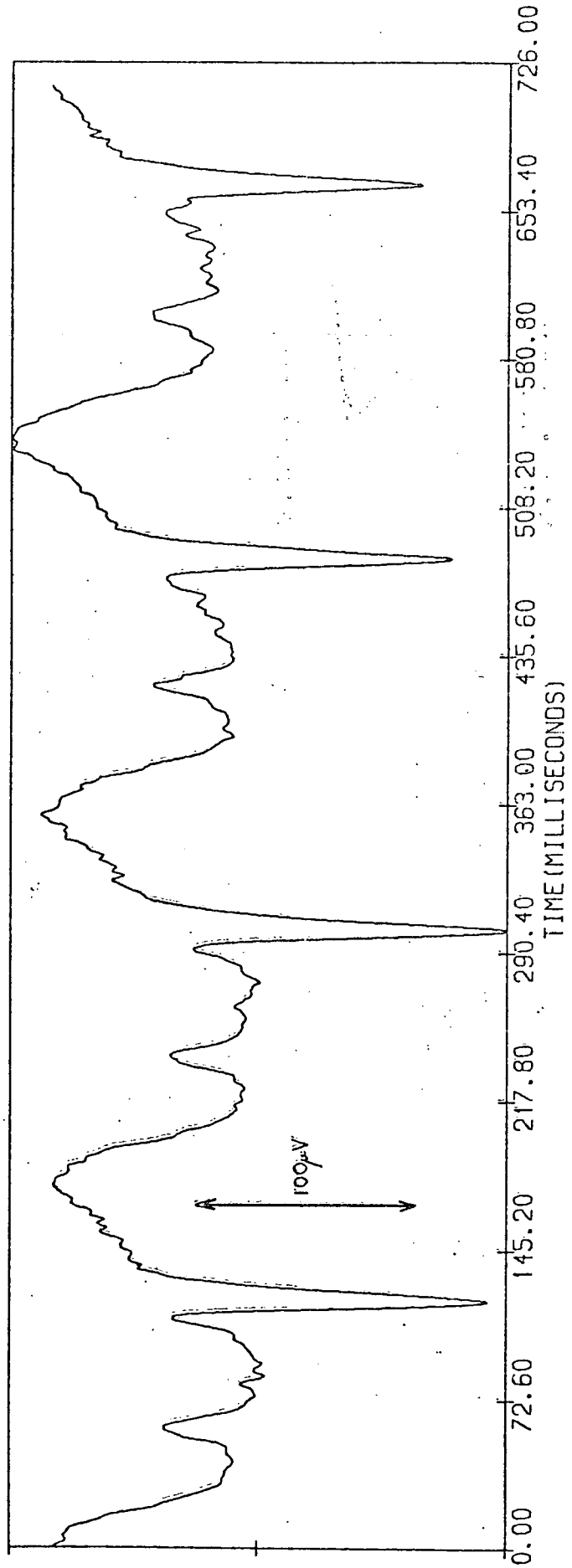

Figure 2.1.1 Avian Electro-Cardiograph Signal

PARAMETER	FREQUENCY	SIGNAL LEVEL
HUMAN		
Body Temperature	DC to 0.1 Hz	35 to 40°C
ECG	0.1 to 100Hz	0.75 to 4mV
EEG	0.5 to 100Hz	10 to 100μV
EMG	10 to 200Hz	0.1 to 4mV
Pulse Rate	0.5 to 4Hz	40 to 210/min.
Blood Pressure	0.5 to 100Hz	0 to 250 mm Hg.
Respiratory Flow	DC to 10Hz	0 to 250 l/min.
Respiratory Rate	0.1 to 4Hz	8 to 150/min.
Stomach pH	DC to 0.1Hz	
AVIAN		
ECG	0.6 to 200Hz	+50 to 200μV
EEG	0.6 to 100Hz	100μV
Deep Body Temp.	DC to 0.1Hz	38 to 43°C
Skin Temperature	DC to 0.1Hz	30 to 40°C

Figure 2.1.2 Physiological Variables

detected by sub-cutaneous silver wire electrodes spaced a few cm apart, close to the heart. Figure 2.1.1 shows a typical time averaged avian ECG signal obtained from an implanted single channel transmitter.

Potentials in excess of a millivolt may be induced in surface electrodes from the contraction of large muscle masses and by the action of the human heart.

Typical values for a range of physiological variables have been collated from a large number of sources and are presented in Figure 2.1.2. A final point relevant to the design of biological telemetry systems is that in many cases a high precision of measurement is not required and data with even 10% error may still be highly significant. Absolute accuracies of better than 1% (equivalent to a signal-to-noise voltage ratio of 40dB in an analogue channel) are rarely required.

2.2 Receiver Performance

The information content of typical biological signals will now be compared with the capacity of a Class II telemetry channel. The base-bandwidth (f_m) and signal-to-noise ratio available at the receiver output are a function of the RF modulation parameters used and the performance of the receiver.

A peak frequency deviation (Δf_c) of 50kHz, and a limit on 'significant emissions' of 150kHz, define the available RF channel. Some receiver performance specifications are listed in the GPO regulations, but as yet (December 1973) no commercially manufactured radio

receivers have received GPO type approval for Class II applications, and the majority of telemetry users operating at 102MHz in the UK do in fact use standard broadcast receivers, which cover the range 88-108 MHz.

The IF bandwidth and discriminator characteristics of such receivers are tailored to suit the reception of standard VHF broadcast transmissions where a peak frequency deviation (Δf_c) of 75kHz is used. A substantially flat baseband response extending to 15kHz for monophonic broadcasts, is available from these transmissions, ie a Modulation Index (D) of 5 is used. Since the frequency spectrum of such a transmission is infinite in extent, any practical definition of bandwidth occupancy must be fairly arbitrary. A general approximate rule of thumb attributed by Rowe (1965)* to J.R. Carson (1937) states that satisfactory reception may be achieved over a transmission bandwidth equal to twice the peak carrier deviation ($2\Delta f_c$) plus twice the frequency of the highest frequency component of the modulating signal ($2f_m$). This rule is widely used in IF filter design, and apparently gives satisfactory results for systems with a Modulation Index (D) = 5, when combined with the additional moderate bandwidth allowances made for local oscillator drift. (Sunde, 1969). If this criterion is applied to a standard broadcast transmission, the predicted 'bandwidth occupancy' is

$$2\ (\Delta f_c + f_m) = 2\ (75 + 15) = 180\text{kHz}$$

* p 103

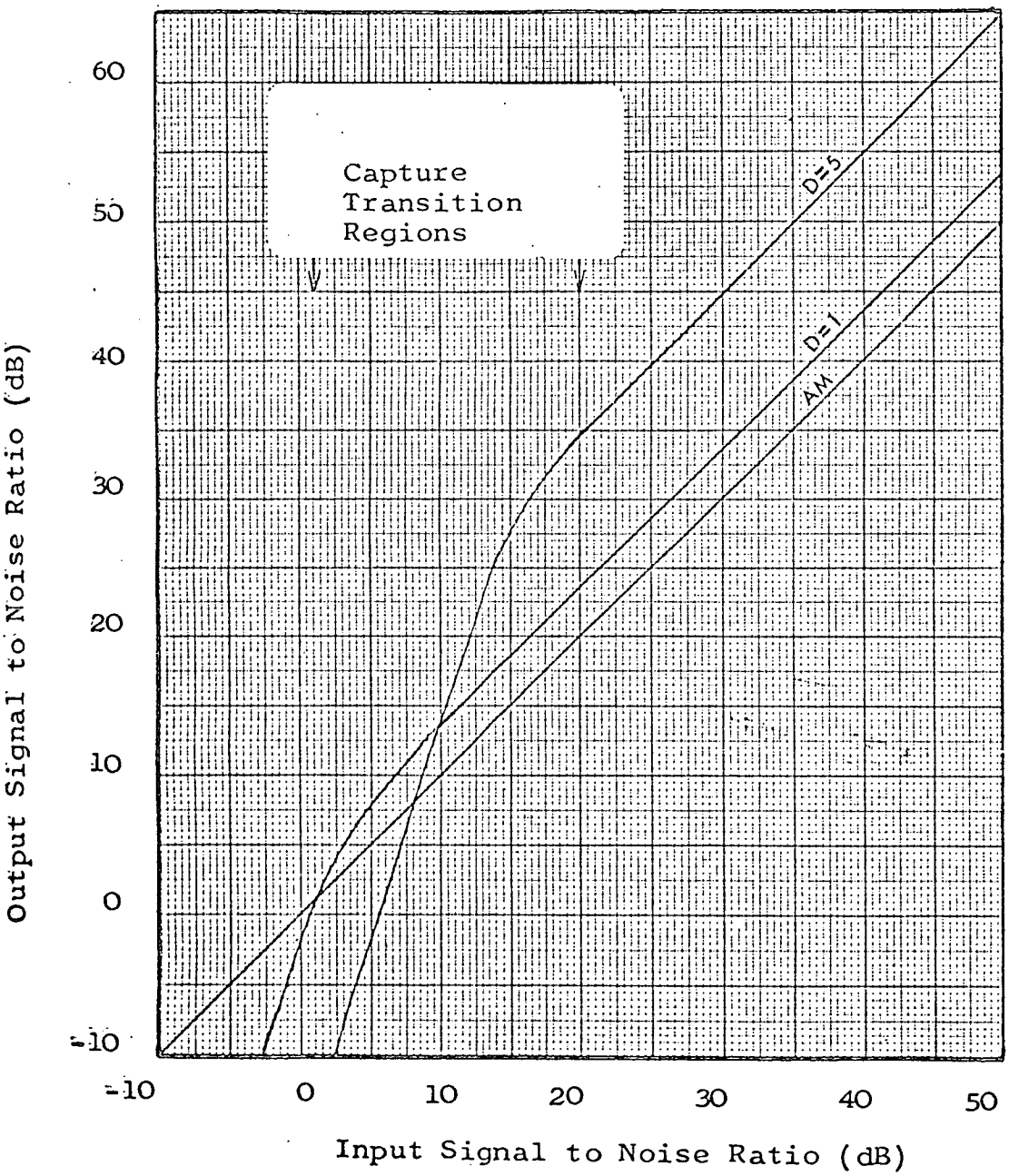

Figure 2.2.1 FM Receiver Threshold Performance

Alternatively, if the transmission bandwidth is such as to pass unattenuated all sideband components of amplitude greater than 1% of that of the unmodulated carrier, then for D = 5 there are eight 'significant' sideband components dispersed symetrically on either side of the carrier, and the bandwidth is given by $2 \times 8 \times f_m$ = 240kHz. (Schwartz, 1959).*

Investigation of some commercially available VHF broadcast receivers has shown a considerable variation in the IF bandwidth used. The narrowest was found to be that of the now discontinued Leak 'Troughline' receiver, where the linear portion of the discriminator characteristics extends over only about 150kHz.

The majority of cheaper mono-receivers (eg Sinclair[10] Henry's Radio[11]) and the Mullard[12] Modules LP1186 and LP1185, are designed for 250 to 300kHz, while the Leak 'Delta FM', designed for stereo-reception, uses a 600kHz IF bandwidth.

The signal-to-noise ratio at the output of an FM receiver is a function of the signal strength available at the aerial input, and the modulation parameters of the transmission. The curves of Figure 2.2.1, based on results obtained by Crosby (1937) and Downing(1964)† reveal the general form of the relationship and show the threshold effect typical of wideband FM systems. The region of these curves between the noise threshold and the threshold of maximum FM improvement is known as the capture-transition region, and occurs where the carrier and the noise are of comparable power. For band-limited

* p305
† p105

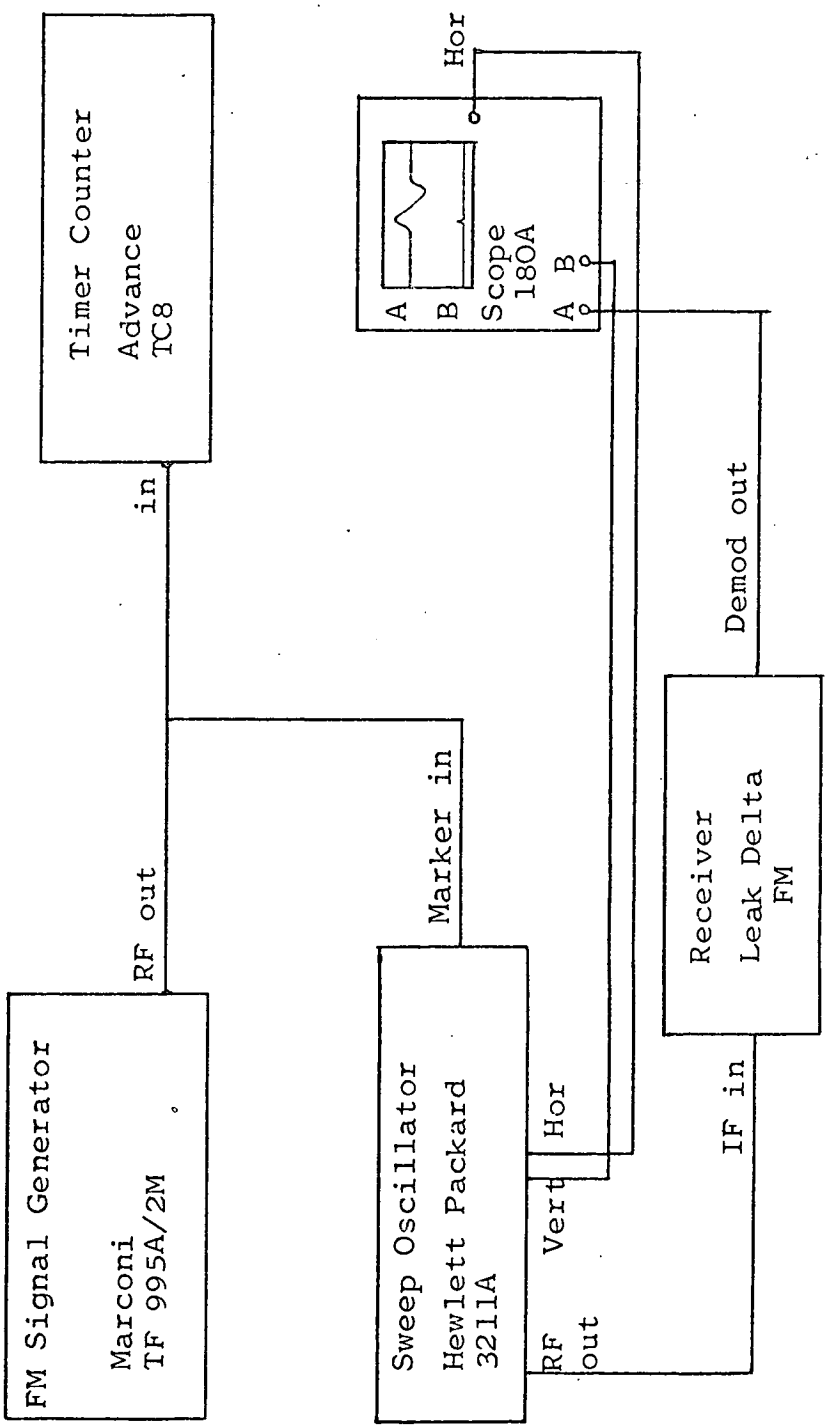

Figure 2.2.2 Measurement of Threshold Characteristics

Gaussian noise, the amplitude probability curve is a Rayleigh Distribution, and the range of input signal amplitude required to move from the noise threshold to the maximum-improvement threshold has been shown by Panter (1967)* to be about 4dB.

At input signal levels above the threshold of maximum FM improvement, the use of an IF bandwidth much wider than that of the transmission causes a wider noise bandwidth at the discriminator output. Since this noise spectrum is restricted by the post-detection baseband filter, only those noise components within the band $f_{IF} \pm f_m$ contribute to the output, and no severe reduction in output signal-to-noise ratio is caused by the wider IF bandwidth.

If the input noise spectrum to the IF strip is assumed to be flat, then the noise power applied to the discriminator is proportional to the IF bandwidth. Consequently, the use of an IF bandwidth much wider than that of the message spectrum might be expected to result in an increase in the input signal level necessary to reach the improvement threshold.

The threshold performance of the 'wideband' Leak Delta FM tuner was therefore investigated using the experimental set-up illustrated in Figure 2.2.2. For large IF input signal amplitudes the entire discriminator response is displayed on the oscilliscope. As the input signal amplitude is reduced, the characteristic breaks into noise at the extremes of the response curve. The

* p 432

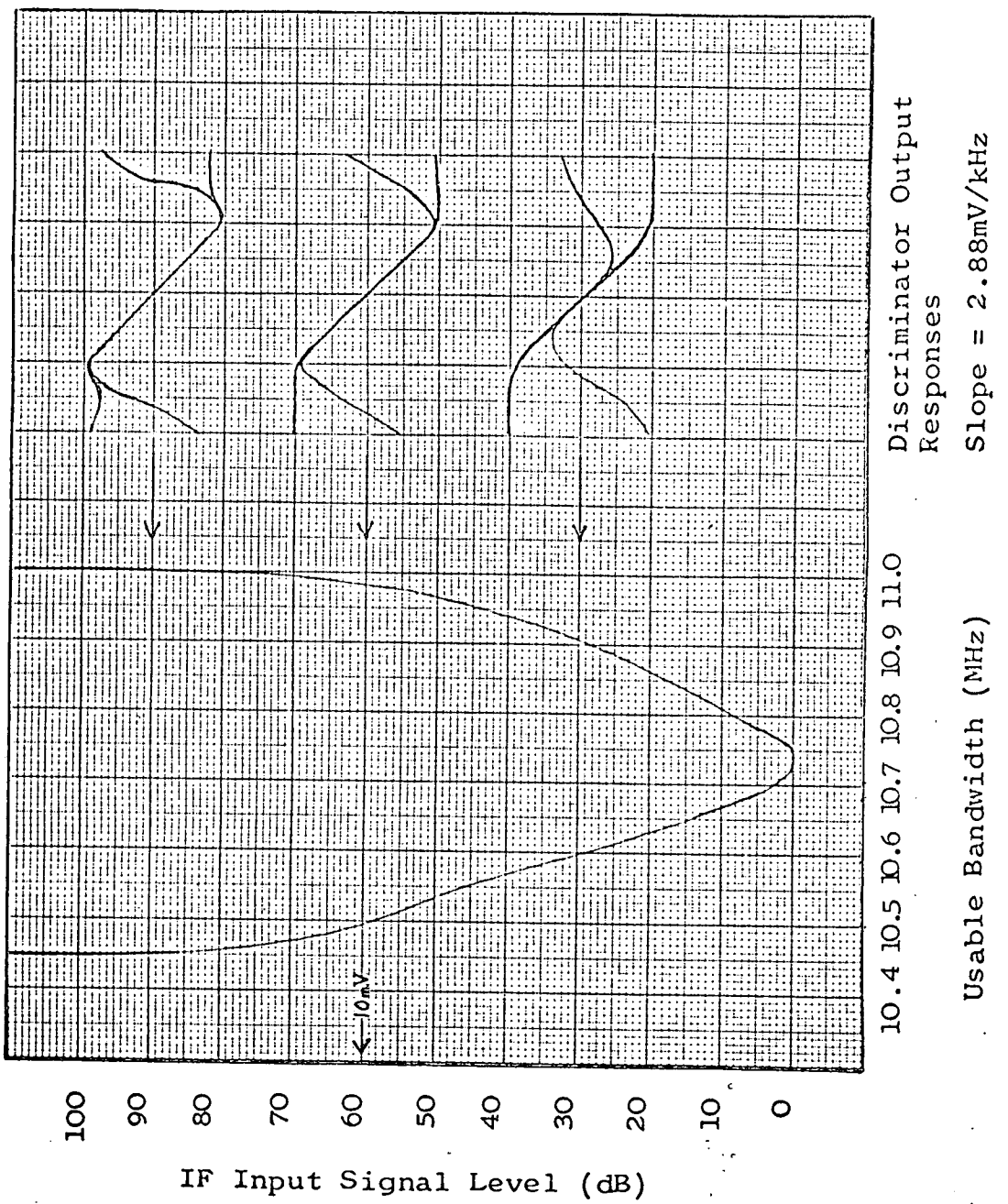

Figure 2.2.3 Threshold Performance of Leak Delta FM Tuner

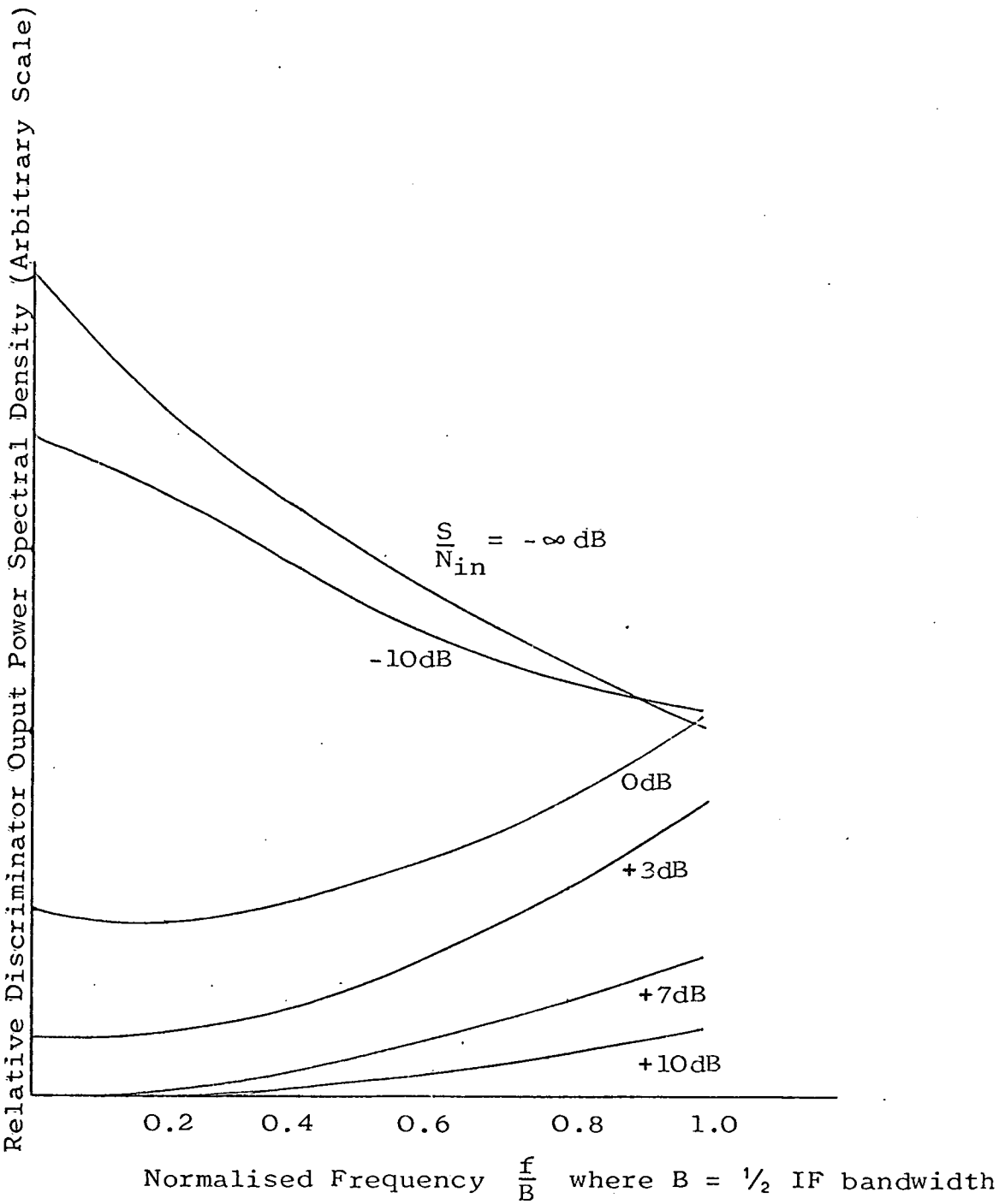

Figure 2.2.4 FM Baseband Noise Power Spectra

range of Δf over which satisfactory capture performance is achieved, is therefore reduced. Figure 2.2.3 shows the results obtained. This performance is obtained because of the use of a linear-phase characteristic in the IF bandpass filter. This is usually justified by the need to minimise phase distortion in the IF strip, which would result in distortion of the demodulated output. A consequence of this is that the resulting amplitude/frequency response of the IF strip deviates considerably from the rectangular 'zonal filter' response so frequently used in theoretical analyses of FM receiver performance. The broad 'low Q' frequency response obtained from the linear-phase filter ensures that large deviation signals are attenuated by the skirts of the IF response, and require a large amplitude input signal for satisfactory capture performance in the discriminator. Conversely, narrow-band signals are passed with virtually no attentuation through the centre of the IF filter response and much lower input signal amplitudes are required for satisfactory capture performance. Figure 2.2.3 represents the situation occurring at the discriminator output, ie before the noise spectrum is modified by the subsequent base-band filter and de-emphasis network.

The curves of Figure 2.2.4 redrawn from Downing (1964)* show that the discriminator noise output power spectrum is parabolic above the maximum improvement threshold and the resulting dominant high frequency noise components are attenuated by the base-band filter. In the capture

*p 104

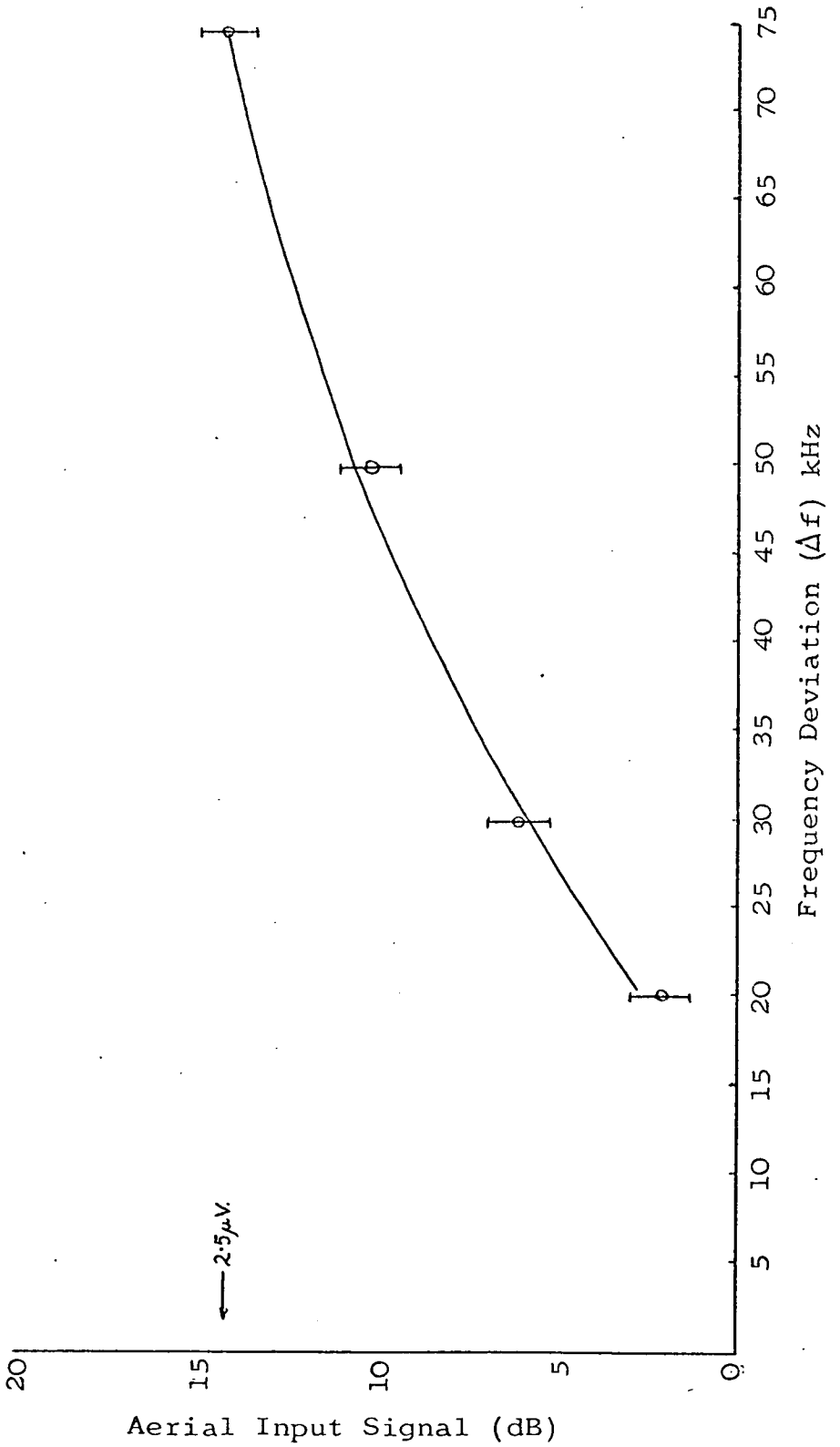

Figure 2.2.5 Narrowband Threshold Reduction - 'Delta FM' Tuner

transition region, however, the impulsive nature of the discriminator output noise causes a flattening of the parabolic power spectrum and results in significant noise components within the pass-band of the base-band filter.

The resulting overall performance of the Leak Delta FM tuner was investigated using a Marconi[13] VHF-FM signal generator type TF995A/2M connected to the aerial input, and a Hewlett Packard[14] HP180 oscilliscope fitted with a type 1801A plug-in connected to the demodulated output. The aerial input required for threshold operation (ie a 30dB output signal-to-noise ratio), was determined as a function of Δf_c.

These results, plotted in Figure 2.2.5, show that because of the threshold reduction to be obtained with narrow band transmissions, no severe reduction in overall system performance is anticipated due to the use of a 'broad-band' entertainment receiver for reception of the Class II transmission.

It is now necessary to consider what choice of modulation parameters available within the Class II constraints, will make best use of the available RF bandwidth.

2.3 Class II Modulation Parameters

Because of the non-linear (exponential) modulation process involved in the generation of an FM wave, the resulting RF spectrum consists of an infinite number of upper and lower sideband components, separated in the frequency domain by all integral multiples of all the modulating frequencies, and all orders of intermodulation

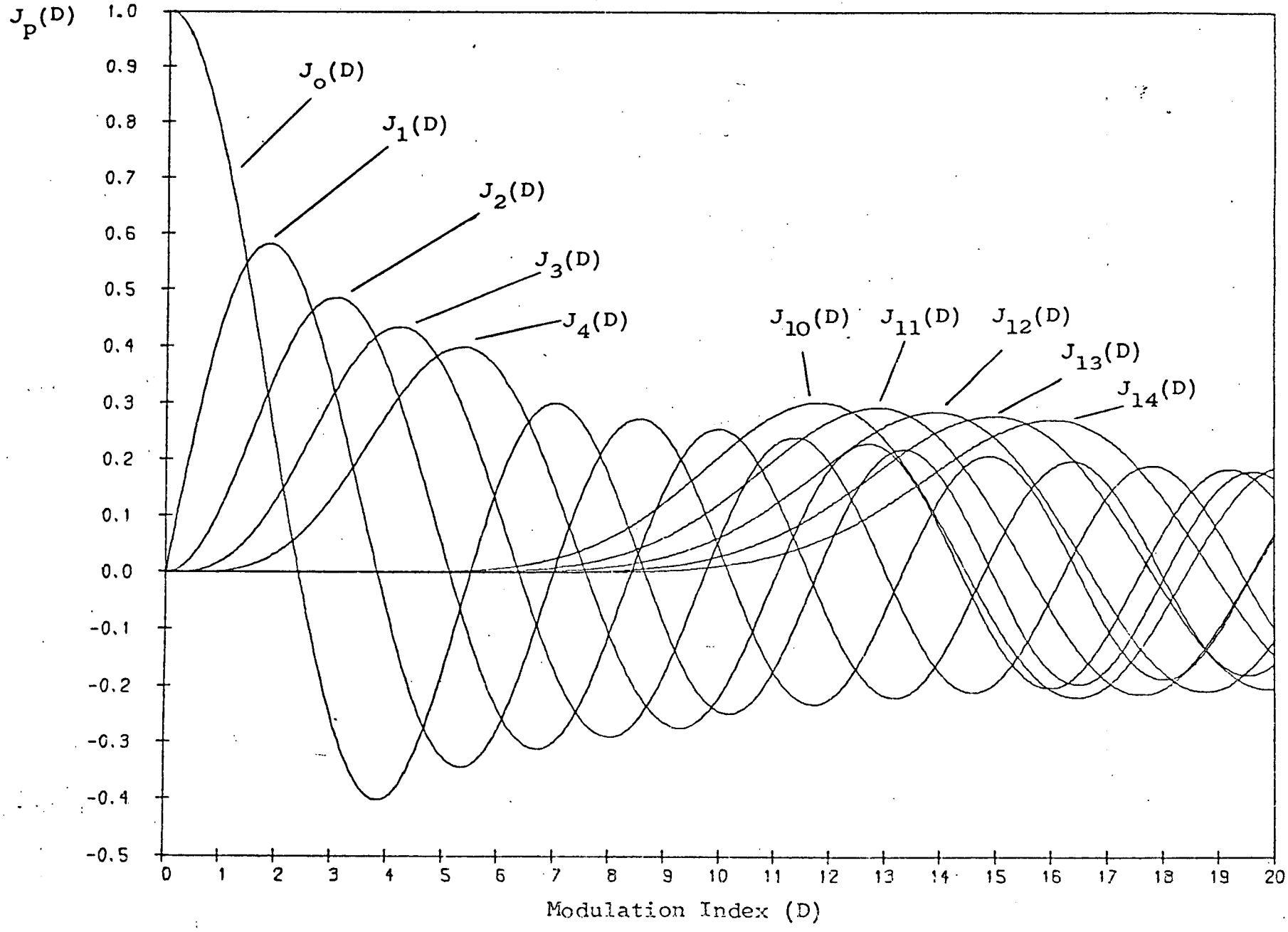

Figure 2.3.1 Bessel Functions $J_p(D)$

products of these frequencies. In the case of modulation by a single sine wave, the amplitudes of the resulting sideband components are described by the set of Bessel Functions ($J_p(D)$) of the first kind, of order (p) and argument (D), the modulation index. (Schwartz, 1959).* Any band-limiting operation performed on this spectrum must result in distortion of the original message waveform, except that 'n'th harmonic distortion caused by the elimination of sideband components due to modulating frequencies greater than $f_m/_n$, will be attenuated by the post-detection base and filter.

Reference to a plot of the relevant Bessel Functions $J_p(D)$, reproduced in Figure 2.3.1, shows that for $D \ll \frac{\pi}{2}$ the only functions of significant amplitude are $J_o(D)$ and $J_1(D)$ representing the amplitudes of the carrier and the two first-order sidebands respectively. Carson's Rule obviously applies in this situation.

With increasing Modulation Index (D), the magnitudes of the higher order Bessel Functions become significant and the number of significant sideband components begins to increase. The higher order Bessel Functions ($p > 20$) are essentially zero for $D < p$, and the number of significant side-band components becomes approximately equal to D. The 'significant' bandwidth for large D then becomes approximately equal to $2\Delta f_c$, and Carson's Rule again provides a reliable estimate of bandwidth occupancy.

For more practical values of D the bandwidth required can be obtained by counting the number of sideband

* pp 120-129

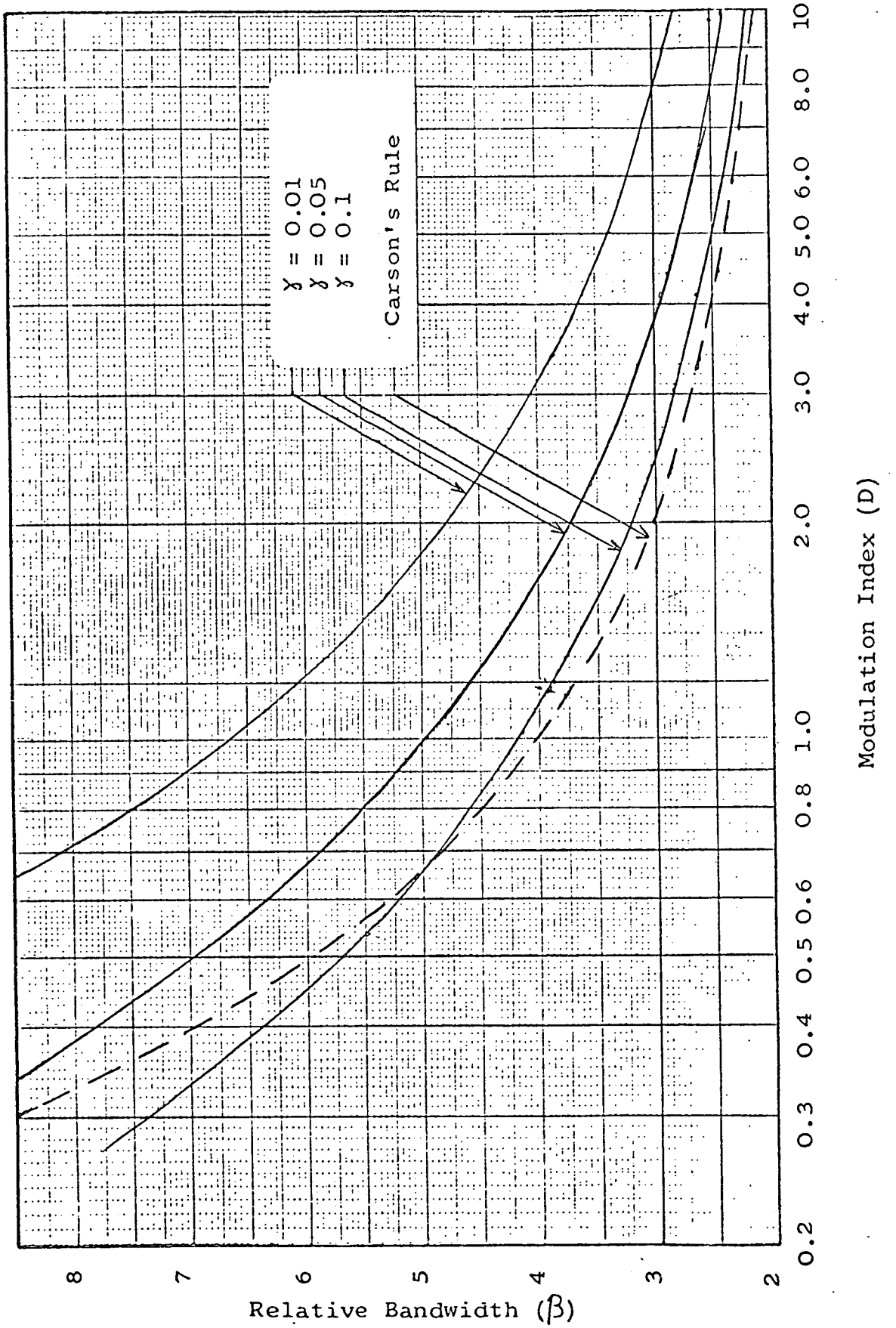

Figure 2.3.2. Bandwidth Requirements in F.M..

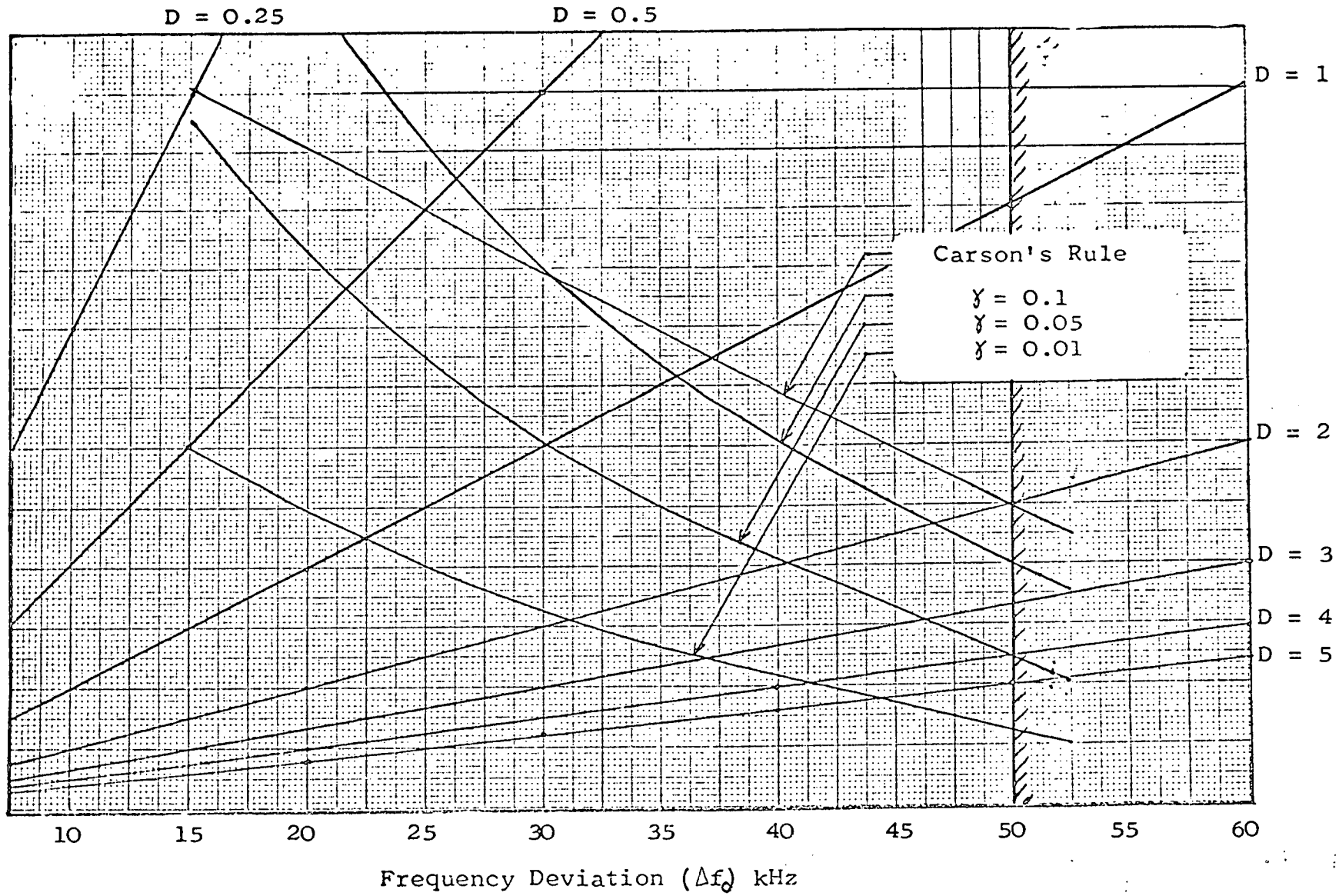

Figure 2.3.3 Available Bandwidth in Class II

components of amplitude greater than some chosen fraction (γ), of that of the unmodulated carrier, since these components are dispersed symmetrically about f_c at intervals of f_m. The resulting estimate of bandwidth occupancy is consequently a function of the definition of significance used.

The computations involved in the estimation of signal bandwidth (B_m), from tables of Bessel Functions have been performed by Downing (1964) who defines the term Relative Bandwidth (β) as:

$$\beta = 2p \frac{B_m}{\Delta f} = \frac{2p}{D} \qquad .. \quad 2.3.1$$

where p is the order (not necessarily integer) of the highest order Bessel Function exceeding the criterion of significance used (γ).

Downing (1964)* has presented this data graphically, as a plot of β as a function of the Modulation Index D for various values of γ. Superimposition of the Bandwidth occupancy curve obtained from Carson's Rule shows that, over a fairly wide range of Modulation Index D, Carson's Rule approximates closely to the criterion $\gamma = 0.1$. These data, redrawn from Downing, are presented in Figure 2.3.2.

Since the GPO specifications do not state the definition of significance to be used in interpreting their regulations, the data of Figure 2.3.2. has been used to estimate the base-bandwidth (f_m) available, within the Class II constraints of $\Delta f < 50$kHz and $B_m < 150$kHz, for various values of γ. These data are presented

* p 91

graphically in Figure 2.3.3. Thus use of the maximum permitted Δf of 50kHz, will allow transmission of a base-bandwidth of 25kHz, if Carson's Rule is applied. Application of more stringent definitions of 'significance' will reduce this to 6.25kHz for the 1% criterion. Reduction of Δf is seen to increase the available base-bandwidth, but this will cause a reduction in the output signal-to-noise ratio, as indicated in Figure 2.2.1.

2.4 Modulation and Multiplexing Techniques

The factors influencing the base-bandwidth and signal-to-noise ratio available from a Class II radio-telemetry link have been examined in the preceding section (2.3). The conclusions indicate than an important factor is the definition of 'significant emissions' used in interpreting the GPO regulations. Since the regulations are in many ways restrictive, it seems reasonable to take advantage of their ambiguity on this point, and to adopt Carson's Rule as the least restrictive definition of significance, especially since it is widely accepted for other applications. (Downing, 1964).*

If this is done, section 2.3 indicates that the Class II channel capacity should be adequate for simultaneous transmission of a small number of biological signals. This may be achieved by one of a large number of possible frequency and time division multiplexing techniques. The actual number of signals that can be handled will depend on the bandwidth and signal-to-noise ratio required of each, and on the efficiency of the multiplexing technique employed.

* p90

Frequency Division Multiplexing (FDM) techniques involve modulation of some property of a sub-carrier signal, eg. frequency, amplitude, phase, and the combination in the frequency domain of a number of such signals, prior to transmission.

Time Division Multiplexing (TDM) techniques involve modulation of some property of a pulse train, eg. amplitude, duration, position and the combination in the time domain of a number of such pulse trains, prior to transmission.

It is therefore necessary to consider the performance of the many available modulation techniques. This assessment must cover both their communication efficiency, and the practicability of providing the necessary circuitry to permit multi-channel operation within the constraints of size, power-consumption etc., dictated by the need for chronic implantation of the transmitter assembly within a relatively small animal.

The performance of practical information transmission systems is limited by two basic constraints. These are the inability of any restricted bandwidth system to respond instantaneously to a step-function input, and the inability of any real system to distinguish small level changes due to inherent noise generating mechanisms. These imply an upper limit on channel capacity (C), given by Shannon (1948) as:

$$C = \frac{1}{\tau} \log_2 n$$ where τ = system response time
n= number of equally probable distinguishable signal levels

The response time (τ) is proportional to the reciprocal of the system bandwidth (B) and:

$$n = 1 + \frac{S_v}{N_v}$$ where S_v = signal voltage, N_v = noise voltage

hence:

$$C = B\log_2 (1 + h)$$ where h = signal-to-noise voltage ratio

If this expression is applied to the input and output of an ideal demodulator (ie, one which does not restrict the channel capacity) then:

$$h_o = h_i^{\frac{B_i}{B_o}}$$ where the subscripts 'i' and 'o' denote the input and output parameters respectively and h_i and h_o are $\gg 1$.

This exponential relationship between h_o and B_i represents the ultimate exchange law between signal-to-noise voltage ratio and channel bandwidth.

The communication efficiency of any practical modulation technique may be similarly expressed by the law which relates its output signal-to-noise ratio to its relative bandwidth occupancy.

For AM, PAM, PM and narrow-band FM ($D \ll \frac{\pi}{2}$) the RF bandwidth is equal to $2f_m$, and all noise components within the band contribute equally to the demodulated output voltage. No noise improvement with increased RF bandwidth occupancy is therefore possible. (Schwartz, 1959)*.

FM systems with $D \gg \frac{\pi}{2}$, PPM and PDM systems use wide-band analog modulation techniques and their output signal-

* pp 291-298

to-noise voltage ratio can be shown to increase linearly with the ratio of transmission bandwidth to signal bandwidth, provided that the signal-to-noise ratio in the channel exceeds the maximum improvement threshold of the demodulator. (Panter, 1965).*

In order to achieve a high communication efficiency in a noisy (Gaussian) channel, it is in general necessary to modify the statistics of the data signal, to conform more closely to the statistics of the channel noise. (Sunde, 1969). Signal pre-conditioning techniques like frequency-pre-emphasis/de-emphasis and volume-compression/expansion may therefore be applied to the analog systems described above, to improve bandwidth utilisation and hence system performance.

In sampled data systems, the signal samples may be quantized not just in time, but in amplitude as well. The quantized amplitudes may then be digitally coded, prior to transmission, to produce a statistically Gaussian signal source. (Sunde, 1969). Coding the input data in this way maximises the significance of the transmitted data and yields an exponential relationship between the output signal-to-noise ratio and the transmission bandwidth. Binary Pulse Code Modulation (PCM) is an example of such a digital technique and is claimed to have the highest communication efficiency of the systems at present in use, requiring 8dB more signal power than the theoretical optimum system to achieve a specified channel capacity within a given bandwidth. (Schwartz 1959)**

* p 432
† p 72
‡ p 73
** p 327

These modulation techniques (AM, FM, PM, PAM, PPM, PDM, PCM) may be combined to form many different types of single and double multiplexed systems. According to Stiltz (1961), those most commonly used in telemetry applications are: FM/FM, FM/PM, PDM/FM, PCM/FM, PAM/FM/FM and PDM/FM/FM. Other techniques used less frequently include FM/AM, PAM/FM, PDM/AM, PPM/AM and PCM/AM.

A comparative analysis of the performance of these systems is tedious but has been attempted in part by Nichols and Rauch (1956), Schwartz (1959) and Sanders (1960). The performance achieved by some of the systems currently in use has been well summarised by Stiltz (1961).

The results of section 2.3 indicate that the ultimate in communication efficiency is probably not required where a small (ie < 6) number of biological data channels is required in a Class II link. The choice of modulation/multiplexing technique may therefore be based largely on considerations of the simplicity, reliability and power consumption of the transmitter hardware, and of the ease with which that hardware might be adapted to suit different combinations of data-signals.

FDM techniques usually require provision at the transmitter of a separate sub-carrier oscillator for each channel with provision for amplitude or angle modulation. Amplitude and phase modulation techniques are not generally employed at sub-carrier level in telemetry systems, but wideband FM is common. (Stiltz, 1961). A typical multi-channel FM/FM system for bio-telemetry has

been described by Fishler et al (1967). Occasionally a single sub-carrier oscillator may be frequency and amplitude modulated by different data signals, as described by Weller and Manson (1972) but this technique is not widely used.

The sub-carrier oscillators used in FDM must be of adequate spectral purity to maintain cross-talk between channels at acceptably low levels. Cross-talk may also be caused by harmonic distortion of the RF baseband spectrum, resulting from non-linearity of the phase characteristic of the transmission channel. (Sunde, 1969)*.

The use of TDM techniques eliminates these problems since the various data channels are combined serially in the time domain and then transmitted 'in parallel' in the frequency domain. The problems of sub-carrier separation and demodulation, however, are merely transferred from the frequency domain into the time domain, ie in FDM adequate guard-bands in the frequency-domain must be provided between each channel to permit channel separation by physically realisable linear-phase filters. Similarly, in TDM consideration must be given to the effects of noise on timing accuracy, and to the provision of synchronisation pulses, to permit sequential de-commutation of the individual channels. A typical TDM system for bio-telemetry is described by Skutt et al (1972).

In terms of hardware at the transmitter, the FDM requirement of a separate sub-carrier oscillator for each channel is replaced in TDM by the need to provide clock

* p353

generation, commutation, synchronisation and pulse generation circuitry common to all channels. This results in a comparative decrease in TDM transmitter complexity relative to FDM, where a large number of data channels is involved. This situation is, however, reversed for small numbers of channels.

The use of digitally coded TDM techniques will realise the ultimate in channel capacity, but at the expense of considerably increased transmitter complexity. A typical PCM transmitter will require an analogue-to-digital converter, buffer store, word and frame synchronisation circuitry, in addition to the commutating circuitry necessary for analogue TDM. Such a system has been developed and described by Rhind (1973) and could be realised in monolithic or multi-chip hybrid form, in a size compatible with implantation in small animals.

Considerations of transmitter complexity, therefore, make FDM attractive where a small number of data channels are required. The total bandwidth of six typical biological signals would be most unlikely to exceed, say, 5kHz, and fairly high modulation-index FM sub-carriers could therefore be used. A number of further points favour this approach. The use of FM sub-carriers enables signals of widely differing bandwidths to be readily accommodated, since the sub-carrier modulation indices may be individually adjusted to achieve the desired noise performance in each channel. In many cases a sub-carrier oscillator may be interfaced directly with a transducer. For example, a thermistor or variable resistance pressure

transducer may be used as the timing resistor of an RC oscillator, to produce a frequency response extending to DC.

If TDM techniques were used, the signal from such a transducer might well require DC amplification to produce a level adequate for reliable commutation and/or pulse modulation.

Another advantage of the FM/FM approach is that the multi-channel signal appearing at the Radio Receiver output may be readily recorded on simple analogue tape recorders, and the individual data signals retrieved at a later date.

The use of sub-carrier frequencies within the audio frequency range could enable some data channels to be monitored by ear. This could, for example, be a convenient form of output for an ECG channel.

On the basis of these considerations, the author has concluded that simultaneous transmission from an implanted transmitter of a small number (probably less than about 6) of biological signals could probably be best achieved by use of an FM/FM multiplex system.

2.5 FM/FM Telemetry

In an FM/FM telemetry system, each data signal is used to frequency modulate a separate sinusoidal sub-carrier oscillator. The sub-carrier frequencies are then linearly combined to form a single composite wave-form which is used to frequency modulate the RF carrier oscillator. The composite signal appears at the receiver output, the individual sub-carrier frequencies are

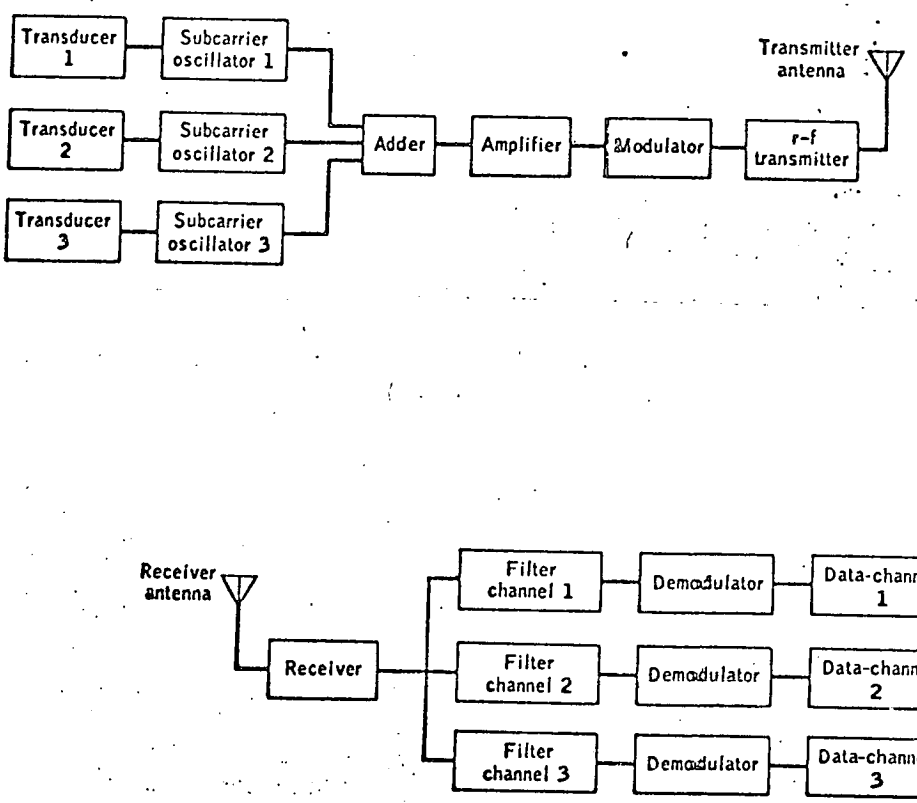

Figure 2.5.1 FM/FM Block Diagram

separated by appropriate filters, and the data outputs obtained from a number of sub-carrier frequency discriminators. Figure 2.5.1 illustrates the functional block diagram of a typical system. This technique has been used as standard practice for many years in the field of Airborne and Missile Telemetry. Recommended performance criteria for such systems were defined in 1948 by the Inter-Range Instrumentation Group (IRIG). These criteria have been recorded in detail by Stiltz (1961), who also reports on the design of the various sytems presently in use.

The signal-to-noise ratio at the output of a data-channel in an FM/FM telemetry system has been shown by Downing (1964)* to be a function of the product of the sub-carrier and the RF carrier modulation indices. In conventional practice, the modulation parameters at sub-carrier level are usually chosen on some common basis, and the RF modulation parameters manipulated individually to optimise the performance of each data channel, and to satisfy the bandwidth constraints of the RF channel. Two systems of sub-carrier frequency allocation are in common use. The choice of modulation parameters to equalise the noise performance of individual data channels in each of the two systems has been analysed in detail by Downing (1964).

Briefly then, the 'constant bandwidth' system uses a fixed modulation index and a fixed frequency deviation (in kHz) for all sub-carrier oscillators. The individual data-channels are therefore of constant bandwidth. The

* p 123
† p 123-127.

signal-to-noise ratios are equalised by use of a 6dB/octave pre-emphasis for the higher frequency sub-carriers.

The 'proportional bandwidth' system uses a fixed modulation index and a fixed percentage frequency deviation for all sub-carrier oscillators. The bandwidths of the individual data channels are therefore proportional to their centre-frequencies and noise equalisation is obtained by use of a 9dB/octave pre-emphasis for the higher frequency sub-carriers.

These pre-emphasis figures are obtained on the assumption of a parabolic noise power spectrum at the receiver discriminator output, due to a flat noise spectrum in the RF channel. In practice, however, internal receiver noise and short-term transmitter frequency instabilities dictate the use of a constant RF modulation index for all sub-carriers lying below a certain frequency. According to Stiltz (1961), the frequency above which pre-emphasis should be applied is not agreed upon by all FM/FM system users, but is generally taken to lie between 5.4 and 14.5 kHz. This contrasts with the pre-emphasis characteristic used in standard broadcast transmissions, where a 6dB/octave pre-emphasis of frequencies greater than 2.1kHz is used to flatten the frequency spectrum of speech and music signals, where most of the signal power is concentrated at low frequencies.

It is, however, a simple matter to obtain the desired de-emphasis characteristic from a broadcast receiver since this is determined by a simple RC filter.

CHANNEL NUMBER	CENTRE FREQUENCY	LOWER LIMIT	UPPER LIMIT	MAXIMUM DEVIATION	FREQUENCY RESPONSE	GUARD BAND
1	400 Hz	370 Hz	430 Hz	60 Hz	6 Hz	88 Hz
2	560	518	602	84	8	73
3	730	675	785	110	11	103
4	960	888	1,032	144	14	170
5	1,300	1,202	1,399	195	20	174
6	1,700	1,572	1,828	255	25	301
7	2,300	2,127	2,473	346	35	302
8	3,000	2,775	3,225	450	45	382
9	3,900	3,607	4,193	585	59	802
10	5,400	4,995	5,805	810	81	995
11	7,350	6,799	7,901	1,100	110	1,812
12	10,500	9,712	11,288	1,575	160	2,122
13	14,500	13,412	15,588	2,180	220	4,760
14	22,000	20,350	23,650	3,300	330	3.10 kHz
15	30,000	27,750	32,250	4,500	450	4.75
16	40,000	37,000	43,000	6,000	600	5.56
17	52,500	48,562	56,438	7,875	790	8.31
18	70,000	64,750	75,250	10,500	1,050	

Figure 2.5.2 IRIG FM/FM Frequency Specifications

The IRIG specifications for a proportional bandwidth system are published in 'IRIG Recommendations no. 161-59 (revised)', entitled 'Telemetry Frequency Utilisation Parameters and Criteria'. The system is based on the use of a peak frequency deviation of $\pm$ 7.5% on all sub-carriers. When allowances are made for 'guard-bands' 18 channels are accommodated within an RF baseband of 70kHz. The peak RF frequency deviation is 125kHz, ie an RF modulation index of 125/70 = 1.78 is used. The recommended sub-carrier frequency bands are listed in Figure 2.5.2, together with the individual data-channel bandwidths, calculated on the use of the recommended sub-carrier modulation index of 5. It is apparent, from this, that the IRIG channels are not well suited to the particular bio-telemetry applications under consideration. A much smaller number of channels with wider data bandwidths would be preferable. Inspection of the frequency response column of Figure 2.5.2 shows that transmission of a relatively 'hi-fi' Avian ECG signal (f_m = 200Hz) could only be achieved on channels 13 to 18. The use of these relatively high sub-carrier frequencies is undesirable for two reasons. Firstly, the restricted RF bandwidth available under Class II conditions (150kHz) would dictate the use of a lower RF modulation index than might otherwise be possible. Secondly, standard broadcast receivers would require slight modification, since their base-band filter responses usually extend to only about 15kHz.

Wider data bandwidths could be accommodated on the lower frequency channels by reducing the sub-carrier

modulation indices, but this is also undesirable for a number of reasons, quite apart from the reduction in the output signal-to-noise ratio which would result.

Figure 2.3.2 shows the increase in sub-carrier bandwidth occupancy that would occur and indicates the consequent danger of adjacent channel interference, unless wider guard-bands were used. As pointed out by Stiltz (1961) if the IRIG recommended sub-carrier filter bandwidths were retained, and the sub-carrier modulation index reduced to unity, the total harmonic distortion due to band-limiting would be greater than 20%. One further point is that the use of relatively high sub-carrier modulation indices will minimise the cross-talk between channels due to intermodulation distortion caused by non-linearities in the RF link. This subject is discussed in detail by Sunde (1969)† and is not considered further here, since a sub-carrier modulation index of 5 is sufficiently high to reduce to acceptable proportions the cross-talk caused by the relatively high levels of phase-distortion occurring in the RF links from missiles and satelites.

The requirements of the bio-telemetry link under consideration would therefore best be met by the provision of a small number of wide deviation sub-carrier oscillators lying below 15kHz.

† p353

CHAPTER 3

THIN FILM HYBRID TECHNOLOGY

3.1 Introduction

A number of currently available microelectronic techniques can provide the degree of miniaturisation required to fabricate an FM/FM telemetry transmitter of a size compatible with implantation in chickens. Monolithic Silicon integrated circuit technology will yield the smallest size for the active circuitry of the transmitter. The process is, however, unable to provide all of the circuit elements required. The high values of capacitor required in typical bio-potential amplifier design would certainly necessitate the use of additional discrete components. Silicon diffused resistors have limited use due to their poor tolerance,and temperature coefficients,* and Silicon junction capacitors have non-linear properties.** These deficiencies may be eliminated by the use of thin-film resistive layers on top of the Silicon passivation, and to a limited extent by the use of Metal/Oxide/Silicon capacitors, but both of these solutions decrease the yield by increasing the chip size and the number of process steps involved. Mask-making and diffusion costs are high, and usually justifiable only where large quantities of identical devices are required.

* Silicon Integrated Circuit Resistors, Technical Communication no 26. The Plessey[15] Company Ltd

**Capacitors for Monolithic Integrated Circuits, Technical Communication no 25. The Plessey Company Ltd

Thick or thin-film hybrid circuit technologies both permit the convenient integration of commercially available Silicon integrated circuit chips from various manufacturers, with ceramic and tantalum dielectric chip capacitors, on substrates bearing high quality resistor and conductor patterns. These hybrid processes are more suited to the small-volume production requirements of this project, and will result in a transmitter of a size compatible with implantation. Both thick and thin-film production processes are currently available within the University of Edinburgh, Department of Electrical Engineering. Some of the reasons why the thin-film process was considered to be more suited to this particular application will now be considered.

The currently available thin-film process is capable of the production of resistor tracks 50μm wide, to a tolerance of ± 5%. This is sufficiently tight to satisfy the great majority of circuit requirements. Tighter tolerances may be readily achieved by providing conductor pads along part of the length of the resistor track. This enables the resistor to be trimmed to the desired value by shorting the pads together with ultrasonic wire-bonds. The thick-film process currently available in the Department of Electrical Engineering, produces resistors, printed and fired, to a tolerance of 12%. (J. Robertson, Personal Communication). Many circuit designs therefore involve individual trimming of resistor tracks. This is tedious if performed manually, and the high cost of automated trimming equipment can only usually be justified where a relatively high volume production is required.

Conventional thick-film layout constraints, dictated by printing and trimming tolerances, permit a range of resistor values of about 25:1,* to be obtained from a single print of a resistor paste. The production of a wider range of resistor values therefore necessitates the use of either inconvenient resistor geometries, or of a second printing operation using a paste of different resistivity. Optimum firing schedules for each individual resistor paste have been developed, and these can produce resistors with a low Temperature Coefficient of Resistance (TCR), usually less than +200ppm/^{o}C. Unfortunately, each paste requires a different furnace profile or ultimate firing temperature for optimum results. If a single resistor paste is printed and optimally fired to produce a low TCR, and the substrate is printed with a second paste and re-fired, then the values of the original resistors may change by about 20% and their TCR increase drastically. It is therefore usual to print and dry each layer individually, and then to fire them all simultaneously. The firing schedule used may then be chosen either to produce the lowest mean TCR of all layers, or to optimise the properties of one particular paste. In contrast, the fine-line definition obtainable from the subtractive thin-film process permits a far wider range of resistor values to be obtained from a single resistive layer. For example, the present process, using a 50μmline width on a 200Ω/square metallised substrate can permit a 100,000:1 (namely 4Ω to 400kΩ) range of resistor values to

* The Thin Film Microcircuitry Handbook Vol 1, Du Pont[16] Electronic Products.

be produced without the use of low-yield geometries. All resistors on a given substrate will therefore have the same low value of TCR, typically less than +100ppm/^{o}C.

Typical multi-chip hybrid circuit layouts involve a high density of conductor tracks in the immediate vicinity of the integrated circuit chips. The substrate area occupied by such interconnections varies as the square of the line definition. At the present time, the typical minimum line width of 250μmused in the thick-film process, could be fairly contrasted with the 50μmline width of the thin-film process. Both of these figures are conservative and could probably be reduced by a factor of two or three times in critical layout situations. The thin-film process is therefore seen to reduce the substrate area devoted to such dense interconnection patterns, by a factor of 25 times.

A further requirement is that the manufacturing process should be economically justifiable for the production of small batches, say 50 off, of different circuits, and that new designs or design modifications should be readily implemented with the minimum time delay and cost.

The high cost of thick-film inks, together with the large amount of ink wasted on the printing screens compared to that actually deposited on the substrates, favour the printing of large numbers of substrates at a time. Where small quantities only are required the costs involved can become prohibitive. Strict quality control of the thick-film process is also difficult to achieve where small batches are produced over long periods of time. The

electrical properties of the printed films are, for instance, a function of the ink viscosity, and this is a function of the 'pot-life' of the inks. The potential low-cost advantage of thick-film hybrids is thus only fully realised where a continuous production process is used.

A further advantage of the subtractive thin-film process is that stocks of 'uncommitted' metallised substrates of defined film parameters may be held, ready for etching as and when required, to any required geometries.

The thin-film process used is described in some detail in appendix I. Some aspects of the process are discussed further in this chapter, in order to demonstrate the extent to which device and circuit design is influenced by the constraints involved in the process itself.

The notation Ni-Cr is used throughout the text to indicate an alloy of Nickel and Chromium of undefined composition. (See appendix I). The form Si-O is similarly used to indicate a mixture of Silicon and Silicon-Dioxide of undefined composition. (See section 3.5).

3.2 Substrate Considerations

Since the electrical properties of thin metallic films are to be used to fabricate resistor and conductor networks, and since such films are not self-supporting, the metals involved are condensed from the vapour phase on to the surface of a 'substrate' whose physical and chemical properties will therefore influence the characteristics of the deposited films. The need to provide a suitable range of resistor values for convenient circuit design dictates the

use of a relatively high sheet resistance, if convenient, or low yield resistor geometries are to be avoided. Where metallic resistive elements are used this means that the resistive layer must be thin, typically less than 100Å. The surface roughness of the substrate material is consequently of prime importance. According to Berry (1968) an ideal substrate material for thin-film work should have:

1. A high volume resistivity.
2. A planar and atomically smooth surface.
3. Chemical inertness.
4. A high dielectric strength.
5. A high thermal conductivity.
6. Compatibility with deposition and all subsequent processing.
7. Ready availability at a low price.

Where work with radio frequencies is involved, a further requirement is obviously a low loss-tangent. The requirement of a high-thermal conductivity is not particularly important in the fabrication of low power devices, and the requirement of an atomically smooth surface can be advantageously replaced in many applications by the requirement of a uniform roughness over the entire substrate area. Where a high mechanical strength is available, expensive encapsulation may be avoided in some applications and low-cost conformal encapsulants may be used. Where substrates of small area are to be produced it is economically desirable to process larger substrates, bearing a number of identical patterns, and then to separate the individual circuits. While this can be done with a diamond saw, the ability to scribe and

crack a substrate is a distinct advantage. Any real substrate material is obviously a compromise between these ideal requirements, and at present a choice must be made between glass, sapphire, silicon, alumina and beryllia.

Sapphire is almost ideal but very expensive. Silicon is also expensive and not widely used except where its semi-conducting properties are exploited. Beryllia is similar to alumina in many respects, but is highly toxic, expensive, and used only where its high thermal conductivity is essential. This leaves a choice, for this application, between the two lowest cost materials mentioned above, ie glass and alumina. At the present time this implies a choice between two specific products, namely 'Corning 7059 Microsheet' and 'MRC Superstrates'.

'Corning 7059 Microsheet' is a Barium Aluminium Borosilicate glass, produced by the Corning Glass Works[17], New York. It is manufactured by a sheet-drawing process, the final surface being fusion-formed from the melt, and having a typical small-scale surface smoothness of 60Å and a typical surface flatness of 0.004 inch/inch. It has a very low alkali content, essential for good resistor stability, of 0.2%. Its Volume Resistivity is high, being $10^{8 \cdot 8}\Omega$cm at 250°C. (Berry, 1968). This glass composition was developed specifically for thin-film applications, and has been widely used for many years. It is the substrate material used in the 'standard process' described in appendix I.

'MRC Superstrates' are manufactured by Materials Research Company Limited[18] of London, and have only recently (1973) become available. They are made of 99.6% alumina, and have a grain-size much smaller than that previously available in alumina substrates. This results in an 'as-fired' small-scale surface smoothness of 1000Å and a typical surface flatness of 0.002 inch/inch. Their physical properties are excellent, their mechanical strength, thermal conductivity and scribability, being much better than 7059 glass.

The cost of the two materials appears closely comparable, except where small sized substrates (less than about 2cm x 2cm) are being purchased. This is due to the relatively higher scribing and packing costs charged by MRC, London. At this substrate size, costs of both materials are about 12p per cm^2.

The use of 'Superstrate' alumina substrates offers a number of potential advantages over 7059 glass substrates. These are:

1. The increased mechanical strength should enable a cheap epoxy conformal encapsulation to be used with increased confidence.
2. The significant and uniform roughness of the surface has been found to double the Ni-Cr film thickness required to achieve a sheet resistance of 200Ω/square. This should improve resistor stability by reducing surface aging effects.

3. Significantly lower Temperature Coefficients of Resistance are observed in 200Ω/square films, ie ≈60ppm/°C for Superstrates as against ≈100ppm/°C for 7059.

4. The higher thermal conductivity of the substrates should reduce the rate of temperature rise of the front surface of the substrate during the gold-film deposition, by improving the heat transfer to the substrate holder. This should minimise the Au/Ni-Cr diffusion which takes place during the Au deposition, which, as mentioned in appendix I, is a source of variation of the final Ni-Cr sheet resistance obtained.

5. The increased surface area under bonding pads should improve the adhesion of appliqued components, (x10 according to MRC).

6. The improved flatness of the substrate should improve fine line definition, by minimising the gap between the substrate and mask during the contact printing operation.

These factors have not yet been fully evaluated and it is therefore intended to fabricate the first transmitters on 7059 glass substrates, to prove their electrical performance. Future devices will probably be made on 'Superstrates' where use will be made of their high mechanical strength, to fabricate an epoxy encapsulated device with an integral battery pack. This is discussed in section 3.8.

3.3 Resistor Considerations

The sheet resistance (R_s) of a thin conducting film is proportional to the resistivity (ρ) of the material and inversely proportional to the film thickness (d), provided that the film is thicker than a certain small value. For Ni-Cr films this value is typically 50Å (Holland, 1961). The sheet resistance is therefore defined as:

$$R_s = \frac{\rho}{d} \quad \Omega/\text{square}$$

The expression 'Ω/square' is commonly used to avoid confusion with absolute ohmic values.

A rectangular resistor of length (l) and width (w) etched in such a film, therefore has a resistance (R) of

$$R = \frac{\rho}{d} \frac{l}{w} = R_s \frac{l}{w}$$

The minimum width (w) of resistor track that can be used is a function of the definition of the photo-lithography process used, and resistor tolerances widen as the track width is reduced. A track width of 50μ has been previously used on the single channel devices mentioned in the introduction, and tolerances of better than ±5% are being readily achieved.

The minimum film thickness (d) than can be used is determined by a number of factors, principally associated with the reproducibility and stability of the film.

Very thin metallic films have a discontinuous 'island' structure and the conduction mechanism involved in charge transfer between these islands can give rise to a negative component in the observed temperature coefficient of resistance, (Swanson, 1967/68). This effect becomes

increasingly dominant in Ni-Cr films thinner than about 50 to 60Å, and effectively precludes the use of Ni-Cr sheet resistances higher than about 300 to 400 Ω/square.

Oxidation of the surface of thin Ni-Cr films during their working life can lead to an increase in resistor values. This long term drift can, however, be minimised by accelerated post-deposition ageing usually involving baking in air at a temperature greater than the working temperature of the final device. The use of a hermetic dielectric protective layer, eg. Si-O, deposited over the etched resistor tracks improves stability further (Keenan, 1973) and inhibits electrolytic corrosion of the tracks which can occur where humidity and a direct potential gradient are present.

The dominant factor determining the minimum film thickness usable in the present Ni-Cr/Au/Si-O film process is the diffusion process at the Ni-Cr/Au film interface (see appendix I). This effect leads to unpredictable Ni-Cr sheet resistances where high values of Ω/square are attempted. The value of 200 Ω/square corresponding to a film thickness of about 80Å, represents a fairly conservative upper limit, and yields adequate reproducibility (±5%) and long term stability for present purposes.

Accurate measurements of the long term stability of the Ni-Cr tracks when protected with Si-O, have not yet been performed. Early data on epoxy encapsulated resistors, however, indicated less than -2% change in resistance after storage for one year at room temperature. Subsequent accelerated ageing tests indicate that this poor stability

is probably associated with the porosity of the epoxy rather than to changes within the film itself.

Minimum line width and maximum sheet resistance can be used to define the maximum value of resistor that can be produced in a given area. This value of 'Ω/mm^2' is an important parameter in circuit design and layout. The 50μm line width and 200Ω/square in previous devices yields a figure of 40kΩ/mm^2, where resistors are fabricated in a zig-zag pattern with lines and spaces of equal widths. When this value was used in estimating the substrate size necessary for realisation of the circuits described in chapter 4, it became apparent that the bulk of the substrate area would have to be devoted to resistor tracks, and that the final substrate area would be inconveniently large. A reduction of the minimum line and spacing to 25μm yields a value of 160k Ω/mm^2 and the resistor tracks no longer dictate the substrate size, which is now primarily influenced by the size of the appliqué components.

3.4 Conductor Considerations

The bulk resistivity of pure gold is 2.04$\mu\Omega cm$ at 0^oC. (Gerritsen, 1956). The anticipated sheet resistance of the 0.5μm thick gold film used in this standard process is therefore 0.0408Ω/square. As pointed out in appendix I, the sheet resistance of the gold film is expected to be higher than that predicted from the bulk resistivity of pure gold, due to the incorporation of Nickel and Chromium in the gold film. Typical 0.5μm gold films produced by the 'standard process', have values of sheet resistance ranging

from 0.06 to 0.09 Ω/square. A value of 0.1 Ω/square is therefore taken as a conservative estimate of the gold film sheet resistance, and this value is used in layout calculations.

Apart from providing the interconnections between resistor tracks on the substrate, the gold layer is used to provide bonding pads for the appliqué components. These are currently being attached using hot-gas reflow soldering and/or conductive silver loaded epoxy resins. A film thickness of greater than about 0.3μm has been found necessary for reliable component attachment using hot-gas reflow soldering. The high purity, density and adhesion of the gold film also facilitates reliable wire bonding using cold-work ultrasonic bonding of aluminium wires or pulsed-thermocompression bonding of gold wires.

The line definition of the conductor tracks is a function of the definition of the photo-resist image and the undercut caused by the gold etchant. This undercut has not proved troublesome in practice, and rarely extends more than 0.5μ from the edge of the photo-resist image. Line widths of 25μ may therefore be confidently used.

3.5 Si-O Film Considerations

The Si-O overcoat which is deposited over the etched Ni-Cr/Au patterns serves a number of purposes. The most important of these is to provide a hermetic seal for the thin Ni-Cr tracks. This improves their long term stability and protects against the possibility of electrolytic corrosion (Keenan, 1973). The film also provides a high degree

of mechanical protection to the tracks during subsequent component attachment and testing operations. Contacts to bonding pads are made through windows etched in the film. These windows also aid the assembly of appliquéd components by controlling the spread of molten solder during hot-gas reflow soldering and eliminating the possibility of short circuits to neighbouring conducts where epoxy-bonding is used.

The Si-O films are prepared by electron-beam evaporation of quartz. Considerable quantities of oxygen are liberated and pumped out during the deposition process, and the final film consists of a mixture of Silicon and Oxygen in non-stochiometric proportions. The resistivity of the deposited films has been found to be at least as high as that of the original evaporant. 'Vitreosil', a 99.9% pure silica supplied by Thermal Syndicate Limited[19] of Wallsend, has been used in this application, and the published resistivity of 2×10^{14} Ωcm has been achieved in films prepared from it.

The adhesion of the film to both glass and Ni-Cr tracks is excellent, probably due to oxygen bonding mechanisms at the interface. Film adhesion to gold is adequate when deposited at substrate temperatures of 300°C, but the deposition conditions described in appendix I yield a film which is under compressive stress. This can give rise to a characteristic fracture pattern, where the Si-O film crosses the 0.5μm high step from the substrate to the gold film. This occurs if the Si-O film is less than about 0.7μm thick.

Si-O films of 1.0μm thick have all survived subsequent aging and high temperature bonding operations, without apparent degradation.

3.6 Appliquéd Component Considerations

At the present time, it is possible to purchase, in the form of unencapsulated chips, virtually any transistor or integrated circuit in current production. Frequently, however, this is not possible in quantities of less than 100 off, due to high handling costs at the distributors. Chip performance specifications are, in general, much looser than those of encapsulated devices, since frequently the chips are subjected to only visual and DC tests before encapsulation. This factor must be taken into account when breadboarding circuits for subsequent hybrid production. Occasionally, tolerances on chip parameters may be so wide as to preclude a 100% yield on the finished hybrid assembly.

Ceramic chip capacitors are presently available from a number of suppliers in this country. These are produced in a range of standard sizes. One of the most common (Vitramon[20] VJ0805, Bowmar[21] R15) measures 2.03 mm x 1.27 mm x 1.27 mm high. These dimensions include the metallised end-terminations for bonding to the substrate. These capacitors are available with a high precision, low temperature coefficient, ceramic dielectric (NPO) in capacities of up to 680pF.* Capacities of up to about 15,000pF are available in the same case size with a 'general purpose' hi-K ceramic dielectric (K1200) suitable for low frequency use, where a high precision and a low temperature-coefficient

*See addendum page 156.

are not required. A detailed analysis of the effects of high-temperature bonding operations on the K1200 material has been performed by Tindall (1970). This work indicates the need for caution in the use of these capacitors for timing and filtering applications.

Unencapsulated tantalum dielectric chip capacitors are available from Union Carbide[22] and Bowmar[21]. These allow capacitances of up to about 100μF to be incorporated in hybrid circuit designs.

3.7 Layout Considerations

A full description of the procedures involved in hybrid circuit layout is beyond the scope of this section because of the multiplicity of possible approaches, and the many different constraints which may be involved in particular cases. This section, therefore, describes briefly the constraints involved and the methods used in the layout of the circuits described in chapter 4.

As stated in section 2.4, an advantage of the FM/FM approach to multichannel telemetry is the ability to multiplex a range of different parameters in a relatively simple and flexible fashion. These parameters will, in general, require specialised circuitry to interface the particular transducer involved to the relevant sub-carrier oscillator. In order to facilitate the production of a range of devices, designed for specific combinations of input parameters, a 'modular' approach to the layout of front-end and sub-carrier oscillator circuitry is appropriate. This therefore involves consideration of the interconnection

requirements of possible combinations of different input circuits, before embarking on the layout of the individual channels. This is discussed further in chapter 4, where the layout of the individual channels is described.

The first step in the layout of a thin-film hybrid is the production, from the circuit diagram, of an interconnection pattern or 'graph' of the circuit. This should incorporate all connections between components and resistor tracks, and should include all bonding pads for external lead wires in the correct orientation. This graph may then be modified to optimise component placement and conductor routing. The length of any critical signal paths may be minimised at this stage, and the number of crossovers may perhaps be reduced by routing conductors between the bonding pads of appliqued components.

Critical components in symmetrical circuits may be placed in close proximity to one another, or symmetrically with respect to any anticipated thermal gradients, to improve circuit performance.

The tight tracking tolerances obtainable from thin-film resistors, simultaneously deposited on the same substrate, may be maximised by laying them out in close proximity. This may be exploited in the design of the load resistors for a long-tailed pair, or the feedback resistors of an amplifier.

An attempt should be made at this stage to foresee any possible future applications of the device which could involve modifications to the basic circuit. Provision for such modifications can usually be simply incorporated at this early design stage, and could well save considerable expense

at a later date.

Once a satisfactory interconnection graph has been developed an estimate must be made of the total substrate area required. The total area occupied by resistor tracks must be calculated. Sufficient area must be provided for bonding pads for appliquéd components and external connections. Allowances must be made at this stage for adequate clearance between appliquéd components and an estimate must be made of the area to be occupied by conductor tracks. The choice of substrate dimensions on which to attempt the final layout must be based on both the area estimated for the circuit itself, and on the availability of suitable packages with the desired number of leads in the desired orientation.

A layout based on the interconnection graph and the physical dimensions of all component parts,may now be attempted. This layout is drawn out at a scale of twenty times its final size on graph paper. The initial stages of this work can be facilitated by the use of cardboard cut-outs to represent appliquéd components, and by representing all resistor tracks as fixed areas of variable dimensions. When a promising topography has been arrived at, the detailed layout can commence, bearing in mind the following constraints.

The substrate metallisation does not extend over the entire area of the substrate, due to the clamping arrangements used during the vacuum deposition stage. An allowance of a 1.0mm wide strip along two opposite edges (usually the shorter pair) must therefore be made for this. The photolithography process used, produces a significant photoresist

'build-up' around the outer edges of the substrate. This thick peripheral layer remains on the substrate after exposure and development of the photoresist pattern, and results in a narrow conducting strip of gold along the perimeter of the etched substrate. An allowance of 0.5mm must therefore be provided around the 'active area' of the substrate, if peripheral short-circuits are to be avoided. Alternatively, the two gold strips so produced can be used as part of the final conductor network, as in the circuits described in chapter 4.

The areas allocated for appliquéd components must reflect the substantial dimensional tolerances of the parts as supplied, and must include an additional area related to the accuracy with which the component may be positioned for bonding. Typically, a distance of 250μm around the maximum dimensions of rectangular ceramic chip capacitors, integrated circuit and transistor chips, is sufficient to allow for reliable positioning, and the spread of any epoxy resin or solder used in the bonding operation. Larger components, such as tantalum chip capacitors or glass encapsulated axial-leaded diodes, which are more awkward to position accurately, should be allowed a clearance of around 500μm.

Bonding pads for ultrasonic wire-bonding may be as small as about three times the wire diameter, but care must be taken in the layout of these pads, that adequate clearance is available for the heel of the bonding tool during the bonding operation.

The design of any hybrid circuit is, of necessity, an

iterative procedure, and repeated attempts at a satisfactory layout are inevitable, especially where, as is the case in this instance, the smallest practical package is required. The application of the general guidelines outlined above, to the layout of the FM/FM telemetry system, resulted in the layout of each data channel within a 'modular' substrate size of 1.0cm x 1.9cm. Each module includes provision for up to eight external leads. These are spaced on 0.100 inch centres, four along each of the shorter edges of the module. This lead spacing is a standard dimension used by a number of micro-electronic package manufacturers, and a suitable range of packages is available from 'Tekform'[23]. These are presently distributed in this country by Dage.[24]

3.8 Encapsulation Considerations

Any encapsulation used for a biologically implanted hybrid microcircuit must perform a dual function. Firstly, sensitive resistor tracks and semiconductor active devices must be protected from the ingress of corrosive body fluids. Secondly, tissue reaction associated with biological rejection of the implant must be minimised by the use of a biologically inert encapsulant. No single material available at the present time satisfies all of these requirements, and a multilayer encapsulation is necessary.

Hybrid circuits intended for applications where the highest standards of reliability are required, e.g. in military and aerospace applications, use hermetic packages of metal with glass-to-metal seals for external connections. Conformal coating or transfer-moulding with epoxy or silicon

resins, is used for less demanding applications. All such resins do, however, have a small but finite water permeability, and cannot therefore be used along with confidence where long term implantation is desired (Mackay, 1970).

Epoxy coating may, however, be used as an initial low-cost encapsulant, and products are currently available whose physical and electrical properties have been optimised for this application. (Eccocoat FT2850)[33]. The devices may then be protected from the ingress of water vapour by dip-coating the epoxy package in molten wax. Paraffin wax is highly impermeable to body fluids but is brittle and does not adhere very well to most surfaces. The addition of up to 50% beeswax improves both of these deficiencies, and produces a tenacious and slightly flexible coating.

An alternative approach,used previously with success (Filshie and McGee, 1974), is to place the substrate in an encapsulation shell of glass loaded diallylpthallate. (Milton Ross Company[25]), and to pour in the molten paraffin wax/beeswax mixture.

Either a hermetic glass/metal package or an epoxy/wax encapsulation will adequately protect the circuitry from the biological environment, but in both cases a final coating of silicon rubber (Hopkins and Williams,[26], 9161), which is biologically quite inert, is necessary to eliminate biological rejection.

This material is, however, quite permeable to water vapour, and all external connections from the device to its battery pack and input leads must therefore be protected

by paraffin wax before the final silicon dip-coating is applied. This minimises the possibility of leakage paths between such connections. Where a metal package is used, the radiating antenna must be external to the package, and must be similarly protected.

As mentioned in section 3.2, 7059 glass substrates were used for the initial devices in order to check the circuit performance obtained from the standard thin-film process. Each sub-carrier oscillator/front-end module was fabricated initially on an individual 1 cm x 1.9 cm substrate. A suitable hermetic package for encapsulation of such a single-channel device is the 'Butterfly Case number 50195' manufactured by Tekform. This package is larger than is necessary, being designed to take a 1.3cm x 2.4cm substrate, and having 5 leads per side. It is, however, a stock item available on a short delivery and was used for the single channel devices. A suitable hermetic package for a two channel device is Tekform's 'Dihedral Case number 70188'. This is designed to take a 2.54cm x 1.9cm (1.0inch x 0.75 inch) substrate, and has ten leads per side. This package therefore is larger in one dimension than required, but should provide enough space to incorporate remote switching circuitry as described in section 4.5.

Devices consisting of more than two channels could be encapsulated in the 'Modular Butterfly' range of packages manufactured by Tekform. These are available to individual order with any number of leads up to fifteen per side at 0.100 inch spacing, or up to thirty per side at a 0.050 inch

lead spacing (part number 50157). The packages mentioned above are illustrated full-size in Figure 3.8.1.

A possible configuration for future devices produced on 'Superstrates' is illustrated in Figure 3.8.2. An epoxy encapsulation could be used to protect the active circuitry and the antenna coil. The Mallory cells used as the power supply could then be mounted on extensions of the ceramic substrate, and be retained by spring clips as illustrated. The package could then be dip-coated, first in wax and then in silicon rubber, to provide a conveniently flat assembly suitable for sub-dermal implantation.

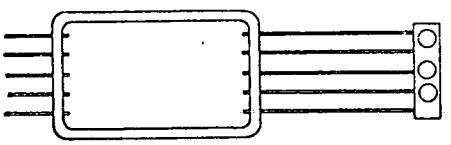

50195

Butterfly Case

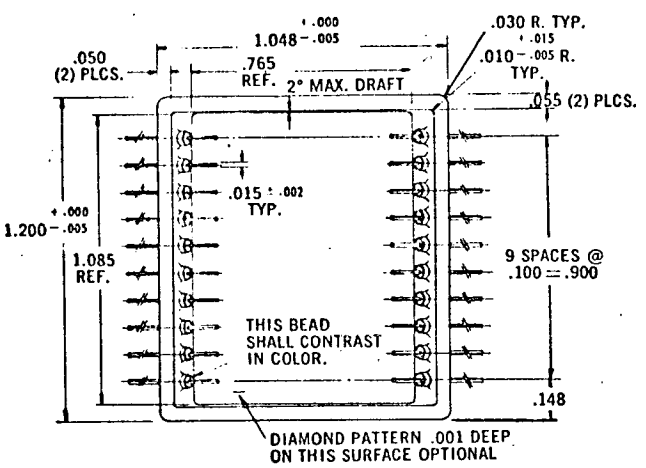

70188

Dihedral Case

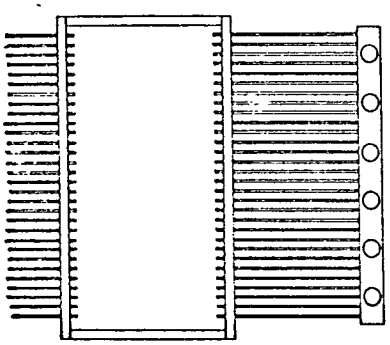

50157

Modular Butterfly Case

Figure 3.8.1 Microelectronic Packages by 'Tekform'

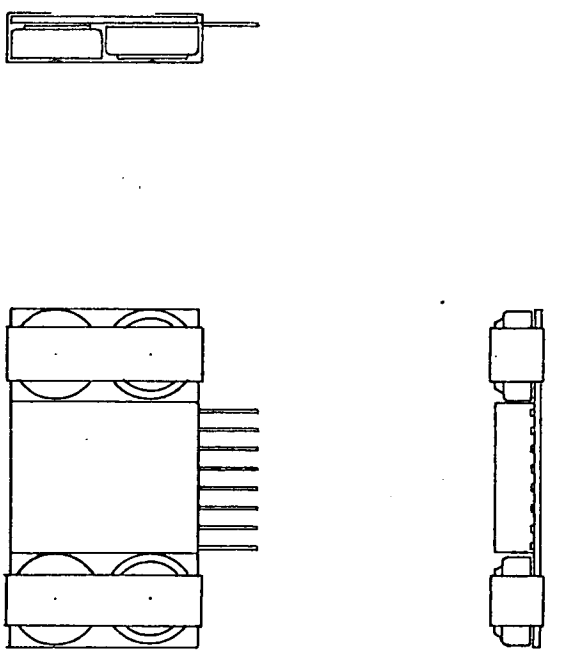

Figure 3.8.2 A Possible 'Superstrate' Encapsulation

CHAPTER 4

HYBRID TELEMETRY DEVICES

4.1 Sub-Carrier Oscillator Design

The fundamental performance requirements of an FM sub-carrier oscillator are a low harmonic content, to minimise interference with other data-channels, and a high modulation linearity, to minimise distortion of the demodulated output waveform. Where such an oscillator is required to form part of a data-channel with a frequency response extending to DC, a high centre-frequency stability is required. Two further requirements related to implanted operation are small size and low power consumption.

The majority of existing subcarrier oscillator designs for FM systems are based on sinusoidal RC oscillators, of either the Wien-bridge or Phase-shifting ladder-network variety. Frequency modulation is frequently achieved by incorporating a variable resistance, or a variable capacitance transducer in the frequency determining network. (Mackay, 1970). Voltage control of the subcarrier frequency may be achieved by replacing the frequency determing resistor with a bi-polar or field-effect transistor. A linear modulation characteristic is, however, difficult to achieve by these methods, especially where wide frequency deviations are required. Alternatively, the frequency determining resistors of a Wien Bridge oscillator may be replaced by a pair of forward-biased Silicon diodes. Such

a system is described by Fishler (1967) who demonstrates how the exponential portion of the forward characteristic of the diodes may be exploited, to yield a linear modulation characteristic from the oscillator. Frequency-modulation is achieved by modulating the diode bias currents.

In general, the current consumption of the RC oscillators described above, is too high for implanted devices, since their low harmonic content is achieved by biasing the transistors in Class A, and operating under small-signal conditions. Wien-bridge oscillators also require AGC circuitry to eliminate clipping of the output waveform, which may otherwise occur, and Fishler's design involves an additional current drain through the diodes themselves.

A novel system based on tunnel-diode sub-carrier oscillators has been described by Robrock II (1967). Frequency modulation is achieved by supplying the tunnel diodes from a variable current-source, but relatively high currents, approx. 1 mA per channel, are dictated by the diode characteristics themselves.

The recent availability of complementary MOS integrated circuits, e.g. the RCA[27] 'COSMOS'* range of devices, has made the use of multi-vibrator circuits attractive for this sub-carrier oscillator application. The fact that the devices consumenegligible power from the supply line except

*See RCA Solid State '74 Databook SSD-203B 'COS/MOS Digital Integrated Circuits'

when actually driving a load, minimises their power consumption. Their high value of input impedance ($10^{12}\Omega$), means that a wide range of resistor and capacitor timing components may be used. Where low frequencies are required, virtually all of the power drawn from the supply is dissipated in the load, and by the R/C timing chain itself. The power consumption of the timing chain may be low, since low-leakage capacitors may be used, and the high value of the device input impedance permits the use of high value timing resistors. The rectangular output waveform does, however, necessitate low-pass filtering to reduce its harmonic content to acceptable levels.

The large voltage swing (virtually equal to the supply-line voltage) available at the output of a 'COSMOS' inverter stage, together with the relatively low signal amplitudes required to modulate the RF carrier oscillator (4.0mV for 50kHz deviation) allow this to be achieved by passive filtering. A simple two-stage R/C filter, the time constants of which were chosen to be equal to the fundamental period, was found to produce second and third harmonic voltage levels of better than -20dB at the filter output. This is a much higher distortion level than that available from a simple Wien bridge oscillator, where levels of less than 0.1% total harmonic distortion may be readily achieved. These harmonic components may well appear within the pass-band of other higher frequency data-channels. These interfering signals will, however, be largely un-correlated in phase with the 'wanted' sub-carrier signals. Interfering

signals of this nature suffer considerable attentuation in conventional frequency discriminators, provided that their amplitudes are sufficiently small to begin with. This 'capture effect', (Downing 1964)* occurs because the resultant average phase of the combined signal is largely determined by that of the 'wanted' signal, provided that its amplitude exceeds that of other signals, by about 4 or 5 dB. The performance of phase-locked discriminators may well be superior in this respect, to that of other types, especially where signals with a high modulation index are involved.(Gardner, 1966).

A number of different 'COSMOS' multivibrator circuits were built and tested, using both the CD 4007 Triple Inverter stage package, and the CD 4047 Astable Multivibrator package. Various frequency modulation techniques were also evaluated using bipolar and field-effect transistors to modulate the charging current of the timing capacitor. The best performance, as regards simplicity, power-consumption, linearity and self-starting ability, was obtained from the voltage controlled oscillator section of the CD 4046 Phase-locked Loop. The phase comparator sections of this integrated circuit are not used in this application and do not consume significant power. The high modulation linearity of this particular multivibrator is achieved by the use of a current-mirror (see RCA '74 Databook SSD-203B), to control the charging current of the timing capacitor. The typical linearity quoted by the manufacturer for operation from a 5.0v supply, is better

* 106-109

than 1% for a ±6% frequency deviation. This figure is measured with a 10kΩ timing resistor, but data is not available from RCA to indicate how this may vary for higher values of timing resistor. Published data at line voltages of 10v and 15v, however, indicate that linearity improves linearly with increasing values of timing resistor. Measurements at 5.0v line voltage were therefore carried out using a 390kΩ timing resistor, and a typical linearity of better than 1% over a ±50% frequency deviation was found. Since high values of timing resistor will be used in all implanted applications, and since deviations as great as ±50% will be seldom required, the linearity of this VCO section should be more than adequate for the majority of biological telemetry applications.

The frequency of these multivibrators varies from 0Hz to twice the centre frequency, in response to a voltage input to the current-modulating transistor, moving from the negative to the positive supply rail. This wide deviation capability could be an embarrassment where sub-carrier channels are closely spaced in the frequency domain, and it may be desirable to limit the maximum frequency deviation, to eliminate adjacent channel interference. The integrated circuit chip includes a 'frequency-offset' facility, whereby an external resistor is used to supply an additional steady current to the current-mirrow. If, for example, this resistor is made equal to one tenth the ohmic value of the source resistor of the FET current modulator, then the maximum frequency deviation may be restricted to 10% of

the centre frequency. This method of limiting the frequency deviation is not well suited to this particular application. The power consumption of the VCO is largely determined by the ohmic value of the timing resistor, which should therefore be as large as is practicable. In thin-film terms, it should occupy as much area as can be made available. In order to limit the frequency deviation to, for example, 10% as described above, means incorporating a second resistor occupying ten times the area of the dominant timing resistor. This results in impractical geometries if a low power consumption and a narrow channel bandwidth are simultaneously required.

An alternative method, more suited to this application, is to restrict the VCO input voltage to a relatively small range of values. This may be achieved, where necessary, if the VCO input is tied to the mid-point of the supply lines by a pair of opposed diodes in parallel. This 'diode-clamp' arrangement permits a voltage swing of about $\pm$ 0.5v at the VCO input, which results in a $\pm$30% frequency deviation if a 5.4v supply voltage is used. Lower maximum deviations may be achieved if the VCO input is tied to a potential divider across the diodes.

The interconnections used are illustrated in figure 4.1.1. Typical measured current consumption, from a 5.4v supply with a timing resistor of 680kΩ, was about 60μA. This figure increased to about 80μA when the device was loaded by the harmonic filter illustrated. These figures apply to a device operating at 22kHz (timing capacitor = 39pF)

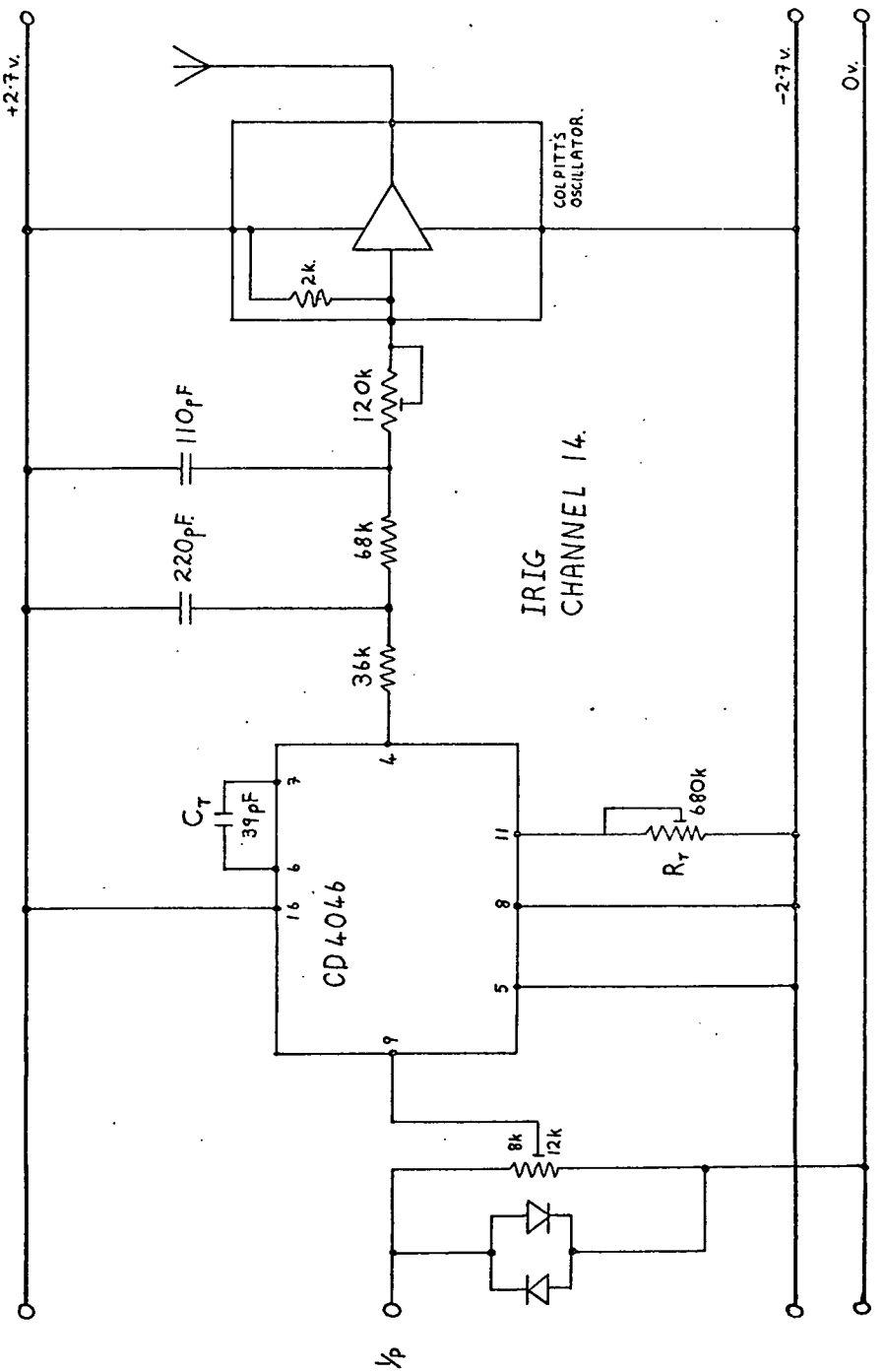

Figure 4.1.1 Sub-carrier Oscillator: Schematic Diagram

i.e. on IRIG channel number 14. Lower frequency devices will consumeslightly less current than this.

Measurements carried out on a dozen CD 4046AE plastic dual-in-line packaged devices showed that the typical specifications published by RCA were quite conservative. For example, the device-to-device centre-frequency variation under given circuit conditions is quoted by RCA as being ±60% for the plastic-packaged devices, operated on a 5.0v supply. All devices tested lay within a ±10% spread. The percentage variation of centre-frequency with supply voltage for all devices tested, was found to be 15% ±1.5% per volt, when tested at around 5.4v supply voltage.

5.4v is a convenient line-voltage for this application, since it may be obtained from a battery pack consisting of four mercury cells (1.35v each). The use of four cells permits the use of a ±2.7v supply with a zero volt reference. This is convenient since it allows the VCO input voltage to be clamped, where necessary, to a low impedance zero-volt reference point, and eliminates the need for an additional potential divider which would otherwise be required.

The relatively flat discharge characteristic obtained from mercury-cells leads to a voltage drop of about 100mV per cell over their useful life. The voltage variation of the four cell pack (400mV) should therefore result in a total frequency shift of 6% ±0.6% for most devices. A typical frequency drift of 0.06%/^{o}C is quoted by RCA, but this low figure means that temperature drift should be

negligible for implanted applications, in comparison with the line voltage variation effect.

The CD 4046 device is available in unencapsulated chip form under the type number CD 4046AH. The chips measure about 0.075 inches square and are 0.005 inch to 0.009 inch thick. They are 'non-gold-backed' and are attached to the substrate using 'Elecolit'[28] 325 conductive epoxy.

Chip interconnection metallisation and bonding pads (0.004" square) are of aluminium and connections to the substrate are made with 0.0007" diameter ultrasonic bonded aluminium wire.

The basic oscillator configuration of figure 4.1.1 is used for all channels. Centre frequency selection is achieved by the use of a variety of values of NPO capacitors in the 0805 case size. Fine tuning is achieved by the use of a tapped timing resistor, provided with bonding pads to permit sections to be shorted out by ultrasonic wire bonds. Harmonic filtering for different frequencies is achieved by the use of fixed resistor values and different values of appliqued chip capacitors. These may be of a hi-K dielectric, and are again of the 0805 size.

4.2 Temperature Channel Design

As mentioned in Section 2.1, studies of the fight/flight syndrome in Gallus Domesticus would be facilitated by telemetry of the avian shank skin temperature. This area, which is not covered by feathers, shows considerable variation in surface termperature in response to vaso-motor changes associated with the fight/flight response. Avian

skin temperature responses have been previously telemetered (Duncan et al 1975) using earlier single channel devices (Filshie and McGee, June 1974). This has been done using externally mounted bead themistors to sense skin temperature, and similar responses have been obtained using a similar themistor just underneath the skin. In this case, the thermistor leads were run sub-dermaly up the shank to a transmitter implanted under the abdominal skin. Experience gained with these devices indicates that a temperature measurement range of 30 to 40°C is suitable for this application, and that typical skin temperature responses can be variations of the order of 1°C occurring within a period of about 30 seconds.

An excellent transducer for this application is manufactured by Yellow Springs Instruments[29], who produce a range of high-precision semiconductor thermistors with an epoxy encapsulation. These devices are about 2mm diameter, have a high sensitivity and are interchangeable with a maximum temperature error of 0.2°C over a range of 0°C to 80°C. A relatively high value of resistance is required for this application, to minimise current consumption and self-heating effects. A suitable thermistor is part number 44015, having a resistance of 1MΩ at 25°C and 603.6kΩ at 35°C, the mid-point of the required temperature range.

The time-constant of the device is defined as the time required to indicate 63% of a new impressed temperature and has a value of 10 seconds maximum in free air,

with the thermistor suspended by its leads, and 1.0 second maximum in a 'well-stirred' oil-bath. These values are, of course, increased where the device is further encapsulated for implanted applications. A typical value of 5 seconds is obtained when the device is wax-dipped and coated in about 0.5mm silicon rubber.

Thermistors of this type have an exponential resistance/temperature characteristic, which may be described by the relationship:

$$R_{(t)} = ae^{b/t} \qquad \ldots\ldots 4.2.1$$

where $R_{(t)}$ = resistance at temperature (t)

a = a constant

b = the 'b-value' of the thermistor

The b-value of the thermistor is effectively a measure of its sensitivity, and has been defined by Becker (1946) as:

$$b = \frac{\ln \left(R_{(t_2)} / R_{(t_1)}\right)}{1/t_2 - 1/t_1} \qquad \ldots\ldots 4.2.2$$

where $R_{(t_1)}$ and $R_{(t_2)}$ are the thermistor resistance values at temperatures t_1 and t_2 respectively.

The b-value is thus a function of both the device characteristics and the temperature range involved. The b-value of the type 44015 device operating over the 30 to 40°C range may be evaluated from the manufacturers' published data as being equal to 4673°K.

Although thermistors of this type have an exponential resistance/temperature characteristic, they may be used in conjunction with a series resistor in a half-bridge

circuit, to produce an output voltage which is a relatively linear function of temperature. The half-bridge output voltage (e_o) is then given by:

$$e_o = \frac{R_T}{R_T + R_r} E_v \qquad \ldots\ldots 4.2.3$$

where R_T = thermistor resistance

R_r = series resistor

E_v = bridge supply voltage

Beakley (1951) has shown how the half-bridge output voltage may be optimally linearised over any defined temperature range by setting:

$$R_r = \frac{b - 2T_o}{b + 2T_o} R_o \ \Omega \qquad \ldots\ldots 4.2.4$$

where R_o is the resistance of the thermistor at the midpoint temperature (T_o) of the range, and b is the b-value in ^oK, evaluated over the appropriate range according to equation 4.2.2.

Beakley has also derived the following expressions for the maximum output temperature error (e_{max}) and the half-bridge current/temperature sensitivity $\frac{dI}{dt}$ (opt), of the optimised half-bridge:

$$e_{max} = 0.03 h_o^3 b^2 / T_o^4 \ ^oK \qquad \ldots\ldots 4.2.5$$

where h_o is the temperature increment (i.e. Range = $T_o \pm h_o$)

$$\frac{dI}{dt}(opt) = \frac{E_v(b+2T_o)^2}{4T_o^2 \, bR_o} \left(1 - \frac{h_o^2 b^2}{12T_o^4}\right) \mu A/^oC \qquad \ldots\ldots 4.2.6$$

When the foregoing expressions are evaluated for the 44015 thermistor over the temperature range from 30 to 40^oC the following results are obtained:

b-value = 4673°K (from 4.2.2)

R_r = 463 kΩ (from 4.2.4)

sensitivity = 138.3 μA/°C (from 4.2.6)

max. error = 0.07°C (from 4.2.5)

If the half-bridge is energised from a 5.4 volt supply, then the mid-point (T_o) output voltage is 3.05 volts, and the voltage output over a 30 to 40°C range is 650mV. Since the total resistance of the half-bridge is in the region of 1MΩ, the bridge current will be about 5μA, and the power dissipated in the thermistor will be about 0.015mW. The dissipation constant of the thermistor is quoted as 1mW/°C in still air, and 8mW/°C when immersed in oil. Even in still air, therefore, the temperature due to self-heating will be of the order of 15×10^{-3}°C.

The 650mV range of voltages appearing at the output of the half-bridge, over a thermistor temperature range of 30 to 40°C, lies well within the linear portion of the voltage/frequency characteristic of the VCO section of the CD 4046. Where a 5.4 volt supply voltage is used, this will result in a sub-carrier frequency deviation of ±16.2% i.e. a modulation sensitivity of 3.24% per °C is obtained.

As mentioned in section 4.1, the maximum frequency drift over the working life of the battery, is anticipated to be in the region of 6%, which is equivalent to a possible temperature error of 1.85°C. This could be expressed as an error of 18.5% of FSD, which is an unacceptably high figure. If, however, a second sub-carrier oscillator is used to monitor the line-voltage variations, then their

two centre-frequencies will track closely together ($\pm$0.6%) over the working life of the battery. If, at the receiver, the output of the sub-carrier discriminator of the temperature channel is referred to the output of the discriminator monitoring the supply-voltage channel, rather than to ground, then the resulting error in the estimate of temperature should be reduced to around 0.26^{o}C. This is equivalent to an error of 2.6% FSD, which is quite an acceptable level for this application.

Obviously, an alternative approach would be to zener stabilise the transmitter power supply, and thus minimise the frequency drift. This would, however, involve running a sufficiently high zener current, to exploit the low dynamic-impedance portion of the reverse characteristic.

The use of a 'reference channel' sub-carrier oscillator, as outlined above, can result in an additional current drain of less than 80μA, and can provide a continuous external indication of the state of charge of the battery pack. This is a particularly useful feature for implanted devices, since the anticipated implanted life of the device could be severely reduced, by failure of the encapsulation. In many multi-channel applications, there will be no need to provide an additional reference oscillator for the temperature channels, since the mean centre-frequency of an AC coupled data-channel could well be used as a reference.

The temperature channel outputs at the receiver could then be referred to a voltage level derived from the output

of the AC coupled channel, by the addition of a buffer stage and an integrating network with a long time constant.

In line with the modular layout approach outlined in Section 3.7, a reference oscillator was included within the 2cm x 1cm area of the temperature telemetry module. This permits the module to be used independently as a single channel telemetry transmitter, since the module also includes an RF carrier oscillator stage. Adequate area for the reference oscillator is available within the module dimensions since, for this application, the thermistor half-bridge may interface directly with the data sub-carrier oscillator. The reference oscillator therefore occupies an area equivalent to that which would be allocated to the pre-amplifier of a bio-potential module.

It was felt desirable in the first instance to fabricate each module of the multi-channel system on a separate 2cm x 1cm substrate. This improves the production yield of the multi-channel devices, by minimising substrate complexity. The circuit diagram of the temperature telemetry module is illustrated in Figure 4.2.1, and the thin-film layout is shown in Figure 4.2.2.

The time constant of the encapsulated thermistor (5 seconds) implies a maximum data bandwidth of 0.032 Hz. If a minimum sub-carrier modulation index of 5 were required (as in the IRIG proportional bandwidth specifications), then the sub-carrier centre frequency could be as low as 0.16Hz. The use of such low frequencies is, however, impractical because of the large areas which would be

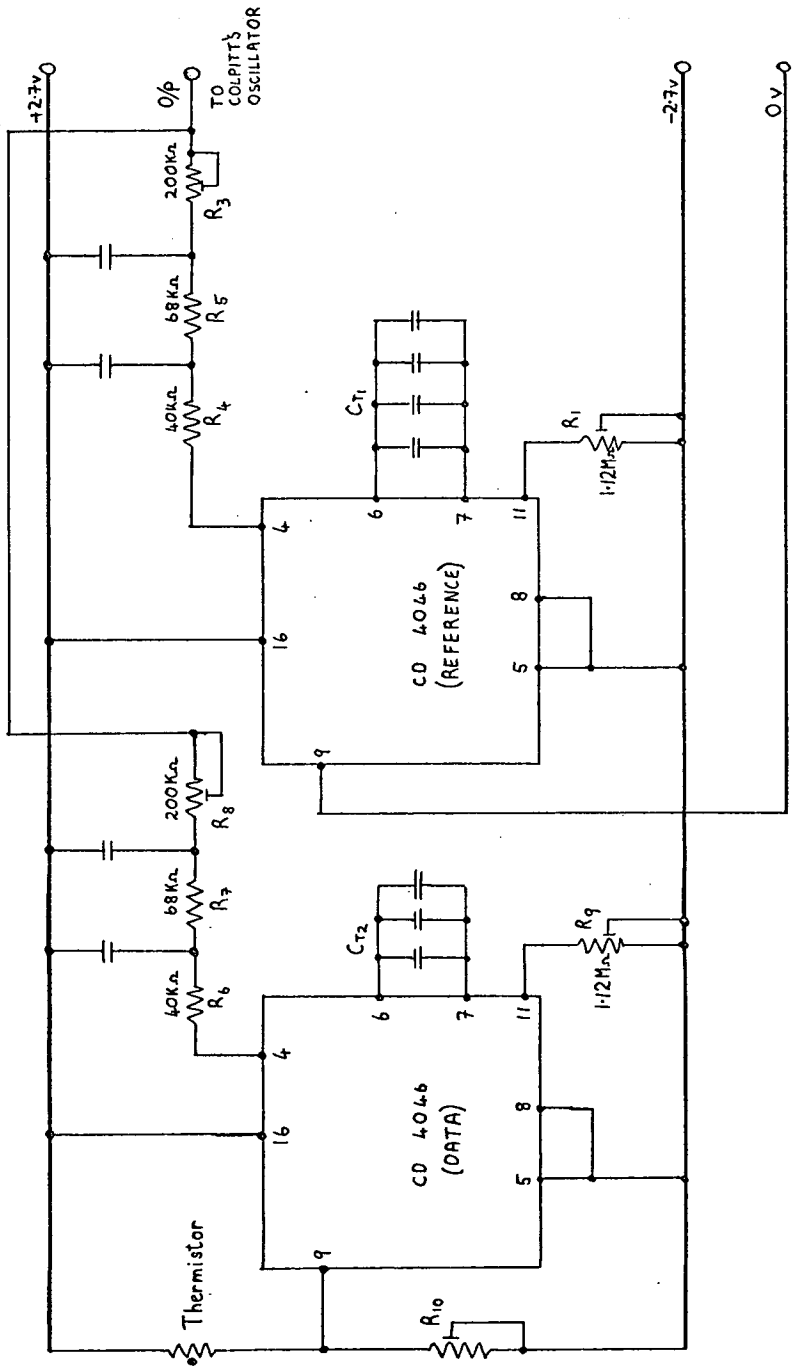

Figure 4.2.1 Temperature Module: Schematic Diagram

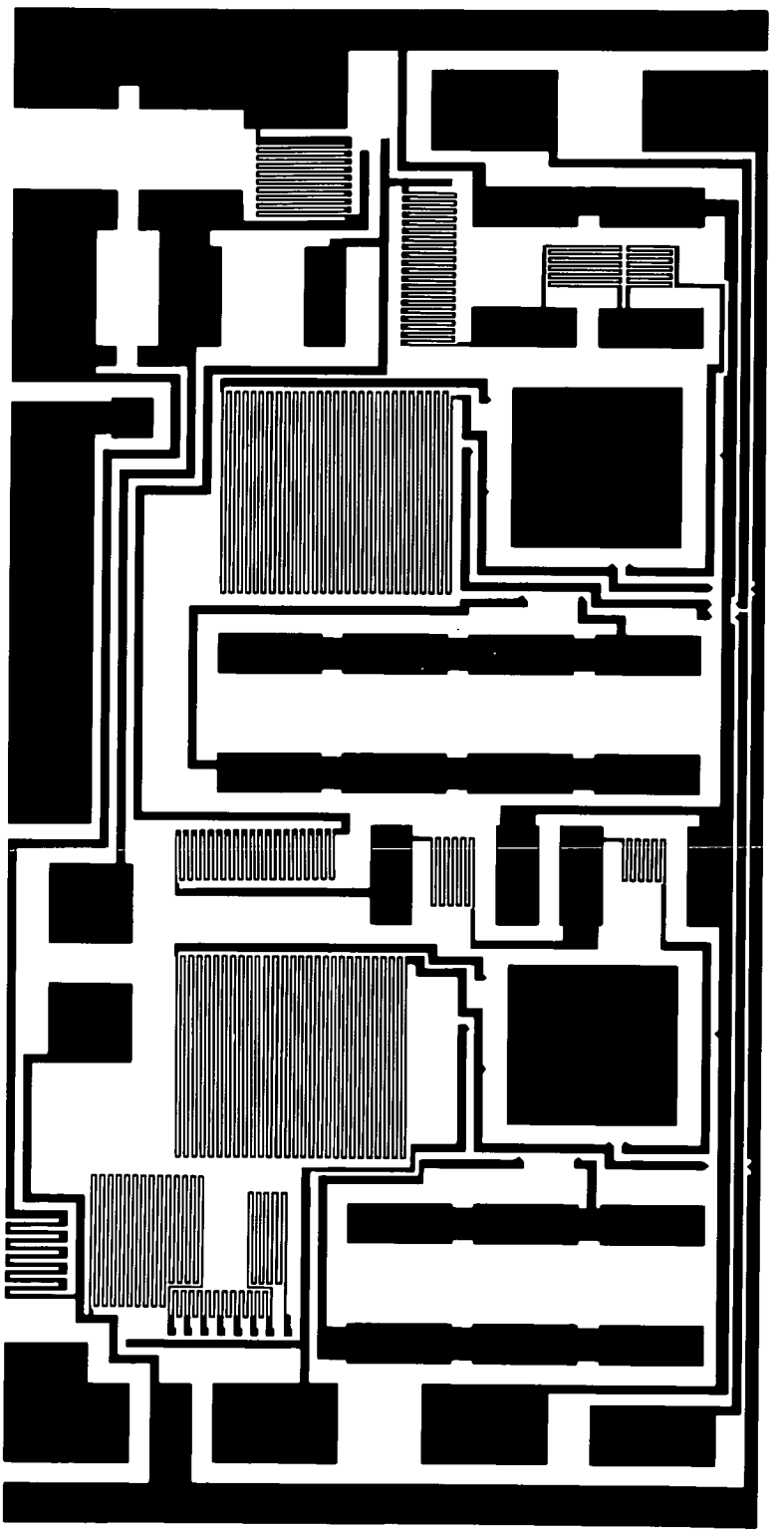

Figure 4.2.2 Temperature Module:
Thin Film Layout

occupied by the frequency determining components. In order to minimise power consumption it is desirable to use a high value of timing resistor.

The provision of gold bonding-pads at the end of each zig-zag track permits the centre-frequency of the individual sub-carrier oscillators to be adjusted, by the use of ultrasonic-bonded shorting links. These pads can also improve the yield on the production of etched substrates, since any open circuit track may be shorted out and the odd short-circuit between tracks may be tolerated. The maximum value of the timing resistors R_1, R_9 as laid out in Figure 4.2.2 is 1.12 MΩ where 200Ω/square substrates are used. This results in a total current consumption for the module of less than 100μA, depending on what timing resistor taps are used. For good frequency stability, it is desirable that high-stability NPO dielectric timing capacitors should be used (C_{T1}, C_{T2}). Although these are available in values of up to 180,000 pF, the largest value obtainable in the most commonly stocked size (0805) is 680 pF.* Provision has therefore been made for use of up to four of these in parallel (2720 pF) for the reference oscillator, and up to three in parallel (2040 pF) for the data oscillator. The nominal minimum centre frequencies of the reference and data oscillators are therefore 164Hz and 218Hz respectively. Since the half-bridge output over the 30 to 40°C range deviates the sub-carrier by 32.4% (equivalent to a 70Hz deviation) the minimum sub-carrier modulation index is 2,200, and an excellent signal-to-noise ratio may therefore be anticipated at the channel output.

*See addendum page 156.

The harmonic filter capacitors may be of the general purpose high-capacitance dielectric type, and values of up to 39,000 pF are available in the 0805 case size. The filter resistors, R_4, R_5, R_6, R_7, need not therefore be very large at these frequencies, except to minimise the power dissipated in them. Values of 40kΩ and 68kΩ were used, since these fit neatly between the capacitor bonding pads. Where relatively wide centre-frequency deviations are used, the capacitor values must be chosen to give adequate harmonic suppression at the lower frequency limit. The amplitude of the fundamental component appearing at the filter output will therefore vary with the centre frequency. This is not expected to be troublesome because of the wide range of input signal amplitudes accepted by the phase-locked sub-carrier discriminators (see Section 4.6). The resistors R_3 and R_8 across the outputs of the harmonic filters, are provided with taps in the same way as the timing resistors. This permits adjustment of the relative amplitudes of the individual components of the multiplexed sub-carrier signal appearing at the input of the RF carrier oscillator. Signal-to-noise ratio performance may thus be 'traded' between the individual channels of a multi-channel system since different RF modulation indices may be provided for each channel, if desired. One major constraint is that the peak-to-peak amplitude of the multiplexed signal must not be such as to cause significant over-modulation of the RF carrier signal. For the Class II oscillator described in Section 1.5, a maximum value of

about 4mVp-p may be used. The criteria used in defining 'significant' over-modulation are fairly arbitrary, since the problem is statistical in nature. The subject is, however, well documented by Downing (1964)*, who investigates the amplitude probability distributions of ensembles of sine waves, whose phases are uncorrelated. A commonly used criterion is that the peak deviation is not exceeded for more than 1% of the time.

The thin film layout includes an integral resistor, R_{10}, forming part of the thermistor half-bridge. This resistor is also provided with taps to permit optimal thermistor linearisation over other defined temperature ranges, in response to possible future applications.

No provision has been made in this circuit for limitation of the data sub-carrier frequency deviation, by the diode clamping method referred to in Section 4.1. This was felt to be hardly worthwhile for the following reasons. The assymetrical voltage-swing at the half-bridge output would necessitate the provision of a reference potential for the diode-clamp. The low sub-carrier frequencies of the temperature channels means that a bandwidth of twice their centre frequencies could well be allocated and would still leave adequate base-bandwidth for the small number of other data-channels liable to be required in the near future.

4.3 ECG Channel Design

Avian ECG signals detected by sub-cutaneous electrodes are of too low an amplitude (180μV peak-to-peak) to modulate

* 127-131

the sub-carrier oscillator described in section 4.1, without preamplification. When the performance of a data-channel based on the use of CD 4046 devices as both the sub-carrier oscillator and the sub-carrier discriminator was investigated using a discrete component breadboard, satisfactory performance was achieved using the IRIG recommended sub-carrier frequency deviation of ±7.5%, at centre frequencies of greater than about 14.5kHz (i.e. on channels above number 13). Use of lower frequency channels than this would therefore require the use of greater percentage deviations. Where a 5.4 volt supply is used, deviations of ±7.5% are achieved with a voltage input to the sub-carrier oscillator of ±150mV. A suitable 'window' for the avian ECG signal has been found previously to be a range of about ±150μV at the preamplifier input terminal. A preamplifier gain of about x1000 (60dB) is therefore suitable for this application. Higher gains will be required where lower frequency, higher deviation sub-carrier channels are used.

With some ECG electrode placements, signal interference due to 'muscle noise' can occur. This interfering signal can be of greater amplitude than that of the wanted ECG signal and also contains harmonic components at frequencies above 200Hz. Both of these factors will cause a broadening of the sub-carrier frequency spectrum, and the possibility of adjacent channel interference, where these are closely spaced in the frequency domain. It is, therefore, desirable to constrain both the amplitude and frequency range of the voltage input to the sub-carrier oscillator. This may be achieved by diode clamping and low-pass filtering.

AC coupling of ECG preamplifier input leads is desirable to minimise electrolytic effects, isolate the amplifier from the high and variable offset potentials associated with the electrode/tissue interface, and to simplify circuit design. High quality tantalum capacitors have adequately low leakage currents for this application, and these are available in chip form in capacities of 10μF in a conveniently small size. Extremely long input time-constants are not required for the relatively fast avian ECG signal, and amplifier input resistances of 100kΩ, giving an input time-constant of 1 second, have previously given excellent results when used with implanted silver wire loop electrodes.

Differential-input preamplifiers are not essential for this application since the use of an isolated implanted telemeter provides adequate rejection of common-mode signals. At present, interest in the avian ECG signal is centered principally on its fundamental rate variation, and the truly bi-polar recording techniques used, for example in vectorcardiography, are not required. Simultaneous multichannel ECG recording could, however, be helpful, insofar as the use of a number of dispersed electrode sites could help to avoid loss of rate information where the ECG signal from an individual electrode is swamped by 'muscle noise'. This could be achieved by use of a number of single-ended-input preamplifiers used in conjunction with a common, implanted, remote-reference electrode, of sufficiently large area to present a low common-circuit impedance.

A single-ended preamplifier was therefore designed

around a triple operational amplifier integrated circuit chip manufactured by Siliconix[30] under type number 4144. This particular device has a number of features commending its use for biological applications.

The current consumption of all three operational amplifiers is set by the value of a single external resistor which controls a triple current-mirror. The frequency response of the amplifiers is a function of their current consumption. Where a narrow bandwidth is required, extremely low consumptions may be achieved. Typically a -3dB bandwidth of 4kHz is achieved for a total current consumption of 70μA per chip (3 amplifiers). A 1.7kHz bandwidth requires only 30μA. Although lower bandwidths may be required for some applications, the use of currents of less than about 30μA require the use of inconveniently large values of external resistors. The ECG preamplifier/subcarrier oscillator circuit therefore consumes about 110μA. Each individual amplifier has a differential input, permitting use of a variety of feed-back configurations, and a single-ended output. Low-frequency open-loop gains of up to 80dB are available from each amplifier and direct coupling is used throughout. The amplifiers do not, however, incorporate an offset-nulling adjustment. For this particular ECG preamplifier application, offset considerations necessitate the use of two AC coupled gain stages. Although the third amplifier is not therefore strictly necessary in this application, it is used to considerable advantage in the design of the EEG channel described in section 4.4, and

for the present small volume production requirements there are advantages in minimising the number of different ICs to be stocked. The circuit diagram of the ECG preamplifier module is illustrated in figure 4.3.1., and the actual lay-out of the resistor and conductor mask is shown in figure 4.3.2. The resistor values indicated on the diagram represent the maximum values of the resistor tracks on the mask. Since adequate space was available within the module size, many tracks were made longer than necessary for the avian ECG application, and these were provided with gold bonding-pads to permit adjustment to the desired values. The etched substrates may therefore be used for a range of other applications, without modification.

The diodes included in the feedback network of the final amplifier produce a 'soft-limiting' of the output signal amplitude at a level of around ±500mV. This results in an effective peak frequency deviation of the sub-carrier oscillator of around ±25%. The potential divider resistor R4 is provided with optional bonding taps permitting the deviation to be limited to ±25%, ±15%, ±10% or ±5%, as desired. The soft-limiting action of the diodes results in an effective 'volume compression', of signals approaching the 500mV level at the output. Where necessary an equivalent 'volume expansion' function may be performed at the data-channel output by the use of a similar diode/resistor combination, with the appropriate signal amplitude. It is desirable to limit the preamplifier pass-band by use of a capacitor across the feed-back resistor, rather than by limitation of the amplifier current consumption. This

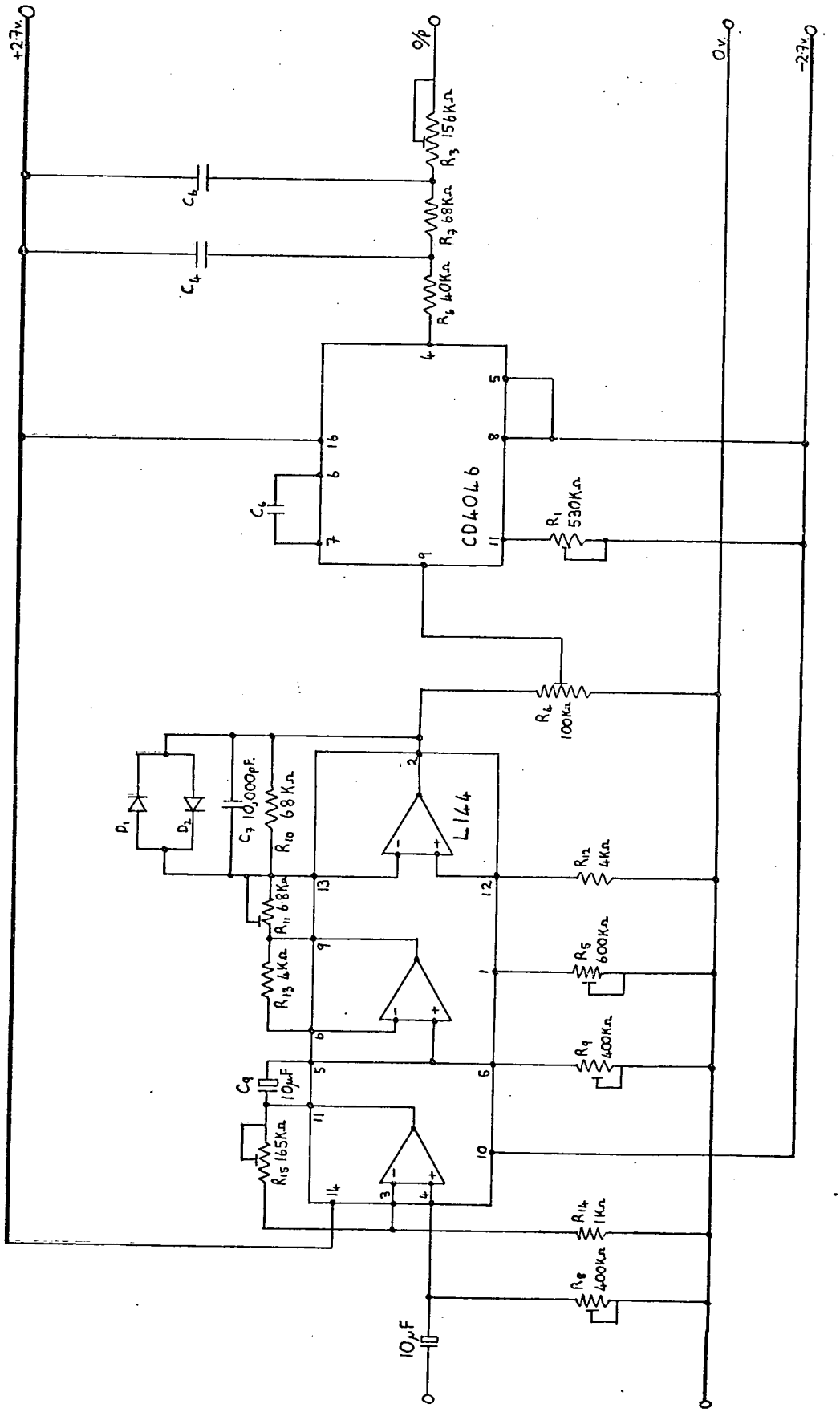

Figure 4.3.1 ECG Preamplifier: Schematic Diagram

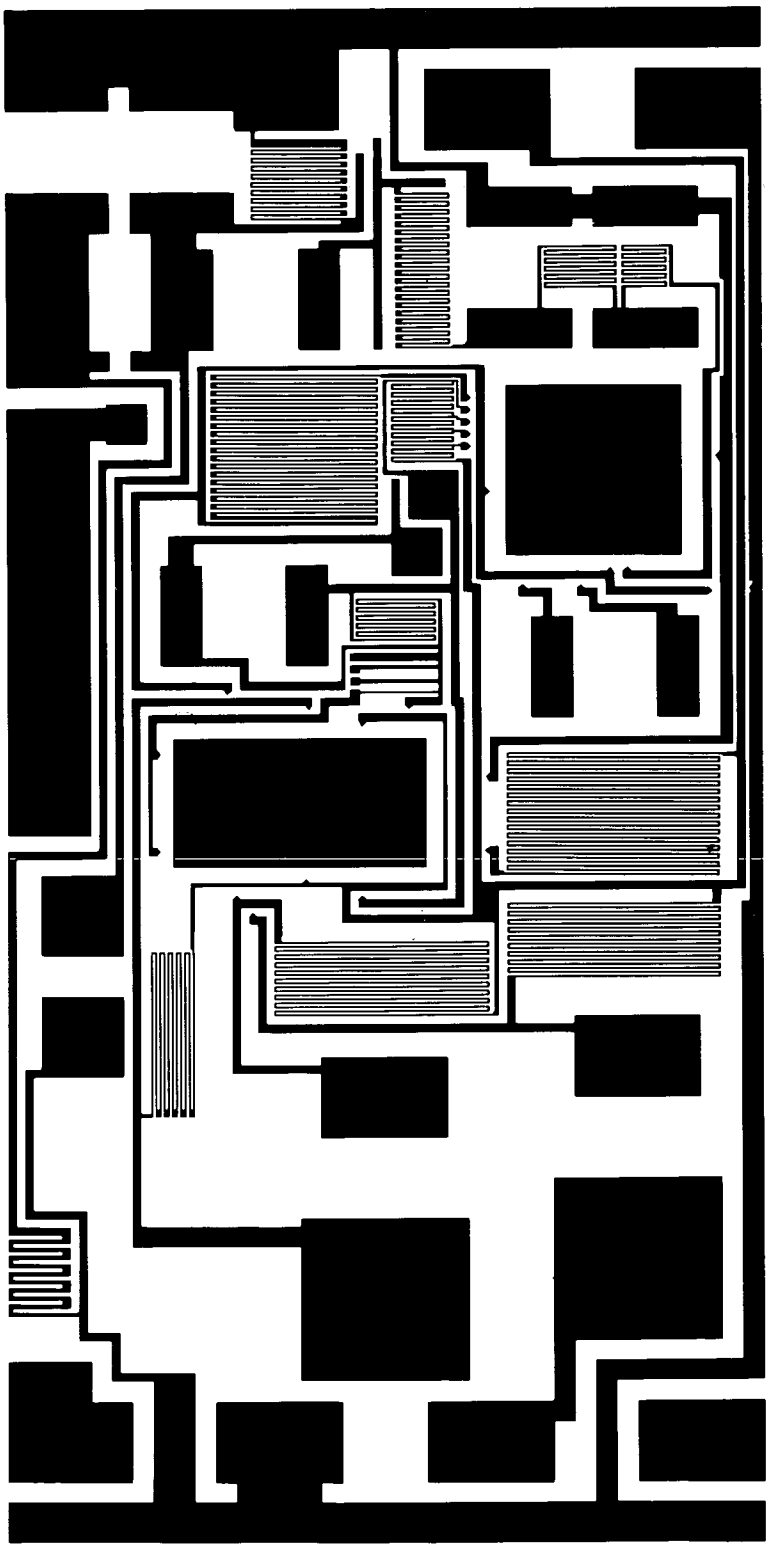

Figure 4.3.2 ECG Module: Thin Film Layout

minimises distortion of signal waveforms approaching the cut-off frequency, since limitation of the supply current produces an apparently slew-rate-limited triangular waveform at high-frequencies. One further point in this design is that the resistor R5 which determines the current consumption, is returned to the zero volt line rather than to the positive supply line, as described in the manufacturers' literature. While this will increase the variation of current consumption with temperature, much lower values of resistor may be used.

4.4 EEG Channel Design

Avian EEG signals from implanted needle electrodes were investigated using a single channel device mounted on the skull of a bird. A high input-impedance was required because of the extremely small active area of the needle electrodes used. These are made of silver and have a tip radius of 100μ. A 10MΩ input impedance was therefore required in order to expand the low-frequency response to about 1Hz. This was achieved by the addition of an n-channel junction FET to the front end of the biopotential telemetry device described by Filshie & McGee (June 1974). Experience gained with this device indicated that a suitable 'window' for the avian EEG was a voltage range of ±75μV at the preamplifier input terminals.

The significant bandwidth of the avian EEG extends from about 1Hz to about 60Hz. Occasionally spikes of about 1 millisecond duration may be observed in EEG traces, and where these are of interest a frequency response extending

to about 2kHz would be useful. Particular interest exists at present in components of the avian EEG signal lying around 3 to 4Hz, since these appear to be related to the state of alertness of the bird (Personal Communication - Dr M. Gentle). The traces received from the single channel devices, however, showed small base-line shifts correlated with rapid head movements. It proved difficult to distinguish these from the signals of interest and it could not be readily established whether these shifts were due to movement artefact potentials appearing at the input terminals, or to RF carrier frequency shifts.

Accordingly, the EEG preamplifier whose circuit diagram is shown in figure 4.4.1 was developed. Apart from providing the possibility of multichannel operation, the use of a sub-carrier data-channel will avoid artefacts due to RF carrier shifts and movement artefact potentials should be attenuated further by the high common-mode rejection, of the differential input preamplifier used.

The final two stages of the preamplifier are identical in design and function, to those used in the ECG design of section 4.3, and are connected to give a voltage gain of ten times.

An additional L144 device is, however, used for the EEG channel, and when this is used in the configuration shown in figure 4.4.1, realises a number of significant performance improvements over more conventional design.

The common-mode rejection ratio of conventional differential input operational amplifier designs is a function

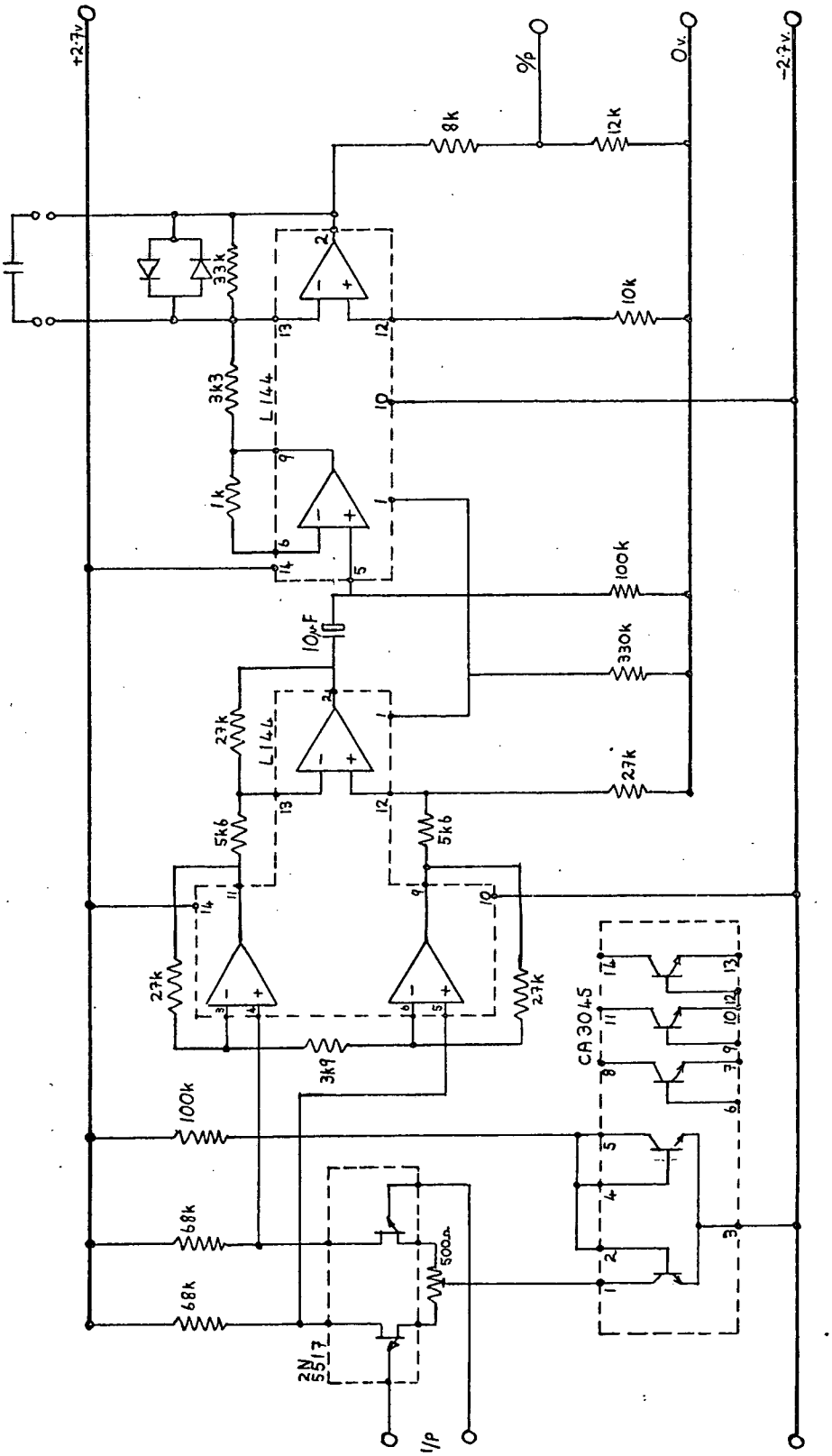

Figure 4.4.1 EEG Preamplifier : Circuit Diagram

of the matching of the two pairs of gain-determining resistors. Where 0.1% tolerance components are used, a common-mode rejection ratio as low as 54dB could result from the resistor mismatch alone. (Electronic Engineering, December 1973, p12).

The common-mode rejection ratio of the 'triple-op-amp' configuration used is much less dependent on resistor matching since the common-mode rejection ratio of the output stage, which is determined by the matching of the two 5.6kΩ and the two 27kΩ resistors, is improved by the gain of the preceding amplifier stages. The gain of these stages may now be adjusted by variation of the 3.9kΩ resistor alone. The input impedance of this configuration is high, being equal to the common-mode input impedance of the operational amplifiers themselves, which is typically in excess of $10^8\Omega$. Significant bias currents (typically 200nA) must however be sunk from the bipolar input devices and this precludes direct coupling to the electrodes themselves. If ac coupling to this stage were used, resistors would have to be provided to sink the bias currents. Input impedances of greater than 10MΩ are, however, required to avoid loading the small diameter needle electrodes (60μ) to be used in future investigations, and so allow the desired low-frequency response to be obtained.

The use of such high values of input resistor would produce unacceptably high input offset voltages, where a high stage gain and operation from a low supply-line voltage (5.4v) are required.

The performance of an n-channel junction field-effect transistor input stage was therefore investigated, since their low leakage currents (typically less than 0.1nA) would permit direct coupling to the electrodes. The configuration illustrated in figure 4.4.1 was found to give a performance adequate for this application. The device type 2N5517 has an excellent low-frequency noise performance (less than $40\mu V/Hz^{1/2}$) and matched pairs are available in un-encapsulated form from Siliconix[30] under the chip type number CDNS01. The performance of a number of pairs of 2N5517 discrete devices was investigated using the long-tailed pair differential amplifier configuration illustrated. The use of the CA3045 monolithic transistor array as a current-mirror supplying the 'tail' improves the common-mode rejection ratio of the stage. Small variations in the forward characteristics of individual devices give rise to an offset voltage across the matched drain-load resistors. The inclusion of a small 'degeneration' resistor in the source circuit as shown, permits this voltage to be 'backed off' by an appropriate choice of tapping point along the resistor. For all pairs of devices tested, it was established that the maximum common-mode rejection ratio (i.e. optimum ac matching) was achieved when the output offset voltage was adjusted to zero. The current consumption of the input stage may be readily adjusted by altering the value of the 100kΩ resistor supplying the CA3045 device.

The voltage-gain, common-mode rejection and noise performance of the FET input stage may all be improved by

increasing its current consumption. With the component values shown, a voltage gain of ten with a common-mode rejection ratio of 69dB was achieved for a current of about 25μA per transistor. The total consumption of the input stage, including the current-mirror, is therefore around 100μA.

As mentioned in section 4.3, the current consumption and frequency response of the L144 devices is set by the value of an external resistor. In this EEG preamp design, this resistor supplies current to both chips and is returned to the zero volt line. The value of 330kΩ as shown, produced a current consumption of about 42μA per chip, and a slew-rate limited frequency response extending to about 2.3kHz. When this was limited to 1kHz by the feedback capacitor across the diodes, a total input referred noise level of 2μV peak-to-peak was measured. Bandwidth limitation to 100Hz, reduced this figure to 1.5μV. The current consumption of the entire preamplifier is therefore around 185μA. The performance obtained is seen to be limited by the need to minimise power consumption and where an improved performance is required this may be readily obtained by the provision of tapping points on the current determining resistors.

The gain of the DC coupled input stages as shown is about 6600 times. Input offset potentials (due to electrochemical effects at the electrodes) of up to about 2mV can therefore be accommodated, at the expense of a reduced common-mode rejection. This EEG preamplifier is more

complex than either the Temperature or the ECG module described previously. Attempts to achieve a satisfactory thin-film layout within the 2cm by 1cm 'module size' have indicated that the components will fit in, but time has not permitted a satisfactory layout to be achieved as yet.

4.5 Remote Switch Design

The preamplifier/sub-carrier modules described in the previous sections of this chapter were designed to realise the desired performance with the lowest power consumption possible within the constraints imposed by the performance of the available active devices and the hybrid production process itself. Nevertheless, the working life of multi-channel devices constructed with these modules is limited by the relatively small capacity of suitable battery packs. A capacity of 167mA hours is about as much as can be obtained without the use of a package, inconveniently large for implantation in chickens.

The current consumption of a three channel device consisting of two ECG channels and one temperature channel, used in conjunction with a 500μA Colpitts oscillator, would be in the region of about 810μA. This would give a useful range of about 15m and a working life of around 200 hours. Since this is inconveniently short for many studies, and since 24 hours of data per day is seldom required, a device capable of switching an implanted transmitter on and off would be useful.

A magnetically actuated bi-stable reed switch marketed under the name 'Logcell', by FR Electronics[31] appeared to

be an attractive solution to the problem, and the performance of these was investigated. The devices were, however, expensive, fragile and actuating them from distances greater than about 1cm required the use of inconveniently large permanent magnets.

The extremely low leakage currents of 'COSMOS' devices combined with their low output resistance made the use of a D-type flip-flop (CD 4013), as a solid-state switch, seem attractive. The possibility of triggering these by means of a burst of RF energy, was therefore investigated, and the circuit illustrated in Figure 4.5.1 was eventually found to give a performance adequate for this application. Since the CD 4013 device is in fact a Dual D-type flip-flop, it was connected to provide a 'divide-by-four' function. This permits independent control of two transmitters, or preamplifiers if desired. The controlled device is connected from the positive line to the CD 4013 outputs, to take advantage of the fact that the 'on' resistance of the n-channel output transistor (200Ω) is less than that of the p-channel output transistor (400Ω).

The burst of RF is generated by a hand-held actuator which consists of a resonant circuit, a micro-switch and a 60v battery. A 20,000pF capacitor charged to 60v is discharged by the microswitch through a rectangular loop antenna. The antenna consists of a single turn of heavy gauge copper wire, whose dimensions are 8cm by 4cm. The resulting RF pulse consists of a damped oscillation at about 2.5MHz. It was found possible to switch the D-type flip-

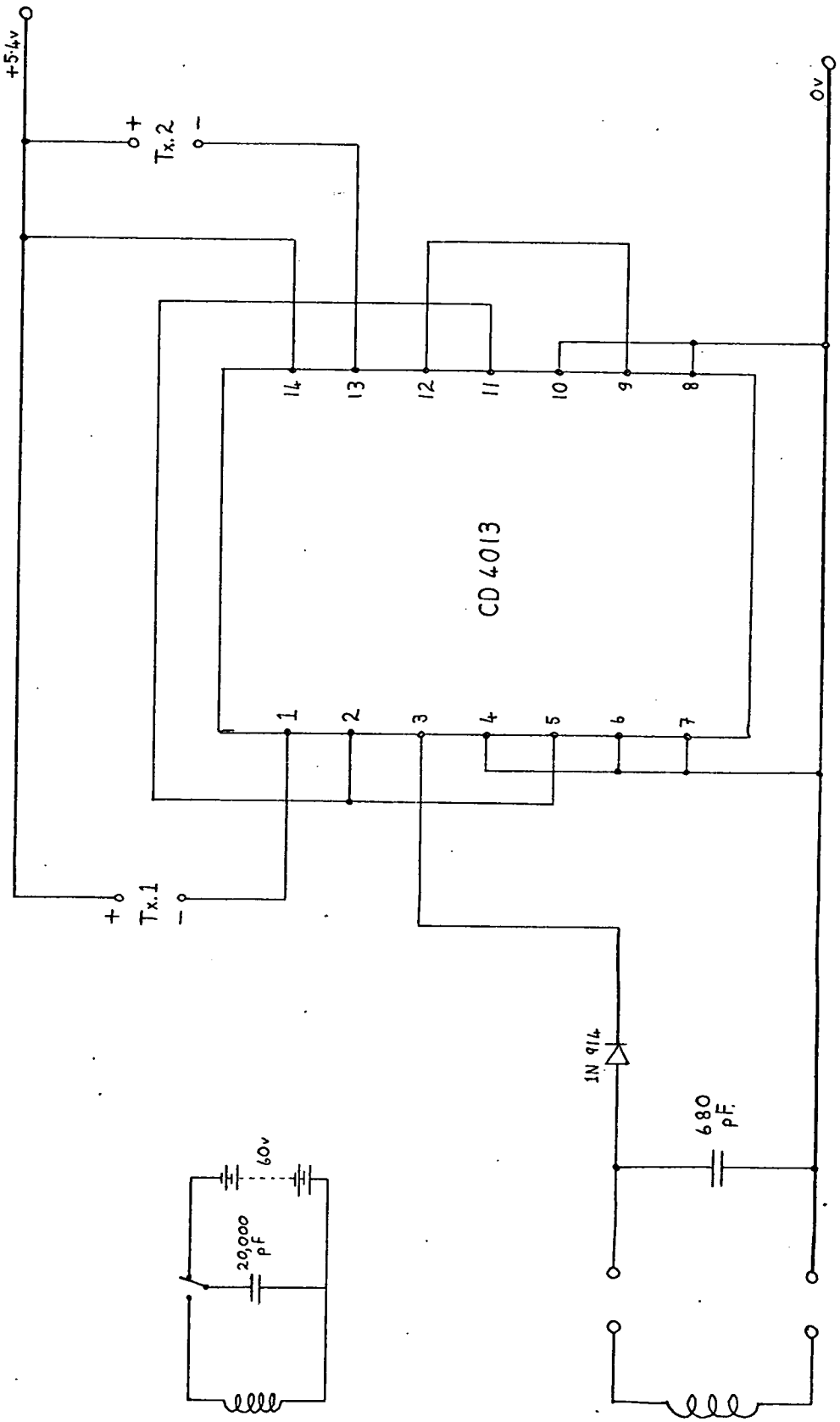

Figure 4.5.1 Remote Switch: Schematic Diagram

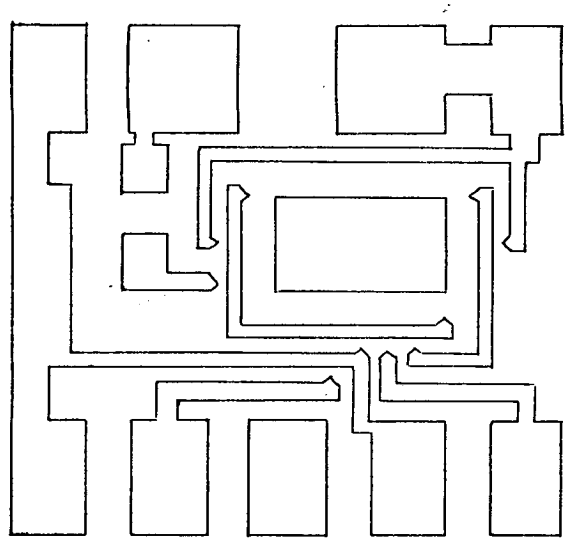

Figure 4.5.2 Remote Switch: Thin Film Layout

flop by means of the pulse appearing at the output of a 'crystal set'. The receiving antenna consists of 30 turns of 36 swg enamel covered wire pile-wound on an Aladdin former type 8A-4387 fitted with an R7 grade 6mm ferrite core. A parallel capacitor of 680pF permits the antenna to be tuned to resonance at 2.5MHz using the ferrite core. The half-wave rectified pulses charge the input capacitance of the flip-flop (5pF) and reliable switching from a distance of around 10cm has been observed to occur. The devices were fabricated in thin-film hybrid form, using unencapsulated flip-flop and diode chips. The substrate size is 6mm by 6mm. The thin-film layout is illustrated in Figure 4.5.2 from which it can be seen that the bulk of the area is occupied by the bonding pads for external lead wires. A considerable area reduction could therefore be achieved where the device can be integrated with the controlled transmitter on the same substrate. When the receiving antenna is implanted sub-dermally, the range of the actuator is reduced to around 5cm. The leakage current of the CD4013 device is around 5 nano-amps at 5v, and a drive current of around 1mA is available from the device.

4.6 Sub-Carrier Discriminator Design

The signal appearing at the output terminals of the radio receiver consists of an ensemble of sinewaves of different frequencies, each frequency modulated by the appropriate message waveform. The function of the sub-carrier discriminators is to retrieve the desired message waveforms with the minimum of distortion, noise, and

crosstalk between channels. A design, typical of the approach used by most workers in the past, is described in some detail by Fishler (1967). He uses an emitter-follower input stage to avoid loading the IF frequency discriminator. This is used to drive a bank of series resonant circuits, each tuned to the appropriate sub-carrier frequency channel. These filters are connected in parallel to the output of the emitter-follower limiter stage. Sub-carrier frequency discrimination is then performed by two parallel driven amplifier stages driving resonant circuits, each slightly de-tuned in opposite directions. The two outputs are then amplitude-detected, added differentially and filtered by a low-pass pi-network filter, to retrieve the desired message waveforms.

An alternative method of recovering the desired message waveforms involves the use of 'phase-locked loops' as sub-carrier frequency discriminators. The subject of phase-locked FM demodulation has been treated in detail by Gardner (1966). Since then, a number of manufacturers have produced monolithic silicon integrated circuit phase-locked loops. The use of a single IC for this application results in a considerable reduction in receiver complexity, and is attractive because of the relative simplicity with which they may be set up for different sub-carrier centre-frequencies, and deviations.

The performance of the RCA COSMOS CD 4046 phase-locked loop was investigated and found to be well suited to this application.

Full design data for FM discriminators using the CD 4046 deviceare published by the manufacturers in Data-File number 637 and Application Note number ICAN-6101. These data were used to design a bank of six sub-carrier discriminators, and these were bread-boarded using discrete plastic DIL packaged devices. The centre-frequency and lock-range of each device was made adjustable by the use of two trimming resistors, and NPO timing capacitors were used. Single-pole loop filters were used and satisfactory performance over the initial design lock-ranges (±10%) was achieved with input signal amplitudes down to about 30mV peak-to-peak. Operation from low-level input signals such as these is achieved by biasing the phase comparator II input to the mid-point of the supply lines, and AC coupling the input signal. Higher level input signals are required where wider sub-carrier deviations are used. Typically, a 300mV input signal level is required for ±90% deviation. Relatively high signal amplitudes are available from the demodulated signal output of the Leak Delta FM tuner (about 3.0v for 50kHz deviation). For the majority of multichannel applications, therefore, the peak-to-peak amplitude for satisfactory capture performance of the CD 4046 sub-carrier discriminators. These devices, however, are capable of locking on to signals outwith their design lock-ranges. This is a function of the type of phase comparator used. A 'phase locked' condition can arise where the VCO capture frequency range covers an harmonic of a low-frequency input signal. The VCO may then run at an

integer multiple of the low frequency input signal.

This is a situation which could well cause trouble in multichannel FM sub-carrier discriminators, where the frequency-multiplexed signal is applied to a bank of parallel driven discriminators. Where relatively wide sub-carrier deviations are used, as is desirable in this bio-telemetry application, it may prove impossible to ensure that the bandwidth of a high-frequency channel does not cover a harmonic of a low frequency channel. Crosstalk or interchannel interference may therefore occur even although the harmonic content of the low frequency sub-carrier is negligible. In order to eliminate this effect, it is necessary to attentuate the amplitude of any such low-frequency sub-carrier signals to a level where the 'capture-effect' will permit satisfactory demodulation of the intended sub-carrier signal. This may be achieved by including a band-pass filter in front of the phase-locked loop discriminator. A high level of signal-suppression is not required, and it was found that an active filter configuration with a Q of 10 eliminated crosstalk to imperceptible proportions. The CD 4046 is provided with a low-impedance buffered output, and data bandwidth limitation may be provided by a suitable time constant applied to this terminal.

Time has not permitted a fuller investigation to be carried out into the optimisation of the discriminator and filter designs, and this will require further attention, particularly where wide deviation sub-carrier channels with narrow guard-bands are required. For present applications,

where only a few data-channels are required, these may be widely spaced within the base-bandwidth available, and relatively simple filter designs should ensure adequate performance.

CONCLUSION

The preceding chapters summarise investigations carried out by the author into the feasibility of producing a multichannel radio telemetry system compatible with chronic implantation in small animals, and the GPO Class II telemetry regulations. Some aspects of RF propagation from implanted devices are considered in Chapter I, and the design of a practical thin film hybrid RF oscillator is presented. The results of investigations into message and channel bandwidths are reported in Chapter II, and reasons are given for the choice of an FM/FM multiplex system.

Various miniaturisation techniques are assessed in Chapter III and the argument in favour of the subtractive thin film hybrid approach is presented. Some aspects of the hybrid technology which lead to constraints in circuit design are also considered. On the basis of the preceding work, a number of component modules of a multichannel system were designed, and some features of these are described in Chapter IV. It is intended to use these modules to construct multichannel telemeters for specific applications. The performance of the whole telemetry system using these transmitters 'in vivo' will then be assessed, and the results obtained will be used to optimise sub-carrier and RF modulation parameters, to suit particular applications.

At the present time, these modules are at different stages of development. A large number of Colpitt's carrier oscillators have been built, and many of these were used,

at 102.36MHz, to replace the 30MHz carrier oscillator used on the devices described by Filshie and McGee (June, 1974). Considerable experience has now been gained in the implanted use of these single channel Class II transmitters and many thousands of working hours have been logged by these Colpitt's oscillators. The earliest of these were fitted with Ferranti[32] μE transistors type BFS46, and later oscillators were built using an equivalent unencapsulated chip transistor, in order to gain experience in chip mounting and wire-bonding techniques. These devices have also performed well in use.

The remote switch described in section 4.5 was chosen as the first device to be produced using unencapsulated 'COSMOS' integrated circuit chips. The production yield on these devices was initially low, and many working devices subsequently failed. The principal production difficulty was associated with the very poor quality of the aluminium metallisation of the chip bonding pads. The spongy nature and poor adhesion of the aluminium film made the ultrasonic wire bonding parameters difficult to optimise. The use of pulsed thermocompression gold wire bonding improved the yield on these early devices. A second batch of 'COSMOS' CD4013 devices purchased more recently showed a much higher adhesion of the chip metallisation and ultrasonic wire bonding is now being used, with a high yield on the finished devices. A few of these switches have been implanted with single channel telemetry devices, and reliable external triggering has been achieved.

When it was felt that sufficient experience had been gained in the handling of unencapsulated COSMOS integrated circuit chips, a start was made to the production of the ECG and Temperature telemetry modules, described in sections 4.3 and 4.2 respectively. At present, about a dozen substrates have been etched to each of the two patterns. These were the first substrates to use the reduced resistor track line width of 25μ and, from the results obtained, a yield of better than 75% is anticipated on the evaporation/photo-lithography process, when the devices are in small batch production. So far, two substrates of each type have been fully bonded up, and all four produced a satisfactory performance.

Both of these modules incorporate a Colpitt's oscillator, which is functionally identical to that described in section 1.5, although the thin film layout is slightly different. The layout change has not significantly affected the performance of the oscillator. Detailed functional tests are at present being performed on these devices, and the initial indications are that all the sub-carrier oscillators produce the anticipated centre-frequencies and deviations. The frequency tracking, with respect to supply line voltage variations of the data and reference channels of the temperature devices, was found to be in the region of 14% ±2% per volt, and the frequency deviation for the designed 10°C range (30°C to 40°C) was measured as ±25%.

The preamplifier sections of the ECG devices were

found to produce the anticipated voltage gains, and frequency responses. The next stage of this work will therefore be to complete the functional tests after the devices have been encapsulated and to gain some experience of the performance of the devices 'in vivo'.

A final layout for the EEG telemetry module has not yet been arrived at, since it was decided to proceed initially with the construction of the two less complicated modules, in order to gain experience of any problems associated with the applique techniques used. Initial layout attempts on the EEG circuit indicate that all components will fit within the 2cm by 1cm module size, but that this represents about the ultimate in packing density that can be conveniently achieved with presently available components.

FUTURE DEVELOPMENTS

The devices described in section 4.2 and 4.3 are considerably more complex than any produced before in this department. Experience gained in etching and bonding of the prototype devices produced to date indicates that they can be produced in quantity with an acceptably high yield. Once data on the overall telemetry system performance has been obtained, then individual data-channel modulation parameters may be modified to optimise the utilisation of the available RF bandwidth. Multichannel devices could then be produced on single substrates, if necessary, in response to requirements for specific combinations of input parameters.

One refinement which would be much appreciated by users of the devices, and which could be fairly readily incorporated into a multichannel system, would be to include an internal calibration function within the telemetry transmitter itself. The IRIG proportional bandwidth telemetry specifications include details of how such a system might operate. (Stiltz 1961). A similar system could be readily implemented in an implanted transmitter, since the use of the remote switch and actuator described in section 4.5 will enable four different modes of operation to be controlled externally. These modes could be:

1. OFF
2. TUNE
3. CALIBRATE
4. DATA

In the 'TUNE' mode, all sub-carrier oscillator input terminals could be shorted to the zero-volt line by, for example, field-effect transistors. In this condition all sub-carrier data channels will produce their centre frequencies. This will permit accurate alignment of the individual sub-carrier discriminators at the receiver output.

In the 'CALIBRATE' mode, an internally generated standardising signal could be applied to all channel inputs. Such a signal could be a low-frequency square-wave of convenient amplitude, generated by a 'COSMOS' multivibrator. This test signal would permit amplitude calibration of the sub-carrier discriminator outputs, and would also allow the frequency responses of the individual data-channels to be readily checked.

In the 'DATA' mode, the actual data signals appearing at the channel inputs would be telemetered. Implementation of this type of system would lead to a slight increase in transmitter complexity, which could well be acceptable because of its utility. An alternative approach, which has much to commend it in some applications, is to dispense with manual remote actuation and to include an internal low-frequency multivibrator to perform the switching function. This could be used with or without the TUNE/CALIBRATE function, to produce a sampled data system, and to prolong the life of the battery pack.

Although the investigations of previous chapters have been concerned with multichannel operation within GPO Class

II regulations, the work relating to bandwidth occupancy of FM signals could be used to interface the FM sub-carrier modules to a number of alternative RF transmitters. Multichannel operation under Class I conditions is obviously quite straightforward as a very wide RF bandwidth is available.

In Class III operation a peak RF frequency deviation of ±5kHz is permitted, and if a wide base-bandwidth were required a poor signal-to-noise ratio at the receiver output could be anticipated. Estimates of the usable base-bandwidth must therefore be based on a thorough examination of the threshold performance of the sub-carrier discriminators used.

Operating licences have recently been granted to users of equipment at 173MHz and at 458.6MHz. Higher RF power levels, viz 10mW and up to 500mW respectively, can be permitted at these frequencies, and the greatly increased range permits the devices to be used for animal tracking experiments in open country. Once again, the FM sub-carrier modules could be interfaced with these devices to permit simultaneous tracking and monitoring of physiological parameters.

Transmitters operating under Class III conditions or at 173MHz or 458.6MHz, currently employ bulk crystal oscillators with multipliers and drive stages, and may therefore only be used with larger animals because of their size and power consumption.

Investigations into the design of RF oscillators,

stabilised by Surface Acoustic Wave devices, are currently being made, and initial results indicate that no fundamental difficulties are involved. The development of such oscillators at 102, 173 and 458.6MHz will open new fields of application for biological telemetry devices, both in intensive care units and with small animals in their natural environments.

A further useful feature of SAW devices is that they may be designed with two output transducers. If these structures are laid out with their finger spacings one quarter of a wavelength apart, then two output signals with a 90^{o} phase-shift may be directly generated. These could be used to drive mutually perpendicular antennae and the resulting circularly polarised radiation field should virtually eliminate signal drop-out, for all transmitter orientations.

APPENDIX I

THIN-FILM HYBRID CIRCUITS

Extracts from
Filshie and McGee (April/May, June 1974)

VACUUM DEPOSITION

A. Equipment

Vacuum deposition of resistive, conductive and insulating films is carried out in a CVC 20E vacuum system. The chamber furniture consists of a heated substrate holder and a Bir-Vac RG II ring-gun with a source-changing mechanism and a shutter. A glow discharge cleaning ring is fitted, and quartz crystal and sheet resistance monitoring facilities are provided. This equipment was constructed largely in the workshops of the Poultry Research Centre and has proved highly reliable in service.

B. Electron-beam gun operation

Two modes of operation of the electron-beam gun are possible, and these may produce films with different properties.

THE DE-FOCUSSED MODE

The crucible may be raised out of the focus of the electron stream, into a position where its side walls are bombarded. Evaporation of material takes place from the evaporant surface, with an energy distribution similar to that in thermal evaporation, i.e. peaking at energies of around 0·2 eV for source temperatures of 2,250°K.[9] The gun may be run under either space-charge-limited conditions, e.g. 250 mA and 1·0 kV, or emission-limited conditions, e.g. 55 mA and 4·5 kV. The evaporation rate and energy distribution is a function of the electron-beam power and is the same for either power-supply condition.

THE FOCUSSED MODE

The crucible may be lowered to a position where the electron stream is concentrated on a small area of the evaporant surface. The thermal resistance of the evaporant and the small spot-size attainable allow much higher effective source temperatures, for the same beam power, than in the de-focussed mod e. Unstable, rate-runaway conditions can occur at high evaporation rates with high electron acceleration voltages. This is due to ionising collisions caused by the focussed electron beam passing through the evaporant vapour. This is to be expected because at practical evaporation rates vapour pressure of the evaporant immediately above the crucible is high (1·3 N/m²) and the mean free path is about 5 mm.[10]

For most metals it is necessary to operate this region, to obtain practical evaporation rates. They can be achieved if the beam current is emission-limited and the evaporation rate is controlled via the filament supply current.

C. Ni-Cr deposition

80:20 Nichrome wire is melted in a shallow amorphous carbon crucible, using an electron-beam spot size of about 10 mm. When the crucible is full the Ni-Cr has a convex upper surface. During deposition, however, the spot is focussed to about 1 mm diameter. This results in the erosion of only a small area of the Ni-Cr surface, the bulk of the evaporant remaining in the solid phase. In view of the similarity of this process to alloy sublimation, film compositions similar to that of the bulk material might be expected.[11] However, films of 200 Ω/square prepared in this way on 7059 glass substrates at 300°C have been shown by X-ray fluoroscopic analysis to have a mean composition of 63:37. This view of the evaporation process is therefore clearly an over-simplification, and significant atomic mobilities must exist within the evaporant, permitting preferential evaporation of the Cr.

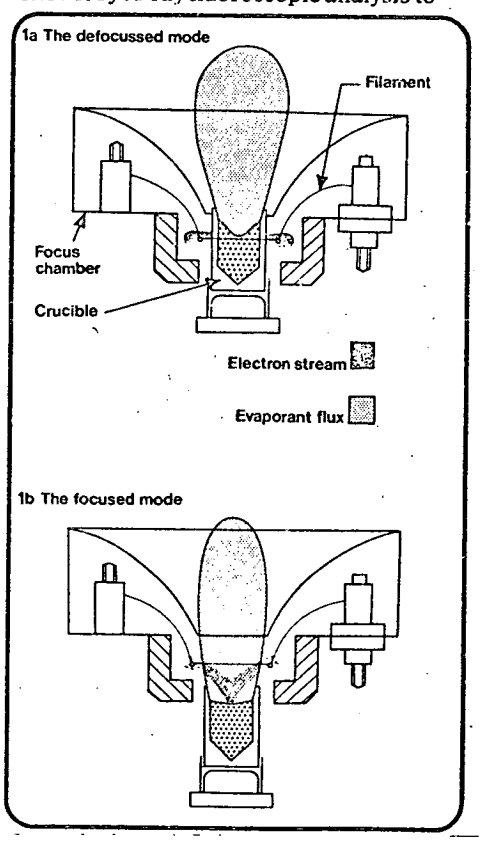

1 Electron beam gun operating modes
1a De-focused mode
1b focused mode

This mode of deposition yields film Temperature Coefficients of Resistance (TCR) which are positive and usually < +100 ppm/°C. If the crucible is topped up with more 80:20 wire, and the contents are melted uniformly as before, the evaporant will become progressively Ni-rich from evaporation to evaporation. This has been observed to result in a mean film composition of 74:26 after about 10 evaporations, with a consequent increase in the positive TCR to around 170 ppm/°C. Both of these TCRs are higher than one would expect from the measured percentage compositions. This indicates significant oxidation of the Cr in the deposited film.[12] This interpretation is supported by the fact that post-deposition ageing at 300°C in air for 12 h causes sheet resistance changes of only around 5%.

The temperature of the front surface of substrates increases during film deposition, due to radiation from the source and the kinetic and condensation energies of the evaporant atoms. Since all of these factors are related to the electron-beam-gun operating conditions, which are manually controlled, the substrate temperature towards the end of a deposition is both unknown and subject to variation from run to run. The source is therefore shuttered shortly before the monitored sheet resistance reaches its intended value. This allows the substrates to cool to 300°C. A drop of up to 1·5% in the monitored sheet resistance, over a period of about 1 min, is usually observed at this stage. If this change is due entirely to a reduction in substrate temperature, an assumed film TCR of +100 ppm/°C implies that substrate temperatures of up to 450°C can be reached. Breitweisser *et al.* report similar temperature rises.[13]

When the monitored sheet resistance stabilises at its 300°C value, a series of brief exposures to the source is made until the desired sheet resistance is attained. Both evaporation rate and accelerating voltage are observed to affect the monitored conductivity. This effect is significant only during exposure to the source and with sheet resistances greater than 10 kΩ/square. There is some evidence that this is due to ion-induced conductivity in the glass substrate. However, since the effect is insignificant at sheet resistances of 200 Ω/square, it has not been investigated further.

D. Ni-Cr substrate interface

Ni-Cr film adhesion to 7059 glass substrates is excellent provided that the substrate temperature is sufficiently high to provide the activation energy required for the oxidation of the initial Cr-rich deposit at the oxygen-rich substrate surface.[12] Electron-beam-evaporated Ni-Cr films have been found to pass the 'Scotchtape Peel Test'[10] when deposited on substrates at above about 150°C. At a substrate temperature of 300°C the film cannot be physically separated from the glass. This may indicate that the energy of formation of Cr_2O_3 is greater than the binding energies of the materials themselves.

These high adhesions are obtainable only on clean substrates and it has been found essential to eliminate the contamination which can occur during source degassing, even with the source shuttered. The evaporants are therefore degassed before loading the substrates into the chamber.

Since cross-contamination of the sources can occur, it is essential that the Ni-Cr crucible be degassed after the Au crucible, as Au contamination of the substrate adversely affects the Ni-Cr film adhesion.

E. Au deposition

Gold wire is melted in a molybdenum crucible and thoroughly degassed. The degassing routine includes the evaporation of gold at twice the desired film deposition rate. This reduces the incidence of particulate ejection of material from the evaporant, which can be troublesome, particularly in the focused mode of operation.

Gold has a vapour pressure of 1·3 N/m² at the fairly low evaporation temperature of 1,397°C. It can therefore be readily evaporated in either the focussed or the de-focussed mode. With the focussed beam accelerating voltages above 3kV can cause runaway conditions if deposition rates greater than about 3·5 nm/s are attempted. Although use of the de-focussed mode largely eliminates this, film adhesions are lower.

F. Au/Ni-Cr interface

This interface is of the diffusion or pseudo-diffusion type.[10] Gold film adhesion is consequently a function of the diffusion or penetration of gold into the Ni-Cr layer. Etching of the gold film using an iodine/potassium iodide etchant also removes the Ni-Cr which was in solid solution in the gold at the interface. The difference between the sheet resistance of the Ni-Cr as deposited and after gold etching is an indication of the interface depth. This has been found to be a function of:-

1. Substrate temperature during gold deposition.
2. Time spent by the substrate at elevated temperatures.
3. Gold deposition rate.
4. Gold film thickness.
5. Gold arrival energies.

The effects of these variables have not been studied in detail, but it has been observed that films of down to 200 Ω/square can be entirely dissolved during over-energetic deposition of gold on substrates at 300°C. Gold film adhesion will in general improve with increasing interface depth. If, however, the interface extends to the substrate surface, film adhesion drops to a low level. The achievement of high and predictable Ni-Cr sheet resistances, together with high levels of

gold adhesion, is therefore critically dependent on the control of all the variables listed above. One may expect the resistivity of the gold film to be increased by the incorporation of either Ni or Cr, by 0·8μ Ω/atomic per cent in the case of Ni, and by 4·65μ Ω/atomic per cent in the case of Cr.[14]

G. SiO_2 evaporation

After etching, the Ni-Cr resistor tracks are protected by the evaporation of SiO_2 from an amorphous carbon crucible. This produces a protective glass layer about 1μm thick over the entire substrate. This film is tenacious, transparent and easily etched in buffered hydrofluoric acid, to produce windows for access to bonding areas. It acts as a hermetic seal for the Ni-Cr tracks, improves their long-term stability[15] and inhibits the electrolytic corrosion which can occur to Ni-Cr when subjected to a dc voltage gradient in the presence of moisture. Its deposition causes less than 1 % change in the Ni-Cr sheet resistance and no measurable change in the Ni-Cr TCR. This may indicate that no further significant exidation or re-structuring of the Ni-Cr is caused by its deposition.

The use of this protective layer has enabled a cheap epoxy package to be used for implantation applications with increased confidence.

H. Standard 200 Ω/square process

The evaporation parameters described in this section are those used for the metallisation of substrates for use in the implantable telemetry devices to be described in part 2. A high Ni-Cr sheet resistance is required to simplify circuit design at low supply currents, and high film adhesion is required for reliable component attachment.

Thirty 7059 glass substrates 25 × 13 mm (1·0 × 0·5 in) are cleaned by ultrasonic agitation for 20 min in a 5 % Decon 90 solution. This is followed by a de-ionised-water rinse. The substrates are blown dry with filtered N_2, loaded into the vacuum chamber and given a final dusting with filtered N_2. These operations are carried out under Class 100 laminar-flow conditions.

The vacuum system is then evacuated to $6·6 \times 10^{-5}$ N/m² and the substrates heated to 300°C. A glow-discharge is then struck in a 6·6 N/m² argon atmosphere and run at 200 W for 15 min. The chamber is again pumped out to $6·6 \times 10^{-5}$ N/m² before film deposition is commenced.

Ni-Cr is deposited at 0·05 nm/s to a sheet-resistance of 168 Ω/square at 300°C. This is done in the focused mode at 40 mA and 4·5 kV (180 W).

Gold is then deposited at 1·5 nm/s to a thickness of 0·5μm; this is done in the focused mode with a 50 mA beam current at 4·5 kV (225 W).

If SiO_2 evaporation is being performed, the cleaning procedure described above is carried out on substrates bearing the etched conductor and resistor patterns. The film is grown at 1·3 nm/s to a thickness of 1·0 μm. This is done with a focused beam of 75 mA at 4·0 kV (300 W).

PROCESS CONTROL

The yield from the evaporation and photolithographic processes is a function of the surface quality of the incoming substrates. A surface scratch as small as 50 μm long and 10 nm deep can completely sever a resistor track. Since such defects are only visible under a microscope, it is considered uneconomic to scan all substrates in this manner. Only a visual inspection for gross defects is therefore performed before film deposition. Great reliance must therefore be placed on the supplier's cutting and packing methods. Thus inexpensive substrates, if of poor quality, can prove to be a false economy.

The metallised substrates are microscopically inspected, with back illumination for pinholes which could cause open circuits, and with oblique illumination for particulate contamination which could damage the emulsion mask.

The sheet resistance of the Ni-Cr layer is checked at this stage by etching a gap in the Au layer of the central metallised substrate of the array, and measuring the resistance and dimensions of the exposed Ni-Cr area. The Au film thickness of the same metallised substrate is also measured on a Talysurf.

Film adhesion is tested on a second metallised substrate by scratching with a scalpel blade, while viewing microscopically, and by pull-testing a 14 SWG copper wire, butt soldered to the film. Acceptable adhesion results in a conchoidal fracture in the glass.

PHOTOLITHOGRAPHY

The initial circuit-layout artwork is cut in Rubylith*, on a coordinatograph, at 20 × final size. A normal integrated circuit first-reduction process is used to produce an emulsion mask on a 50·8 mm square plate.

The following procedure effectively uses an etched gold pattern as a high adhesion, in-contact mask for the Ni-Cr etchant and minimizes undercut in the Ni-Cr pattern. Variability of undercut of the gold layer affects the Ni-Cr track widths so produced. Since the gold layer is 0·5 μm and the Ni-Cr tracks at present in use are 50 μm wide, this presents no problem. The tendency of the Ni-Cr etchant to penetrate pinholes is also minimized by the two layer mask (Au + photoresist).

The following photolithographic processes are carried out in a humidity- and temperature-controlled environment.

Shipley** AZ135OH photoresist is used for the metal etching. Because of its positive working nature, only a single coating is required for exposure to the two masks involved. Resist is spun on at 3,000 rpm for 30s, air dried and given a low temperature bake. Optimum photoresist exposure and development times are established before processing each batch of metallized substrates. This minimizes line width variation due to variation in the viscosity of the photoresist, the intensity of the ultra-violet source and the activityof the developer.

The resist film is then exposed through the

* *Ulano Graphic Art Supplies Inc, New York*
** *Shipley Chemicals Ltd, Coventry*

first mask, which consists of the resistor and conductor patterns. The developed photoresist pattern is then rinsed, dried and examined under a microscope before the first etch is performed. This is done under filtered illumination, to avoid exposure of the photoresist. Any faulty patterns are stripped and reprocessed.

The unprotected gold is removed in an iodine/potassium iodide etchant and the Ni-Cr is etched with a ceric sulphate/sulphuric acid etchant. The metallization patterns are examined after this first etch. Open circuit patterns are rejected and short circuit patterns may be stripped and reprocessed.

The substrate is then exposed through the second mask, which contains the conductor pattern only. After development the gold is removed from the top of the previously-etched resistor tracks, which are then examined under a microscope for pinholes, etc, and for any deviation from design line widths. Any significant Ni-Cr undercut after the standard Ni-Cr etch process indicates a reduced film adhesion at either the Ni-Cr substrate interface or the Au/Ni-Cr interface.

All circuits passing this final inspection are probed manually and the resistance of all Ni-Cr tracks are tabulated. Shipley AZ resist stripper is used after etching and the substrates are rinsed in de-ionized water and blown dry before being returned to the vacuum chamber for deposition of the protective glass layer.

Contact windows are subsequently produced in this layer by a similar photolithographic technique, using Kodak Thin Film Resist, and a buffered hydrofluoric acid etchant. The change to a negative working resist at this stage avoids the use of a darkfield mask, with its inherent alignment difficulties.

Ni-Cr track resistance values are again tabulated and compared with their previous values. Substrates showing deviations of more than $\approx 5\%$ are rejected as potential failures. Open circuit Ni-Cr tracks occasionally occur at this stage. The mechanism involved is not understood at present, but may be due to Ni-Cr mobility or oxidation during the SiO_2 deposition at points where damage to the substrate surface had caused a localized weak spot in the Ni-Cr film.

The line widths of 50 μm at present in use are fairly easily achieved with this process, and overall yields greater than 75% can be obtained on the film deposition and photolithography processes.

DEVICE ATTACHMENT

Miniature chip capacitors with ceramic and tantalum dielectrics are available from a number of manufacturers. This makes it possible to produce circuits using capacitors from $\approx$ 3 pF to 100 μF. Active devices in the Ferranti micro-E package, toroidal inductors and ceramic trimming capacitors are also at present in use.

All these components and the connecting wires to the substrates are reflow soldered to the substrate bonding pads using a hot nitrogen jet. The circuits are then probed and dc levels are tabulated. An ac function test is also carried out before and after encapsulation.

The principal cause of failure of devices after encapsulation appears to be solution of the gold metallization in the solder joints. This is not associated with the initial bonding operation which is easily controllable within fairly wide limits. If, however, a solder joint is remelted during the attachment of an adjacent component, de-wetting will eventually occur associated with oxidation of the Ni-Cr surface. This produces a joint which may be visually and electrically satisfactory but prone to subsequent failure.

A hot-work ultrasonic chip bonder has been designed and constructed by the Poultry Research Centre workshops. This together with a K & S Model 484 ultrasonic wire bonder, enables current design work to be based on the use of face up bonded integrated circuit chips.

ENCAPSULATION

The earliest transmitters to be implanted were encapsulated in a rectangular-section glass envelope with crimped glass/metal seals for battery and transducer leads. The encapsulated device was similar in appearance to an EA50 valve but somewhat larger. The antenna coil was a circular loop of 30 mm diameter, mounted externally to the hermetic encapsulation.

Current devices, on 25 × 12·5 mm (1·0 × 0·5 in) substrates, are potted in glass-filled diallylpthalate boxes which are 8 mm deep, and can incorporate flush-mounted sockets for external leads. These boxes also contain a 12 mm square antenna. The box is then half filled with silicone rubber and the device is set to the desired carrier frequency by use of the trimming capacitors. The box is then filled up flush with a two-part epoxy potting resin.

For implantation the box and its external battery pack are dip-coated in silicone rubber to eliminate biological rejection of the device (Fig 1). This encapsulation has proved satisfactory in use, although it is of finite aqueous permeability. Devices have been implanted for up to two months without deleterious effects.

Some devices potted in paraffin wax, instead of the silicone/epoxy package, have recently been implanted and appear satisfactory in use. It is hoped that the lower water-permeability of the wax will prove beneficial in this application and its low melting point allows the carrier frequencies to be set conveniently, by use of a hot screwdriver.

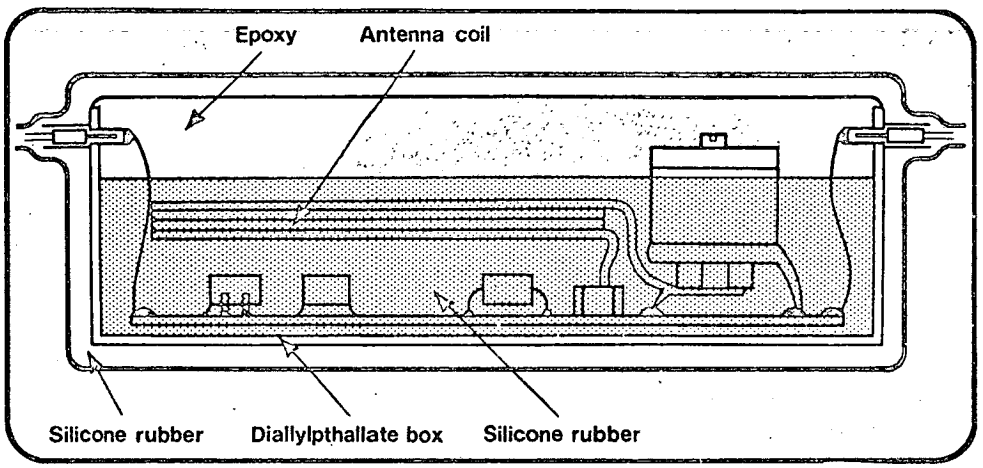

1 Cross-section of encapsulated device

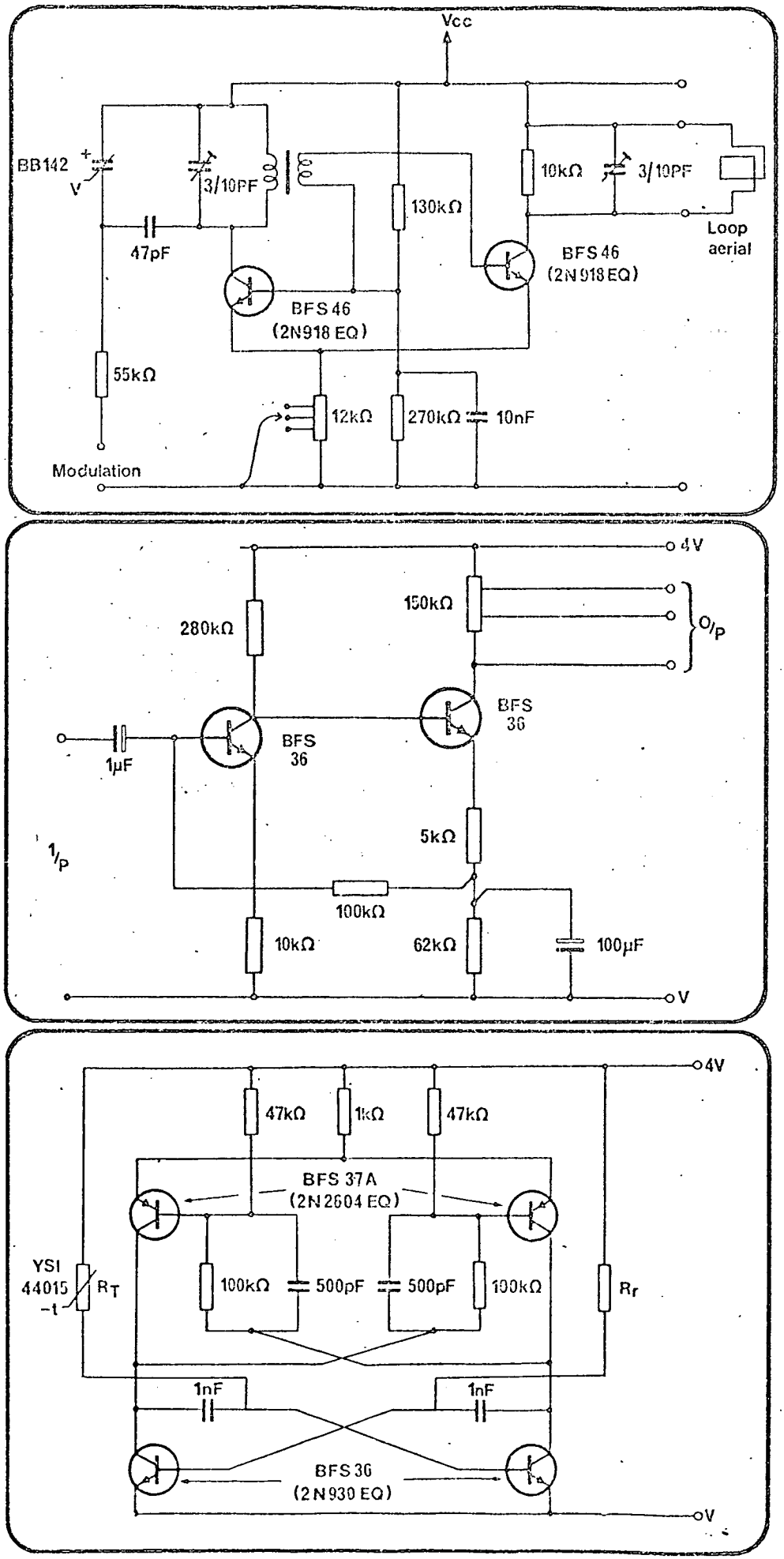

2 'Tempsens' and 'ECG' device schematics

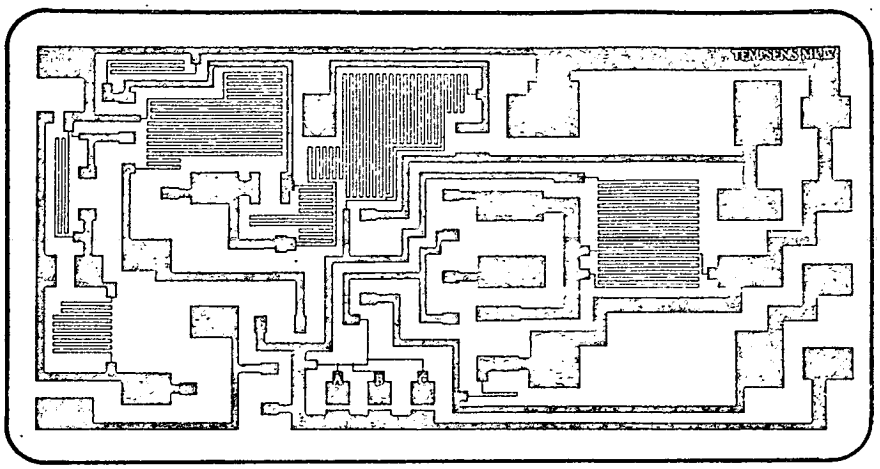

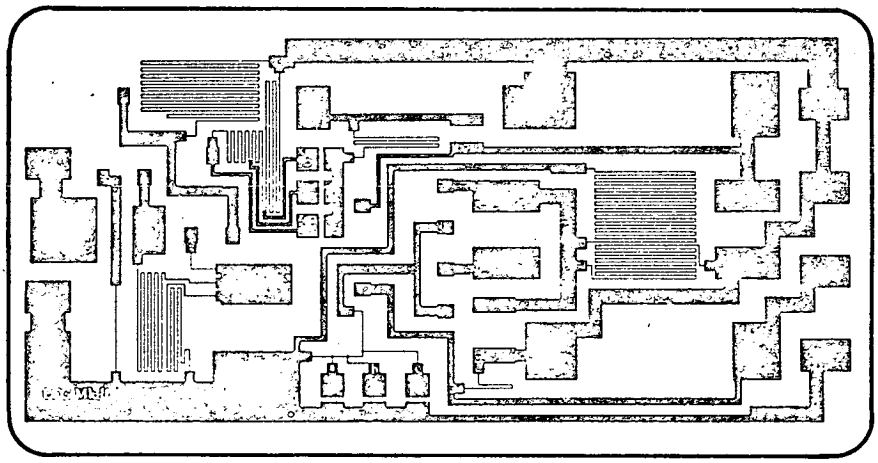

3 'Tempsens' and 'ECG' photo-masks

TELEMETRY TRANSMITTERS

Two types of implantable radiotelemetry devices are at present being produced, using the process described in this paper. These we have referred to as the 'ECG device' and the 'Tempsens device'. Both operate under 'Class I' conditions as defined by the GPO and are tunable over the range 26 to 30 MHz. The circuit diagrams of these devices are shown in Fig 2 and their thin film layouts in Fig 3. Both devices use the same two-transistor oscillator stage, in which frequency modulation is achieved by the application of a signal voltage to a varicap diode in the tuned collector circuit of one transistor. The antenna coil is part of the tuned collected circuit of the second transistor. Because of their close proximity, there is a stray coupling capacitance between the two resonant circuits. This capacitance must therefore be isolated from its surroundings, and this is achieved by wrapping metallized self-adhesive tape around the rf end of the package.

The 'EEG device' combines this carrier oscillator section with a two-stage voltage pre-amplifier, on the same 25 × 13 mm substrate. This device was originally intended for telemetry of the avian ECG signal, of about 180 μV peak-to-peak obtained from implanted leads. The preamplifier specifications are, however, suitable for telemetry of many sorts of bio-potentials and the avian EEG has been successfully monitored from cortical electrodes.

The 'Tempsens device' used the carrier oscillator in conjunction with a four-transistor multivibrator whose mark/space ratio is controlled by the resistance of a thermistor. Other variable-resistance transducers could be used to monitor parameters other than temperature.

A brief list of the main performance specifications of these devices is given in Fig 4.

Both of these devices were designed for implanted operation and this has necessitated their low current consumption of about 200 μA, to maximize battery life. With a 4 V supply line they typically operate at about one-twentieth of the GPO maximum permitted power and give a useful range of about 2 m if operated in a low noise environment. The power output of the rf stage is governed by the value of the emitter resistor. This resistor is arranged in sections which can be sorted out, allowing the power output to be increased, if necessary, to yield an acceptable signal-to-noise ratio at the receiver output.

The devices are typically powered by a battery of three mercury cells of 160 mAH capacity, connected in series. This pack weighs about 5-6 g and gives about 28 d continuous operation. The application of these devices is limited by the compromise which must be made between battery weight, useful range and life.

ACKNOWLEDGEMENTS

The authors wish to thank Professor W E J Farvis of the School of Engineering Science, University of Edinburgh and Mr J Murray and Dr A D Milne (the past and present Directors of the Wolfson Microelectronics Liaison Unit) for affording the facilities of the department and for the most helpful advice

R.F. OSCILLATOR SECTION (Tempsens & E.C.G. devices)

Carrier frequency	26·0 to 30 MHz
Carrier deviation	100 KHz
Deviation sensitivity	≃1 KHz/mV
Current consumption (V_{cc} = 4·00 V)	120→225 μA

VOLTAGE PREAMPLIFIER SECTION (E.C.G. device)

Voltage gain	×200
Frequency response	—3dB at 1·4 Hz 6 KHz
Input impedance	100 KΩ
Current consumption	22 μA
Total input referred noise voltage (near field conditions)	3 μV
Input voltage range	3→500 μV (without attenuators)

SUBCARRIER OSCILLATOR (Tempsens device)

Centre frequency	2 KHz
Duty cycle	10% to 90%
Current consumption	60 μA
Temperature sensitivity (with Y.S.I. thermistors)	5%/°C
Linearity (10°C span) (with Y.S.I. thermistors)	<0·1°C
Package dimensions	28 × 13 × 8 mm
Package weight	5→6 gm

4 'Tempsens' and 'ECG' device performance specifications

REFERENCES:

(9) Beavitt, A R, Turnell, R C and Campbell, D S. 'Study of energy distribution and neucleation of evaporated gold using a velocity selector', Thin Solid Films, 1, (1967), pp 3-11.

(10) Berry, R W, Hall, P M and Harris, M T. Thin Film Technology, Van Nostrand, Princeton, (1968).

(11) Holland, L, Thin Film Microelectronics, John Wiley and Sons Inc, New York, (1965).

(12) Swanston, J G and Campbell, D S. 'Structural and electrical properties of 80:20 Ni-Cr Thin Films', Thin Solid Films, 1, (1967), pp 183-202.

(13) Breitweisser, G, Varadarajan, B W and Wafer, J. 'Influence of Film condensation and source radiation on substrate temperature', Journal of Vacuum Science and Technology, 7, (1970), pp 274-277.

(14) Gerritsen, R N 'Metallic conductivity, experimental part' in: Encyclopaedia of Physics, 19, ed Flugge, S, Springer Verlag, Berlin, (1956), p 210.

(15) Holland, L, Vacuum Deposition of Thin Films, Chapman and Hall, (1961), p 251.

REFERENCES

Barr (1972) — A telemetry system for recording body temperatures of large numbers of caged rodents. Barr, R.E. Med. and Biol. Eng. 10 pp 677-684.

Beakley (1951) — The design of thermistor thermometers with linear calibration. Beakley, W.R. J.Sci.Inst. 28 pp 176-179.

Becker (1946) — Becker, J.A. et al, Trans AIEE 65 pp 711-724.

Berry (1968) — 'Thin Film Technology' Berry, R.W., Hall, P.M. and Harris, M.T., D. Van Nostrand Co. Ltd, Princeton, New Jersey.

Bolie (1962) — Theory for a loop antennae in a conductive medium. Bolie, V., in 'Biotelemetry'. (ed. Slater), Pergamon Press, London.

Brown (1971) — A miniature transmitter suitable for telemetry of a wide range of bio-potentials. Brown, M.W., Electroencephalography and Clinical Neurophysiology, 31 pp 274-276

Buchanan et al (1968) Measuring the radio frequency field strength of implanted transmitters. Buchanan, H. et al. USAF School of Aerospace Medicine, Report Number SAM-TR-68-33.

Carson (1937) Variable frequency electric circuit theory with application to the theory of frequency modulation. Carson, J.R. and T.C. Fry. Bell System Technical Journal 16 (October), pp 513-540.

Castelfiori and Dubini (1972) Radiotelemetry system for fetal monitoring. Castelfiori, S. and S. Dubini in 'Biotelemetry' (ed. Kimmick and Vos). Meander, N.V. Leiden. pp 237-245

Connor (1972) 'Antennas' Connor, F.R. Edward Arnold (Publishers) Ltd, London.

Crosby (1937) Frequency modulation noise characteristics, Crosby, M.G. Proc. IRE 25 no. 4 (APRIL) p 472.

Downing (1964) 'Modulation systems and Noise' Downing, J.J. Prentice-Hall Inc. New Jersey.

Dummermuth (1970) Numerical analysis of EEG data IEEE Transactions on Audio and Electroacoustics AU 18, no. 4. pp 404-411

Duncan et al (1974) Radiotelemetry of avian shank temperature using a thin film hybrid microcircuit. Duncan, I.J.H., Filshie, J.H. and McGee, I.J., Med. and Biol. Engineering, (in press).

Filshie and McGee (May 1974) Thin film hybrids for biomedical radiotelemetry. Part I: A film deposition process using electron-beam evaporation. Filshie, J.H. and I.J. McGee Electronic Equipment News, April/May 1974, pp 92-94.

Filshie and McGee (June 1974) Thin film hybrids for biomedical radiotelemetry. Part II: Production of implantable devices. Filshie, J.H. and I.J. McGee Electronic Equipment News, June 1974, pp 62-65.

Fishler (1967) FM/FM Multiplex radiotelemetry system for handling biological data. Fishler, H., N. Peled and S. Yerushalmi. IEEE. T.BME 14 no. 1 (January), pp 30-39.

Gardner (1966) 'Phase Locked Techniques' Gardner, F. John Wiley & Sons, New York.

Gerritsen (1956) 'Metallic conductivity: experimental part' Gerritsen, R.N. in 'Encyclopedia of Physics, 19' (ed. Flugge, S.) Springer Verlag, Berlin.

Green and Shore (1969) A two-channel transmitter for telemetry of cat electrocorticograms. Green, D.M., and J.R. Shore. J.Physiol. 203 no. 1 (July) pp 1P-2P.

HMSO (1968) 'Medical and Biological Telemetry Devices' Performance Specifications Numbers W6802/3/4, Her Majesty's Stationery Office, code 885438, London.

Holland (1961) 'Vacuum Deposition of Thin Films'. Holland, L. Chapman & Hall Ltd, London.

Kennan (1973) Nickel-Chromium resistor failure modes and their identification. Keenan, W.F. and W.R. Runyan. Microelectronics and Reliability, 12 pp 125-138.

Kimmick & Vos (1972) 'Biotelemetry' ed. Kimmick, H.P. and J.A. Vos. Meander N.V., Leiden.

King (1956) 'The Theory of Linear Antennas'. Kings, R.W.P. Harvard University Press, Cambridge, Mass.

Ko et al (1972) The radiation from an electrically small circular wire loop implanted in a dissipative homogeneous spherical medium
Ko, W.H. et al.
Annals of Biomed. Engineering, 1 pp 135-145.

Ko and Neuman (1967) Implant biotelemetry and micro-electronics.
Ko, W.H. and M.R. Neuman.
Science 56, pp 351-360.

Kraus (1950) 'Antennas'
Kraus, J.D., McGraw Hill Book Company Inc., New York.=

Lewis (1973) The design, performance and limitations of SAW oscillators.
IEE Conference Proceedings no. 109 (September 1973) pp 63-72.

Lin and Ko (1968) A study of microwatt powered pulsed carrier transmitter circuits.
Lin, W.C. and W.M. Ko.
Med. and Biol. Engineering 6, pp 309 - 317.

Mackay (1957) Endoradiosondes
Mackay, R.S. and B. Jacobson.
Nature, 179 (June 1957) pp 1239-1240.

Mackay (1965) 'Bio-medical Telemetry' (1st edition).
Mackay, R.S. John Wiley & Sons Inc., New York.

Mackay (1970) 'Bio-medical Telemetry' (2nd edition).
Mackay, R.S. John Wiley & Sons Inc., New York.

Marshal and Celebi (1970) A tunable sub-miniature biotelemetry transmitter.
Marshal, D.A. and G. Celebi.
Physiology and Behaviour 5 pp 709-712.

Michael and Weller (1968) Recording myometrial activity in freely moving Rhesus Monkeys by telemetry.
J. Endocrinology 42 pp 357-358.

Nichols and Rauch (1956) 'Radio Telemetry'
Nichols, M.H. and L.L. Rauch.
John Wiley & Sons Inc., New York.

Panter (1965) 'Modulation, Noise and Spectral Analysis'
Panter, P.F.
McGraw Hill Book Company, New York.

Rhind (1973) Studies in low power digital telemetry and data systems.
Rhind, W.G., PhD Thesis, University of Edinburgh.

Riley (1970) Radio telemetry system for transmitting deep-body temperature. Riley, J.L. Cornel Vetinarian, 60 pp 265-273.

Robrock II (1967) A six channel physiological telemetry system. Robrock II, R.B. and W.H. Ko. IEEE T.BME 14 no. 1 pp 40-46.

Rowe (1965) 'Signals and Noise in Communications Systems' Rowe, M.E. D. Van Nostrand Company Inc., New Jersey.

Sakrison (1968) 'Communication Theory, Transmission of Waveforms and Digital Information' Sakrison, D. John Wiley & Sons Inc., New York.

Sanders (1960) Communication efficiency comparison of several communication systems. Sanders, R.W. Proc. IRE 48 April 1960. pp 575-588

Schwan (1960) Characteristics of absorption and energy transfer of microwaves and ultrasound in tissues. Medical Physics Vol. 3 (ed. Glasser, O.) Yearbook Publishers, Chicago.

Schwan and Piersol (1955) Absorption of electromagnetic energy in body tissues: II, Physiological and Clinical Aspects. Amer. J. Phys. Med. 34 pp 425-448.

Schwartz (1959) 'Information Transmission Modulation and Noise'
Schwartz, M.
McGraw Hill Book Company Inc., New York.

Shannon (1948) A mathematical theory of communication.
Shannon, C.E.
Bell System Technical Journal, 27 pp 379-423 and pp 623 -658.

Shannon (1949) Communication in the presence of noise.
Shannon, C.E.
Proc. IRE 37, p 10.

Skutt et al (1972) The use of telemetry to obtain physiological data during exercise.
Skutt, H.R., R. Kertzer and R.B. Fell.
in 'Biotelemetry' (ed Kimmick & Vos)
Meander N.V., Leiden.

Stalberg and Kaiser (1972) Long term EEG telemetry.
Stalberg, E. and E. Kaiser.
in 'Biotelemetry' (ed Kimmick & Vos)
Meander N.V., Leiden. pp 307-316

Stiltz (1961) 'Aerospace Telemetry'
Stiltz, H.
Prentice Hall, Englewood Cliffs, New Jersey.

Sunde (1969) 'Communication Systems Engineering Theory'
Sunde, E.D.
John Wiley & Sons Inc., New Jersey.

Swanson (1967/68) Electrical conduction in island structure Ni and 80:20 Ni-Cr films.
Swanson, J.G., D.S. Campbell and J.G. Anderson.
Thin Solid Films, 1 pp 325-342.

Tindall (1970μ The effects of in-process heating on K1200 monolithic multilayer chip capacitors.
Tyndall, R.F. in INTER/NEPCON '70 Proceedings. Milton S. Kiver, London.

Weller and Manson (1972) A three channel telemetry system compatible with the British Medical and Biological Telemetry Regulations.
Weller, C. and G. Manson.
in 'Biotelemetry' (ed Kimmick & Vos)
Meander, N.V., Leiden.

LIST OF ADDRESSES OF MANUFACTURERS AND ORGANISATIONS REFERRED TO IN THE TEXT

1. Poultry Research Centre (ARC), Kings Buildings, West Mains Road, Edinburgh EH9 3JS.
2. University of Edinburgh, Department of Electrical Engineering, Kings Buildings, Mayfield Road, Edinburgh EH9 3JL.
3. Leak, manufactured by Rank Radio International, Bradford Road, Idle, Bradford.
4. GPO Radio Regulatory Division, General Post Office, London EC1.
5. Royal Radar Establishment, Great Malvern, Worcs.
6. Airmec, now under RACAL Instruments Limited, 55 St. Mary's Road, Maidenhead, Berks.
7. Alladin Components Limited, Greenford, Middlesex.
8. Dynatel, Spur Road, North Feltham Trading Estate, Middlesex.
9. Mallory Batteries Limited, Gatwick Road, Crawley, Sussex.
10. Sinclair Radionics Limited, London Road, St. Ives, Huntingdon PE17 4JH.
11. Henrys Radio, 303 Edgeware Road, London W2 1BW.
12. Mullard Limited, Mullard House, Torington Place, London WC1.
13. The Marconi Company Limited, Wetham, Essex.
14. Hewlett Packard Limited, 224 Bath Road, Slough, Bucks, SL1 4DS.
15. Plessey Semiconductors, Cheyney Manor, Swindon, Wilts.

16. Du Pont de Nemours International SA, Geneva, Switzerland.
17. Corning Glass Works NY, distributed by Carsberg & Froud Limited, Springwood Industrial Estate, Rayne Road, Braintrea, Essex.
18. Materials Research Company, 303 Ballards Lane, London N12 8NP.
19. Thermal Syndicate Limited, PO. Box 6, Wallsend, Northumberland.
20. Vitramon (Europe) Limited, Wycombe Lane, Wooburn Green, Bourne End, Bucks.
21. Bowmar Instrument Limited, 41-45 High Street, Weybridge, KT13 8BB.
22. Union Carbide UK Limited, Leaside, Aycliffe Industrial Estate, Near Darlington, Co. Durham.
23. Tekform Products Company, 2770 Coronado Avenue, Anakein, California 92806.
24. Dage (GB) Limited, Haywood House, 64 High Street, Pinner, Middlesex.
25. Milton Ross, 14 New Road, Watford, Herts.
26. Hopkins & Williams, Freshwater Road, Chadwell Heath, Essex.
27. RCA Solid State Europe, Sunbury on Thames, Middlesex, TW16 7HW.
28. Elecolit, distributed by Industrial Science, Leader House, 117-120 Snargate Street, Dover, Kent.
29. Yellow Springs Instrument, distributed by Sasco, PO Box 2000, Crawley, RH10 2RU.

30. Siliconix Limited, Morriston, Swansea, SA6 6NE.

31. FR Electronics, Wimbourne, Dorset, BH21 2BJ.

32. Ferranti Limited, Gem Mill, Chadderton, Oldham O29 8NP.

33. Emerson & Company (UK) Limited, Colville Road, Acton, London W3.

34. Home Office, Radio Regulatory Department, Waterloo Bridge House Waterloo Road. London SE1 8UA

A D D E N D U M

NPO capacitors with a larger capacitance per unit volume have recently been made available by Bowmar. The maximum value now available in the 0805 case size is now 1500 pF.